EVALUATION OF HYDROPHOBICALLY MODIFIED LOW MOLECULAR WEIGHT CHITOSAN AS A POTENTIAL NONVIRAL VECTOR FOR DNA VACCINE DELIVERY

A Dissertation
Submitted to the Graduate Faculty
of the
North Dakota State University
of Agriculture and Applied Science

By

Buddhadev Layek

In Partial Fulfillment
for the Degree of
DOCTOR OF PHILOSOPHY

Major Department:
Pharmaceutical Sciences

March 2014

Fargo, North Dakota

North Dakota State University
Graduate School

Title

Evaluation of hydrophobically modified low molecular weight chitosan as a potential nonviral vector for DNA vaccine delivery

By

Buddhadev Layek

The Supervisory Committee certifies that this ***disquisition*** complies with North Dakota State University's regulations and meets the accepted standards for the degree of

DOCTOR OF PHILOSOPHY

SUPERVISORY COMMITTEE:

Dr. Jagdish Singh
Chair

Dr. Sanku Mallik

Dr. Bin Guo

Dr. Rhonda Magel

Dr. John Ballantyne

Approved:

03/28/2014
Date

Dr. Jagdish Singh
Department Chair

ABSTRACT

Gene therapy has great potential in disease prevention and treatment. The purpose of the proposed research was to advance the development of safe and effective nonviral polymeric vectors for targeted gene therapy and DNA vaccine delivery. A series of hydrophobically modified chitosan derivatives with increasing degrees of chain length, substitution, and hydrophobicity was synthesized via carbodiimide mediated coupling reaction. The chemical structure of the polymers was determined using proton nuclear magnetic resonance (^{1}H NMR), fourier transform infrared (FTIR) spectroscopy, and elemental analysis. These polymers form micellar structures in aqueous environment and effectively condense plasmid DNA (pDNA) into nanoscale polyplexes. The acyl chain length, degree of substitution, and hydrophobicity of the substituent had great impact on the particle size, pDNA binding strength, in vitro pDNA release profile, cellular uptake, and in vitro gene transfection efficiency of the polymer/pDNA polyplexes. The hexanoic acid grafted chitosan [NAC-6(15)] and L-phenylalanine grafted chitosan (AGC-F) with a 15% degree of amino substitution demonstrated significantly ($p < 0.05$) higher gene transfection in HEK 293 cells, and their transfection efficiency surpassed the transfection capacity of FuGENE HD. The NAC-6(15) and AGC-F polymers were mannosylated to provide selective antigen presenting cell (APC) targeting, thereby facilitating cellular uptake to ultimately improve the overall immune response to the DNA vaccine. The chemical composition of the mannosylated copolymers was analyzed by ^{1}H NMR spectroscopy. These polymers efficiently condense pDNA into nanosized polyplexes with net positive surface charges. The resultant polyplexes demonstrated excellent protection of the condensed pDNA from enzymatic degradation by deoxyribonuclease (DNase). The synthesized mannosylated polymers exhibited 7-fold greater cellular uptake than chitosan in RAW 264.7 cells, which

express mannose receptors, mainly via the receptor-mediated endocytosis without affecting biocompatibility. The in vitro transfection efficiencies of mannosylated polymer/pDNA polyplexes were significantly ($p < 0.05$) higher than other polymers and FuGENE HD. An in vivo study in Balb/c mice using hepatitis B surface antigen encoding pDNA as a model DNA vaccine reflected good efficacy and biocompatibility of the delivery system. Therefore, hydrophobically modified mannosylated chitosan derivatives have the potential to be a safe and efficient APC targeting gene carrier for DNA vaccine delivery.

ACKNOWLEDGEMENTS

I would like to express my deepest and sincere gratitude to my graduate supervisor Prof. Jagdish Singh, for giving me the opportunity to work on this exciting and challenging project. His excellent guidance, immense knowledge, constructive criticism, constant motivation, understanding, and patience helped me throughout my research and writing of my thesis. I could not have imagined having a better supervisor and mentor for my Ph.D. study.

Besides my major advisor, I would like to extend my sincere thanks to my graduate supervisory committee members, Prof. Sanku Mallik, Prof. Bin Guo, Prof. Rhonda Magel, and Dr. John Ballantyne, for their guidance, encouragements, and suggestions throughout the study.

I wish to express my gratitude to Mike Chambers and Dr. John Ballantyne of Aldevron LLC, Fargo, ND for providing plasmid DNA for our research. My special thanks to Prof. Kenneth Rock of Dana Farber Cancer Institute, Boston, MA for providing DC 2.4 cells for our study.

I would like to offer my warmest and heartfelt thanks to my colleagues and friends Dr. Manas K. Haldar, Gitanjali Sharma, Dr. Rhishikesh Mandke, Dr. Mayura Oak, Dr. Rinku Dutta, Lindsey Lipp, and Sushant Lakkadwala for their help and support during my studies. I also thank my friends Abrez, Nimish, and Vinay for making my stay here enjoyable.

The five years at the Department of Pharmaceutical Sciences will always remain some of the best years of my life. All faculty, staff, and students have been extremely supporting and I know that I will rarely meet nicer people anywhere in the world. My special thanks go to Jean and Janet for their help, support, and assistance.

I gratefully acknowledge financial supports from the National Institutes of Health, the Fraternal Order of Eagles, the Department of Pharmaceutical Sciences, NDSU, and the North Dakota Experimental Program to Stimulate Competitive Research (NDEPSCoR).

I wish to acknowledge my family members for their love, sacrifice, understanding, and unconditional support without which I would not have been reaching this milestone.

Last but not the least, I would like to thank my wife Mayna and my son Nil for their sacrifice, cheering me up, and standing by me through the good times and bad.

DEDICATION

Dedicated to my parents,

Chhaya and Kartick Chandra Layek

my wife,

Mayna

and son,

Swapnanil

TABLE OF CONTENTS

LIST OF TABLES

LIST OF FIGURES

LIST OF ABBREVIATIONS

AAV…….....Adeno-associated virus

AFM.……..Atomic force microscope

AGC……....Amino acid grafted chitosan

AGC-A……L-alanine grafted chitosan

AGC-F……L-phenylalanine grafted chitosan

AGC-F-Man……...Mannosylated AGC-F

AGC-I…….L-isoleucine grafted chitosan

AGC-L……L-leucine grafted chitosan

AGC-V……L-valine grafted chitosan

ANOVA……..Analysis of variance

APC…….Antigen presenting cell

BCA……Bicinchoninic acid

CMC…….....Critical micelle concentration

DAPI…….....4',6-diamidino-2-phenylindole

DLS…….Dynamic light scattering

DMEM…..**.....**Dulbecco's Modified Eagle's Medium

DNA……...Deoxyribonucleic acid

DNase…….Deoxyribonuclease

EDC……1-Ethyl-3-(3-dimethylaminopropyl) carbodiimide

ELISA…….Enzyme linked immunosorbant assay

EMEM……Eagle's minimal essential medium

EtBr……Ethidium bromide

FACS……..Fluorescence activated cell sorting

FBS…….Fetal bovine serum

FITC……...Fluorescein isothiocyanate

FTIR…….....Fourier transform infrared

GFP…….……Green fluorescent protein

HBsAg…….....Hepatitis B surface antigen

HBV…….....Hepatitis B virus

HEK 293…….Human embryonic kidney 293

IFN-γ……...Interferon-γ

IgG……..Immunoglobulin G

IL-4…….Interleukin-4

ITC…….....Isothermal titration calorimetry

kb…….....kilobases

kDa……..…kilodalton

MR……..Mannose receptor

MTT……3-(4,5-dimethylthiazol-2-yl)-2,5-diphenyltetrazolium bromide

Mw……..Molecular weight

MWCO……...Molecular weight cut-off

NAC…….....N-acyl derivative of chitosan

NAC-6……N-hexanoyl chitosan

NAC-6(5)……...NAC-6 with 5% of hexanoic acid substitution

NAC-6(15)…….NAC-6 with 15% of hexanoic acid substitution

NAC-6(25)…….NAC-6 with 25% of hexanoic acid substitution

NAC-6(15)-Man…….Mannosylated N-hexanoyl chitosan

NAC-8……N-octanoyl chitosan

NAC-10……..N-decanoyl chitosan

N/P ratio…….Ratio of free amino groups on the polymer to phosphate groups in DNA

NHS……N-hydroxysuccinimide

^{1}H NMR……..Proton nuclear magnetic resonance

pβ-gal……..Plasmid DNA encoding β-galactosidase

PBS…….Phosphate buffered saline

PBST……..Phosphate buffered saline containing 0.2% (v/v) Tween 20

pDNA…….Plasmid DNA

PEG…….Polyethylene glycol

PEI……..Polyethyleneimine

pGFP……..Plasmid DNA encoding green fluorescent protein

pHBsAg……..Plasmid DNA encoding HBsAg

PLL…….Poly-L-lysine

RNA……Ribonucleic acid

rpm…….Revolutions per minute

SD……...Standard deviation

TAE……Tris-acetate-ethylenediaminetetraacetic acid

1. INTRODUCTION

Gene delivery has emerged as a new paradigm in medicine due to its tremendous therapeutic potential. Initially, transfer of exogenous genetic materials to host cells was considered as an experimental tool to understand gene function and its regulation. With the rapid advancement in molecular biology and genetic understanding of cellular processes and disease pathogenesis, gene delivery is becoming an integral part in developing an effective prophylactic or therapeutic strategy against various inherited or acquired diseases. The basic concept of gene therapy involves the delivery of nucleic acids (DNA, RNA, small interfering RNA, and anti-sense oligonucleotide) that manipulate gene expression in a desired cell population and thereby alter cellular processes and responses. However, the systemic delivery of naked therapeutic genes is unrealistic because of their non-specificity to the target cells, rapid clearance by mononuclear phagocytic system, and susceptibility towards nuclease-mediated degradation. Additionally, the large size, hydrophilic nature, and high anionic charge density are considerable barriers for efficient cellular uptake of the naked gene. Therefore, the primary challenge for gene therapy is the development of carriers or physical methods that assist safe and efficient transfer of the therapeutic gene to targeted cells without degradation of the delivered gene. Researchers have pursued numerous delivery systems for gene transfer, which are broadly categorized as viral and nonviral delivery systems. Figure 1 shows the distribution of different vectors used in clinical trials of gene therapy.

1.1. Barriers for nonviral gene delivery

Successful in vivo gene delivery requires that the pDNA is delivered to the target cell population, efficiently taken up by the cell, and transported to the appropriate cellular compartment. Multiple anatomical and cellular barriers limit the overall efficiency of gene

delivery by nonviral methods (Figure 2). Anatomical barriers such as epithelial and endothelium cell linings as well as the extracellular matrix surrounding the cells prevent direct access of nucleic acids to the desired cells. Endonucleases present in blood and extracellular matrix can degrade the free and unprotected DNA within 30 min (Kawabata et al., 1995). Furthermore, systemic delivery of DNA-loaded colloidal particles leads to rapid clearance from the circulation due to extensive uptake by the phagocytic Kupffer cells in the liver and the residential macrophages in the spleen, thus preventing transportation to any organ or tissue (Al-Dosari and Gao, 2009). In addition, DNA directly injected into a tissue drains rapidly into the lymphatics (Choate and Khavari, 1997; Levy et al., 1996). Crossing the plasma membranes is considered to be the most critical rate limiting step for efficient gene expression.

pDNA is typically 10^3 to 10^4 base pairs in length, has a molecular weight of 10^6-10^7 daltons, has a supercoiled tertiary structure in aqueous solutions, has an hydrodynamic diameter of greater than 100 nm, and has a surface charge ranging from –30 mV to –70 mV (Shea and Segura, 2001). This large size and high negative charge density of naked DNA prevents its diffusion through the cell membranes unless its entry is assisted by creating transient pores via physical techniques (Villemejane and Mir, 2009) or through different active cell uptake mechanisms such as endocytosis, phagocytosis, or pinocytosis (Medina-Kauwe et al., 2005). Following uptake via endocytosis, macromolecules trapped within the endosomes usually transform into digestive lysosomes unless some escape mechanism is used to interrupt this maturation process. Upon their escape from endosomes, DNA in its free form or as complexes with vectors must travel through cytoplasmic space filled with viscous fluid and a network of cytoskeleton matrix and traverse the nuclear membrane to get transcribed. Multiple delivery systems have been developed to overcome the barriers of stability, charge density, size, and

biodistribution. To date, no single gene delivery method is capable of overcoming all of these barriers.

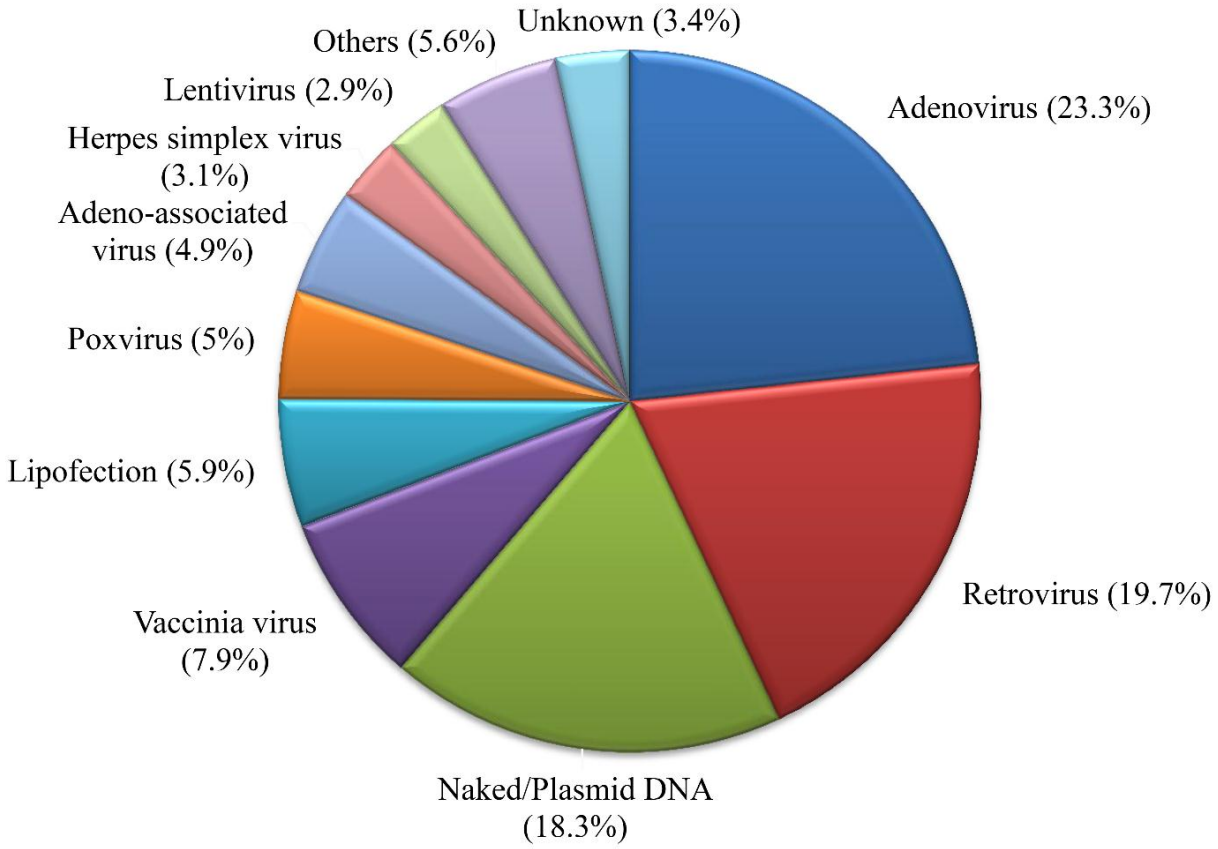

Figure 1. Gene delivery vectors used in clinical trials (n = 1843). Adapted from J. Gene Med., 2012. Current as of January 2012.

1.2. Viral delivery systems

Viruses are naturally evolved vectors which efficiently deliver their genes into host cells. This ability made them favorable for engineering virus-based carrier systems for the transfer of therapeutic genes. Viral vectors have an established history of efficacy and have been used in the vast majority of clinical trials conducted so far. The most commonly used viral vectors include retrovirus, lentivirus, adenovirus, and adeno-associated virus.

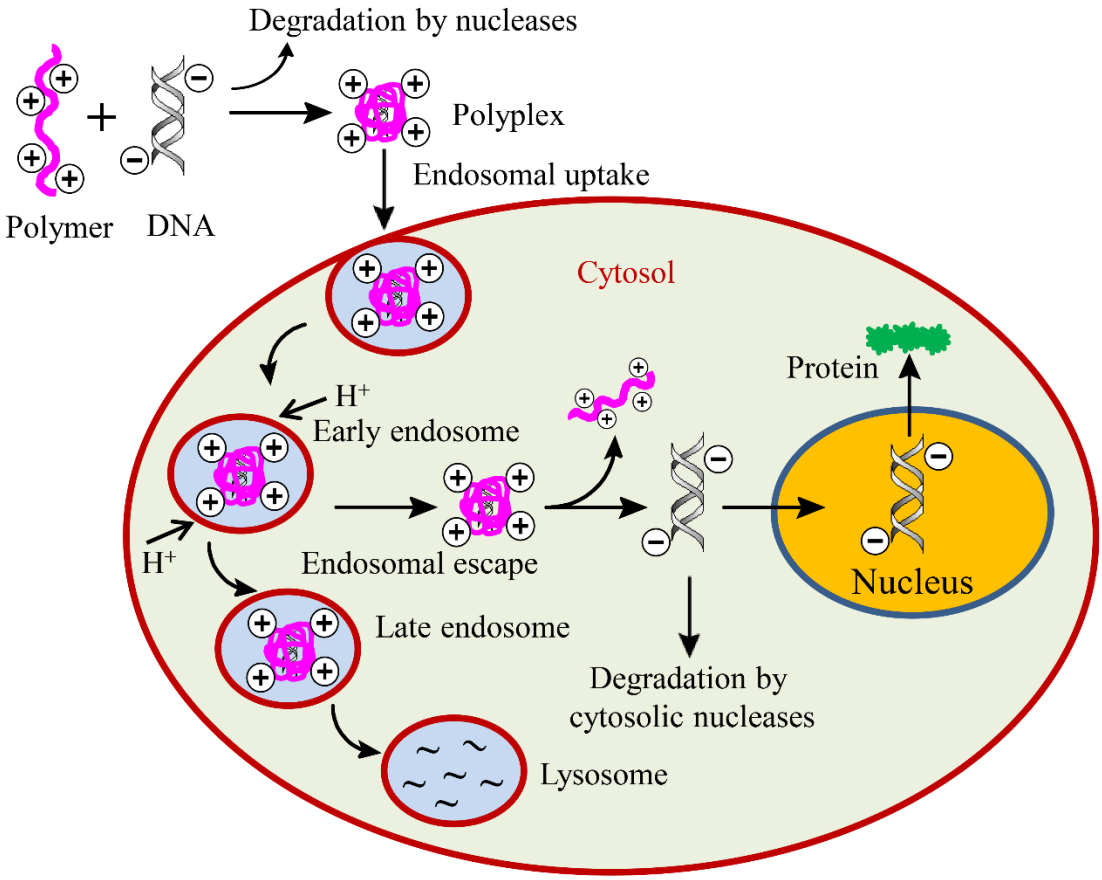

Figure 2. Schematic representation of major barriers to the chemical nonviral vector-mediated gene delivery.

1.2.1. Retroviral vectors

Retroviruses are among the first viral vectors to be designed and comprise 19.7% of current clinical trials (Ginn et al., 2013). They are small RNA viruses with single-stranded RNA genomes of 7-12 kilobases (kb) (Zhang and Godbey, 2006). Following entry into host cells, the viral genome is converted into linear double-stranded DNA by means of a reverse transcriptase enzyme encoded by the virus itself. The obtained viral-DNA is then integrated into the host's cell genome leading to sustained transgene expression (Smith, 1995). The retroviral vectors used for gene delivery must be manipulated to make them replication-defective so that they are capable of transfecting their target cells and delivering their viral payload, but unable to produce and release

new virions to induce pathogenic effects. This can be accomplished by replacing the trans-acting viral genes (gag, pol, and env) with the genes that are to be delivered. The most commonly used recombinant retroviruses are Moloney murine leukemia viruses (MuLV) and lentiviruses.

The major advantages of retroviral vectors include their capability of stable integration into the host genome, generation of sufficient viral titres for efficient gene transfer, infectivity for broad range of target cell types, and capacity to carry reasonable sizes (< 8 kb) of foreign genes (Walther and Stein, 2000). However, these advantages are often accompanied by some serious disadvantages which can create hurdles for their clinical applications. The most common disadvantages include instability of some retroviral vectors, possibility of insertional mutagenesis due to the random insertion of viral genetic material into host DNA, difficulty in targeting of viral infection or gene expression, and the requirement for cells to be actively dividing for integration of MuLV-derived retroviral vectors (Walther and Stein, 2000).

Lentiviruses (e.g., HIV-1) are a specialized class of retroviruses that have the ability to infect and integrate into non-dividing cells (Vigna and Naldini, 2000). Like other retroviral vectors, they also integrate into the host genome at arbitrary places, which can disturb the normal function of cellular genes and may promote the development of cancer (Poeschla et al., 1998). However, studies have demonstrated that lentiviral vectors have a lower tendency to integrate in places that potentially cause cancer and did not increase tumor incidence (Cattoglio et al., 2007; Montini et al., 2006).

1.2.2. Adenoviral vectors

Adenoviruses are non-enveloped DNA viruses containing a linear double-stranded DNA of about 35 kb and are known to cause mild infections in humans (Smith, 1995). The major advantages of adenoviral vectors include their ease of production, high level of gene expression,

and ability to transfect non-dividing cells (Chailertvanitkul and Pouton, 2010). Currently adenoviral vectors are the most commonly used vector for gene delivery applications which consists of 23.3 % of all clinical trials (Ginn et al., 2013). The attachment of adenoviruses to the host cells is mediated by high affinity binding between the viral fiber capsid protein and the Coxsackie-Adenovirus Receptor present on the surface of the host cell (Miyazawa et al., 1999), while internalization takes place via endocytosis upon interaction with αv-integrins (Nemerow and Stewart, 1999). It is reported that the adenoviruses reach the host cell's nucleus primarily via a microtubule-mediated intracellular translocation mechanism (Bailey et al., 2003; Greber and Way, 2006). After entering into the nucleus, the viral DNA does not integrate into the host genome, but replicate as epichromosomal (Verma and Somia, 1997). The major challenge for adenoviral vectors is their high immunogenicity which prevents long-term transgene expression making them inappropriate for treatment of diseases demanding sustained transgene expression (Robbins and Ghivizzani, 1998). However, these vectors may be useful in conditions where high-level but transient transgene expression is desired such as in restenosis and cancer.

1.2.3. Adeno-associated viral vectors

Adeno-associated viruses (AAVs) are small, nonpathogenic, non-enveloped, single-stranded DNA viruses belonging to the Parvoviridae family (During, 1997). They require co-infection with an adeno or herpes simplex helper virus for their replication (Li et al., 2005). AAV are one of the most promising gene delivery vectors due to a number of favorable features such as the ability to infect a wide range of cells, low level of immune response, and long-term gene expression in dividing and non-dividing cells (Smith-Arica and Bartlett, 2001). However, there are a few drawbacks to using AAV, including the small size of the transgene it can carry (up to 4.5 kb) and the difficulty in viral production (Wright et al., 2003).

1.2.4. Poxviral vectors

Poxviruses represent a heterogenous group of viruses (vaccinia virus, avipoxviruses, smallpox virus etc) belonging to the Poxviridae family. They are large, complex, enveloped viruses containing a linear double-stranded DNA of about 200 kb. Several unique features of poxviral vectors make them an efficient carrier for gene delivery. The main advantage of these vectors is their large insertion capacity for foreign genes. More than 25 kb of foreign DNA can be stably inserted into the viral genome without compromising infectivity or other essential functions (Kim and Gulley, 2012). Poxviruses carry out their replication entirely within the cytoplasm of the host cells and the viral genome does not integrate into host DNA, so it has no risk of mutation. Most importantly, poxviral vectors have proven safe, effective, and infect most of the mammalian tissues including dividing and non-dividing cells. There are some challenges in utilizing poxviruses for gene delivery due to their complex structure and biology, so further studies are needed to improve their safety and to diminish the risk of cytopathic effects (Walther and Stein, 2000).

1.2.5. Herpes simplex viral (HSV) vectors

HSV is an enveloped, DNA virus containing a linear double-stranded genome of about 150 kb (Burton and Glorioso, 2000). It is a potential candidate as a gene delivery mainly because of its large insertion capacity for foreign genes (30-50 kb) and its natural tropism for the central nervous system (Walther and Stein, 2000). HSV has a broad range of host cell types, and can infect dividing and non-dividing cells. Furthermore, the recombinant HSV vector may readily be developed with high titre and purity. However, the major limitations of HSV include possible toxicities, risk of recombination, and transient transgene expression (Walther and Stein, 2000).

1.3. Nonviral delivery systems

Safety issues such as carcinogenicity, immunogenicity, and inflammation as well as restrictions in nucleic acid cargo size impose serious concerns for clinical applications of viral vectors (Check, 2005; Hacein-Bey-Abina et al., 2003; Raper et al., 2003; Thomas et al., 2003). The challenges confronted with viral vectors have accelerated the search for alternative, nonviral vectors (Needham et al., 2012; Pack et al., 2005). Nonviral vectors are broadly categorized as physical and chemical methods. The most commonly used physical methods are electroporation, sonoporation, gene gun, microinjection, and hydrodynamic injection. The physical methods rely on the delivery of nucleic acid via the application of physical forces to enhance the permeability of the cell membrane. In contrast, chemical vectors use natural or synthetic carriers to deliver nucleic acids into cells. The materials used are usually less toxic and non-immunogenic compared to their viral counterparts. Additionally, cell or tissue specificity can be attained by harnessing a cell specific ligand in the design of chemical or biological vectors while physical methods can offer spatial precision. Other potential advantages of nonviral vectors include ease of large-scale production, no limitations over their payload capacity, and potential for repetitive administration (Al-Dosari and Gao, 2009).

However, the major disadvantages of nonviral vectors for clinical applications are low transfection efficiency and in many cases, the gene expression is transient (He et al., 2010). Therefore, the most critical point that should be taken into consideration in gene therapy is the development of a suitable vector that enhances the expression of the delivered gene in a desired cell population. Some major nonviral delivery systems with their distinct benefits and shortcomings are discussed below.

1.3.1. Physical methods

1.3.1.1. Electroporation

Electroporation involves the use of high-voltage electric pulses for a very short duration (microseconds to milliseconds) to induce transient and reversible breakdown of the cell membrane. This transient and permeabilized state can be exploited to load cells with a large variety of molecules, either through diffusion in the case of small molecules, or through electrophoretic forces allowing transport through the destabilized cell membrane, as is the case for DNA transfer (Gehl, 2003). This technique has been routinely applied for in vitro and in vivo gene transfer for more than three decades (Neumann et al., 1982; Heller et al., 1996; Mir et al., 1999; Medi et al., 2005; Jazi et al., 2012). Typically, in vivo electroporation is performed by injecting DNA locally or systemically followed by application of electric pulses for a few milliseconds. Several parameters such as the type of electric pulse, pulse lengths, pulse amplitude, number of pulses, the interval between each pulse, electrode design, size of the delivered DNA, and type of target tissue have been shown to greatly influence the efficiency of gene transfer (Medi et al., 2005). In vivo electroporation is considered as safe, efficient, and reproducible compared to other nonviral approaches (Al-Dosari and Guo, 2009). Moreover, when parameters are optimized, this technique can induce transfection efficiency equal to that generated by viral vectors (Andre and Mir, 2004).

Despite the high gene transfer efficiency, several aspects associated with this technique need to be improved to make it practical for human applications. Electroporation is generally effective only within the ~ 1 cm region between the electrodes, and this causes transfection of the cells in large areas of the tissues difficult. Electroporation is also difficult to use in internal organs, surgical procedures are required to implant and explant electrodes. Most importantly, the

application of high voltage can cause irreversible tissue damage as well as affect the stability of genomic DNA (Al-Dosari and Guo, 2009; Gao et al., 2007).

1.3.1.2. Gene gun

The gene gun, also known as biolistic particle delivery system, was first designed for gene transfer in plants in 1987 (Klein et al., 1992). This device injects cells with genetic information using heavy metal microparticles coated with pDNA. Generally, tungsten, gold, or silver particles are employed as the gene carrier (Mhashilkar et al., 2001; Miyazaki et al., 2006). The particles are accelerated to high velocity to penetrate the target cells using compressed inert gas such as helium. Gas pressure, particle size of the gene carrier, and dosing frequency are key parameters in determining the penetration efficiency, degree of tissue damage, and overall gene transfection efficiency (Uchida et al., 2002).

The gene gun mediated gene transfer has been extensively studied for intradermal, intramuscular, and intratumoral genetic immunization (Miyazaki et al., 2006). The major advantages of gene gun over other in vivo gene delivery approaches include no need of toxic adjuvants for gene carrier, receptor independent gene delivery, no restriction for DNA size, high repeatability, and hassle free production process for DNA loaded microparticles (Lin et al., 2000). However, the major disadvantages of this method are shallow penetration of DNA into tissues and short-term gene expression (Mhashilkar et al., 2001; Niidome and Huang, 2002).

1.3.1.3. Sonoporation

Sonoporation is a promising nonviral strategy that utilizes ultrasound waves to transiently increase the cell membrane permeability of macromolecules such as DNA, RNA, protein, and other agents (Miller et al., 2002; Newman and Bettinger, 2007). Though the exact mechanism of sonoporation is not fully understood, it is believed that ultrasound energy mechanically creates

nonspecific pores on the plasma membrane via hyperthermia and acoustic cavitation to enhance the permeability of the target cells (Deng et al., 2004; Pitt et al., 2004).

Ultrasound has many potential advantages as a gene transfer system, due to its safety, simplicity, and flexibility (Pitt et al., 2004; Ferrara, 2010). The gene transfection efficiency of sonoporation could be further improved by combining with microbubles. Microbubles or ultrasound contrasting agents enhance permeability by lowering the cavitation threshold for applied ultrasound energy. Recent studies suggested that pDNA binding cationic microbubles are more efficient compared to neutral microbubles in gene delivery (Wang et al., 2012). However, the transfection efficiency of sonoporation greatly depends on the ultrasonic parameters such as frequency, pulse length, acoustic pressure, duty cycle, and repetition rate as well as microbuble parameters such as size, shell material, gas species, surface rigidity, and interfacial tension.

1.3.1.4. Hydrodynamic injection

The hydrodynamic gene delivery technique uses high pressure as a driving force for gene transfer. The rapid injection of a large volume of naked DNA solution (8–12% of body weight in 3-5 s), leads to a reversible increase in endothelial lining permeability and transient pore formation in hepatocyte membranes facilitating intracellular diffusion of the DNA molecules (Zhang et al., 2004). The safety and simplicity of hydrodynamic injection allows for a wide range application of this technique for efficient gene transfer in internal organs, especially the liver (Al-Dosari et al., 2006; Suda and Liu, 2007). The effectiveness of hydrodynamic gene therapy depends on capillary structure, structure of the cells encircling capillaries, and applied hydrodynamic pressure (Gao et al., 2007; Suda and Liu, 2007). Until recently, the application of this method for in vivo gene delivery in humans was ruled out mainly due to the need for a large injection volume that is beyond the acceptable limits for patients. However, the use of a ballon

catheter and the development of a computer-controlled injection device have made it suitable for human use (Fabre et al., 2008; Suda et al., 2008).

1.3.2. Chemical methods

Chemical vectors such as cationic lipids, polypleptides, and cationic polymers can condense negatively charged DNA into nanocomplexes via electrostatic interactions. The complexes protect DNA from nucleases degradation, facilitate cellular uptake, and intracellular delivery. This section describes the brief summary of chemical vectors extensively used for gene transfer.

1.3.2.1. Cationic lipids

Cationic liposomes pioneered by Felgner et al. (1987) are still the most extensively investigated and commonly used nonviral approach for gene delivery into cells. Currently, hundreds of cationic lipids have been utilized for in vitro and in vivo transfection of mammalian cells. The chemical structures of some representative cationic lipids are depicted in Figure 3. They share the common structural features of a positively charged head group and hydrophobic tail attached via a linker group. The most frequently used hydrophilic head groups include primary, secondary, tertiary, or quaternary amines. However, imidazole, guanidine, pyridinium, and phosphorus groups have also been used. The cationic head group is essential for binding with negatively charged phosphate groups in nucleic acids. The hydrophobic tails are typically aliphatic chains, cholesterol, or other types of steroid rings. The most common linkages between hydrophilic head and hydrophobic tail are ester, ether, amide, or carbamate and can greatly affect the chemical stability and biodegradability of the cationic lipid.

The transfection efficacy of cationic lipids differs dramatically depending on the structure of the lipids (such as overall geometric shape, the types of lipid anchor, the number of charged

groups per molecule, and the type of linkage), the charge ratio used to form lipid/DNA complexes, and the properties of co-lipids (Wasungu and Hoekstra, 2006). Due to the electrostatic interactions, the cationic liposomes spontaneously form complexes with negatively charged nucleic acids and such unique compacted complexes are termed lipoplexes. In lipoplexes, nucleic acids are surrounded by cationic lipids which provide them efficient protection against nucleases degradation and can facilitate endosomal escape of the contents (Hoekstra et al., 2007). Furthermore, due to their positive charges, lipoplexes tend to interact with negatively charged proteoglycans of cell membranes via electrostatic interactions that may facilitate adsorption mediated cellular uptake of the lipoplexes.

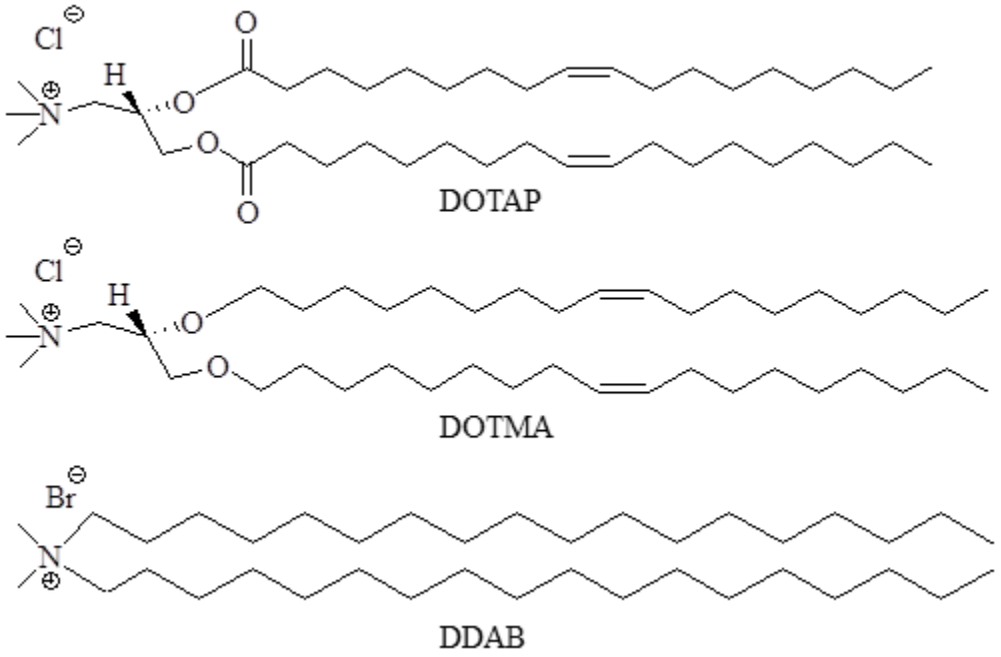

Figure 3. Chemical structures of some commonly used lipids in nonviral gene delivery. DOTAP: 1,2-dioleoyl-3-trimethylammonium-propane (chloride salt); DOTMA: 1,2-di-O-octadecenyl-3-trimethylammonium propane (chloride salt); DDAB: dimethyldioctadecylammonium (bromide salt).

In general, cationic lipid based gene delivery systems have the advantages of being inexpensive, easy to formulate, and possessing a reasonably simple transfection procedure (Rao

and Gopal, 2006). Moreover, cationic lipids can be engineered to impart tissue or cell specificity to improve the overall efficacy of delivery system (Guo and Huang, 2011; Kong et al., 2012; Sharma et al., 2013). However, their transfection potency needs to be further enhanced, and the potential toxicities such as formation of aggregates with blood components and tendency to induce acute inflammatory response have to be resolved for in vivo application (Al-Dosari and Gao, 2009). As of June 2012, lipofection, which involves cationic lipid/DNA complexes have been used in 111 clinical trials and represent 5.9% of all trials (Ginn et al., 2013).

1.3.2.2. Cationic polymers

Cationic polymers have also been extensively used for gene transfer because of their capability of forming electrostatic complexes (polyplexes) with negatively charged DNA under physiological conditions. These polyplexes improve the hydrodynamic properties of DNA and provide its efficient protection from nuclease degradation. The most noticeable difference between cationic polymers and cationic lipids is that the former does not contain a hydrophobic moiety and is soluble in water (Elouahabi and Ruysschaert, 2005). Compared to cationic lipids, cationic polymers have the distinct advantage of condensing DNA into a relatively small size (Gershon et al., 1993; Ruponen et al., 1999). This can be critical for gene transfer, as small particles are favorable for cellular uptake and downstream gene expression. The most commonly studied cationic polymers for gene delivery include polyethyleneimine (PEI), poly-L-lysine (PLL), and chitosan.

PEI is the most extensively studied gene carrier and is often considered the gold standard of nonviral vectors. PEI was first introduced to gene transfer in 1995 (Boussif et al., 1995). It exists in either linear or branched structures. PEI contains a very high density of primary, secondary, and tertiary amino groups of which 80% remain unprotonated at physiological pH.

The unprotonated amines exert significant buffering capacity over a wide pH range and promote the escape of polyplexes from the lysosomal degradation pathway, resulting in enhanced gene transfection (Behr, 1997). PEI offers significantly higher transfection and protection against nuclease of the transferred gene than other cationic polymers such as PLL possibly due to its higher charge density resulting in efficient complexation of the gene. However, the high charge density of PEI is also responsible for its greater degree of cytotoxicity. The transfection efficacy and toxicity of PEI depends on its various properties such as molecular weight, degree of branching, polymer to DNA weight ratio used, and the size of the polyplex (Thomas et al., 2005). The high toxicity and non-biodegradable nature of PEI is the hurdle for its in vivo application. Several strategies such as chemical conjugation of targeting ligands to PEI (Gabrielson and Pack, 2009; Kursa et al., 2003; Tian et al., 2011), steric stabilization of PEI with inert polymers such as polyethylene glycol (PEG), dextran, or pluronic triblock polymers (Al-Dosari and Gao, 2009), and use of synthetic high molecular weight PEI derived from low molecular weight PEI by polymerization through biodegradable disulfide linkage (Gosselin et al., 2001) have been utilized to improve transfection efficiency while reducing its cytotoxicity.

PLL was the first cationic polymer utilized for in vitro and in vivo gene transfer (Thiersch et al., 2013; Wu and Wu, 1987). It is a biodegradable linear polypeptide of the amino acid L-lysine synthesized by polymerization of N-carboxyanhydride of lysine (Zhang et al., 2004). PLL can effectively condense DNA into nanoscale stable polyplexes and improve their cellular uptake. However, the gene transfection efficiency of PLL-based polymers is lower as compared to PEI, which can be attributed to its inability to protect the polyplexes from endolysosomal degradation pathway (Akinc and Langer, 2002). The DNA condensing and transfection efficiency of PLL increases with higher molecular weight, but is also accompanied

by undesirable high cytotoxicity. Several approaches such as design of amphiphilic PLL by conjugation with PEG (Ziady et al., 2003), addition of buffering moieties to PLL backbone (Pichon et al., 2001), and conjugation of targeting ligand (Curiel et al., 1991; Mislick et al., 1995) have been attempted to improve its transfection efficacy while reducing cytotoxicity.

Chitosan is a linear copolymer of randomly distributed β-(1-4)-linked N-acetyl-D-glucosamine and D-glucosamine residues produced by alkaline deacetylation of chitin. Chitin is derived from the exoskeleton of crustaceans (e.g., crabs, shrimps, and lobsters) and cell walls of fungi (Riva et al., 2011; Rane and Hoover, 1999) and is the second most abundant biomaterial in nature after cellulose (Rinaudo, 2006). Chitosan is a general term applied to chitins which are sufficiently deacetylated to form soluble amine salts. Since the degree of polymerization and deacetylation of chitins are highly variable, chitosan is not exactly defined in terms of its chemical composition (Jones and Mawhinney, 2005). The general chemical structure of chitosan is shown in Figure 4.

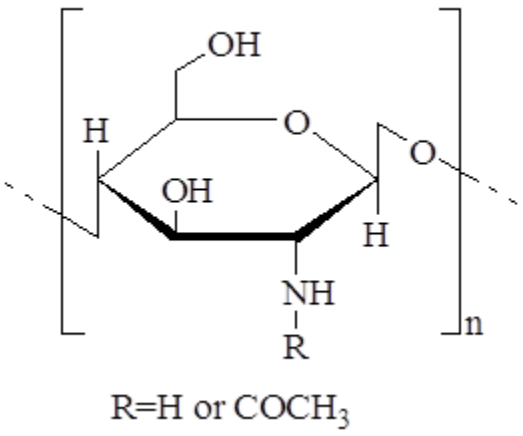

Figure 4. General chemical structure of chitosan. Degree of deacetylation (R = H) varies from 60 to 100%.

Chitosans are commercially available in different types and grades that widely varies in molecular weight (ranging from 10000 to 1000000 Da), degree of deacetylation (varies from 60

to 100%), and viscosity (Genta et al., 1998). Most of the functional properties of chitosan depend on its molecular weight, degree of deacetylation, and charge distribution (Dodane and Vilivalam, 1998). The primary amine group of the chitosan has a pKa value of ~6.5, which leads to a protonation in neutral to acidic solution with a charge density dependent on pH and the degree of deacetylation value.

Chitosan offers several potential advantages such as excellent biocompatibility, low cytotoxicity, low immunogenicity, and high cationic charge density (Lee et al., 2005; Shu and Zhu, 2002). Due to its cationic charge, it can form polyelectrolyte complexes with negatively charged DNA through electrostatic interactions, thereby condensing it into small particles and protecting it from DNase I &II degradation (Chang et al., 2010; Koping-Hoggard et al., 2001; Huang et al., 2005). However, the gene transfection efficiency of chitosan is significantly influenced by different formulation parameters such as molecular weight, degree of deacetylation, charge ratio of the primary amine of chitosan to phosphate groups on DNA, pH of the transfection medium, serum concentration, and cell types (Ishii et al., 2001; Kiang et al., 2004; Köping-Höggård et al., 2001; Romøren et al., 2003; Sato et al., 2001; Mao et al., 2010). Moreover, the presence of abundant primary amines and hydroxyl groups on the chitosan backbone make it amenable to various chemical modifications. These modifications, when precisely controlled, lead to desired physicochemical and biological characteristics of chitosan (Prabaharan, 2008).

The clinical applications of unmodified chitosan however have been limited by its low gene transfection efficiency. Studies have reported that the low transfection efficiency of a chitosan-based delivery system is primarily attributed to the poor water solubility at physiological pH, poor cellular uptake, and incomplete dissociation of DNA within cells due to

strong interaction between chitosan and DNA (Chen et al., 2008a; Lu et al., 2009). Several modifications of chitosan side chains using hydrophilic (Park et al., 2000; Germershaus et al., 2008), hydrophobic (Hu et al., 2006; Liu et al., 2003; Sajomsang et al., 2009), and both hydrophilic-hydrophobic moieties (Wang et al., 2011) have been reported to enhance the transfection efficiency of chitosan. Modification with hydrophilic units improves the water solubility and increases the plasma circulation time of the polyplexes. Hydrophobic modifications are expected to enhance the adsorption of the polymer/DNA polyplexes on the lipophilic cell membrane, confer efficient DNA protection from nuclease degradation, and assist intracellular DNA dissociation (Kim et al., 2007). Moreover, conjugation of hydrophobic segments to chitosan resulted in amphiphilic cationic polymers which could easily self-organize to form micelles in aqueous milieu. These polymeric micelles can not only facilitate efficient DNA condensation but also improve the stability of DNA polyplexes for in vitro and in vivo environments (Chen et al., 2011). These distinct benefits of hydrophobic modification encourage the possibility of developing amphiphilic chitosan derivatives with enhanced gene transfection efficiency.

Another major shortcoming of chitosan-based DNA delivery systems is its poor cell specificity, which is especially essential in successful DNA vaccine development that requires efficient delivery of antigen-encoded DNA into specific cells (Sun et al., 2012). The professional APCs such as macrophages and dendritic cells play a crucial role as effector cells in the initiation of immune responses to foreign antigens. These cells are highly efficient in internalizing and processing of antigens for presentation to T-lymphocytes (Mellman and Steinman, 2001). The additional co-stimulatory signals are then produced by the APCs leading to proliferation and differentiation of lymphocytes. Hence, there is tremendous prospective in developing DNA

vaccines that efficiently target APCs with a DNA delivery vector. It has been reported that mannose receptor (MR) is abundantly expressed on the surface of APCs (Taylor et al., 1990). Therefore, conjugation of mannose on the delivery vector can trigger the MR-mediated endocytosis, leading to enhanced efficacy of a desired DNA vaccine.

1.4. Hepatitis B

Hepatitis B is a serious liver infection caused by the hepatitis B virus (HBV). It is a major global health problem which affects about one third of the world's population (around 2 billion people) (Lavanchy, 2004). The virus is transmitted through infectious blood and other body fluids such as semen and vaginal fluids. The infection can cause acute and chronic liver diseases and puts people at high risk of death from cirrhosis and hepatocellular carcinoma (Larkin et al., 1999). The World Health Organization (WHO) has estimated that there are approximately 360 million chronic carriers of HBV, many of whom are at high risk for development of serious illness such as liver cirrhosis and hepatocellular carcinoma (WHO, 2009).

There is no specific treatment available for acute hepatitis B. Chronically infected individuals can be treated with drugs including interferon alpha and antiviral agents to slow the progression rate of liver cirrhosis, reduce incidence of hepatocellular carcinoma, and increase long term survival, but the treatment can cost thousands of dollars per year and is not available to most patients in developing countries. Hepatitis B, its complications, and the difficulties associated with treatment lead to about one million deaths per year. Therefore, immunization programs are the most efficacious way to reduce global HBV-related morbidity and mortality.

1.4.1. Current vaccines for hepatitis B

The prevention and control of infectious diseases such as hepatitis B depends on the availability of safe, effective, and affordable vaccines. The first vaccine for hepatitis B became

available in 1981, which was plasma-derived. The current recombinant hepatitis B vaccine was marketed in 1986 and has gradually replaced the plasma-derived vaccine. The active component of recombinant hepatitis B vaccine is hepatitis B surface antigen (HBsAg) and is produced in genetically engineered yeast or mammalian cells. This protein vaccine is safe and immunogenic, yet a very high rate of low or non-responders is apparent (Rendi-Wagner, et al., 2002). Moreover, current protein based vaccines are expensive, require multiple shots to achieve an optimal immune response, and are not effective in chronic HBV carriers. A course of three doses of vaccine is needed, the second dose at least one month after the first immunization and the third dose being administered six months after first immunization, to ensure an adequate level of anti-HBsAg antibodies. The number of doses and the length of time required for the development of adequate immune response is a major limitation in offering protection to the individuals with high risk.

The protection against HBV is reported to be dependent on immune memory after vaccination (Banatvala and Van Damme, 2003). Patients with acute hepatitis B exhibit detectable polyclonal cytotoxic T-lymphocyte (CTL) and T helper 1 (Th1) cell responses toward viral antigens, whereas these responses are absent or weak in chronic HBV carriers (Ferrari et al., 1990; Wieland and Chisari, 2005). Therefore, restoration or reactivation of HBV-specific immune responses is essential for chronic hepatitis B therapy (Wieland and Chisari, 2005).

1.4.2. DNA vaccines for hepatitis B

DNA vaccination or genetic immunization is a novel approach to immunize individuals against deadly diseases. It involves the immunization of host cells with pDNA encoding the antigen(s) against which an immune response is sought. DNA vaccines use host cells as bioreactors for in situ production of target antigen (Tang et al, 1992). This form of antigen

processing and presentation leads to activation of both major histocompatibility complex (MHC) class I and II pathways resulting in the induction of both cytotoxic cellular and humoral immunity (Encke, J. et al., 1999; Srivastava and Margaret, 2003). The induction of CD8+ CTLs mediated immune responses caused by DNA vaccines make them useful for the immunotherapy of chronic HBV infection (Michel and Loirat, 2001). Moreover, studies in nonhuman primates showed that DNA vaccine encoding HBV antigen induced high antibody titers that achieve levels required for HBV protection in humans (Michel and Loirat, 2001). The hepatitis DNA vaccine was also shown to induce protective antibody responses in humans who have not responded to conventional vaccination (Rottinghaus et al., 2003). Hence, DNA vaccines may offer an alternative therapeutic strategy to treat chronic HBV infection.

1.5. Statement of the problem

Lack of safe and effective gene delivery systems is the primary reason for the absence of eagerly awaited gene-based medicines including DNA vaccine. Thus, the development of novel delivery systems is of paramount importance in the overall success of gene therapy. The type and magnitude of immune responses induced by DNA vaccines can be influenced by the formulation and route of administration. The possible approaches to improve the immunogenicity of DNA vaccine are through efficient presentation of antigen to professional APCs or increasing the amount of antigen available for presentation. Considering the large population of APCs in the skin, intradermal delivery of DNA vaccine using an APC targeting delivery system will facilitate the cellular uptake and ultimately improve the overall immune response to the DNA vaccine.

The proposed research was directed towards the development of a safe and highly efficient chitosan-based nonviral vector for delivery of a HBV DNA vaccine encoding HBsAg antigen. The hydrophobically modified APC targeting nanomicelles were expected to overcome

the major barriers for gene transfer such as cell specificity, cellular uptake, and endosomal escape, and result in enhanced expression of the transferred gene.

The hypotheses for the present study were as follows:

1. The grafting of short chain hydrophobic moiety on chitosan backbone would introduce hydrophobic regions in the polymer, leading to formation of cationic nanomicelles in an aqueous environment. These micelles under optimized formulation conditions will condense pDNA to form nanocomplexes (polyplexes) and provide efficient protection of pDNA against nuclease degradation. The polymer/pDNA polyplexes will be biocompatible, nontoxic, and effectively transfect cells both in vitro and in vivo.
2. The introduction of mannose to hydrophobically modified chitosan will provide selective APC targeting, and thereby facilitate the cellular uptake and ultimately improve the overall immune response to the DNA vaccine. The intradermal delivery of pDNA encoding HBsAg using mannosylated polymers will induce efficient cellular and humoral immune responses in Balb/c mice model.

To test these hypotheses, the following specific aims were designed:

1. To derivatize low molecular weight chitosan with either short chain hydrophobic moieties such as short chain fatty acids and hydrophobic amino acids alone or both hydrophobic moieties and APC targeting ligand mannose to obtain graft polymers, which self-assemble to form cationic nanomicelles in aqueous environment.
2. To evaluate the polymer/pDNA polyplexes as gene carriers:
    (a) To investigate the pDNA condensing ability of the polymers using dynamic light scattering (DLS) method and agarose gel retardation assay.

(b) To evaluate pDNA protection capacity of polyplexes using the DNase protection assay.

(c) To study the cellular uptake and in vitro transfection efficiency in different cell lines

3. To study in vitro and in vivo biocompatibility of nanomicelles by cell viability assay and histological analysis, respectively.

4. To study cellular and humoral immune responses with intradermal delivery of HBsAg encoding DNA vaccine in Balb/c mice model.

The study is intended to result in the development of highly efficient, biocompatible, nontoxic, cationic nanomicelles to deliver HBV DNA vaccine in vivo in Balb/c mice.

2. SHORT CHAIN FATTY ACID CONJUGATED CHITOSAN FOR GENE DELIVERY: EFFECT OF FATTY ACID CHAIN LENGTH

2.1. Introduction

Chitosan [β (1→4) linked 2-amino-2-deoxy-β-D-glucan] is a linear copolymer of N-acetyl-D-glucosamine and D-glucosamine produced by alkaline deacetylation of chitin. Chitosan and its derivatives have been extensively used in various biomedical applications (Hirano et al., 1991; Jayakumar et al., 2010; Muzzarelli et al., 2000) due to their biodegradability, excellent safety profile, low immunogenicity, favorable physicochemical properties, and ease of chemical modification (Lee et al., 1998; Li et al., 2010; Zhu et al., 2008). At low pH (below the pKa of 6.5), primary amines of the chitosan backbone remain positively charged and can form complexes with negatively charged DNA through ionic interactions, thereby condensing it into small particles and protecting it from DNase I &II degradation (Chang et al., 2010; Koping-Hoggard et al., 2001; Huang et al., 2005).

However, the main drawback of chitosan-based delivery systems is their low transfection efficiency at physiological conditions. The low transfection efficiency of chitosan-based delivery systems is primarily attributed to the poor water solubility at physiological pH (Chen et al., 2008a) and the inability to release DNA after endosomal escape due to strong interaction between chitosan and DNA (Lu et al., 2009). Several modifications of chitosan side chains using hydrophilic, (Park et al., 2000; Germershaus et al., 2008) hydrophobic, (Hu et al., 2006; Jayakumar et al., 2010; Liu et al., 2003; Sajomsang et al., 2009) and both hydrophilic-hydrophobic moieties (Wang et al., 2011) have been reported to enhance the transfection efficiency of chitosan. Modification with hydrophilic units improves the water solubility and increases the plasma circulation time of the polyplexes. Hydrophobic modification of chitosan

alters polyplex interaction with the cell membrane, facilitates intracellular DNA dissociation, and improves water solubility (Kim et al., 2007).

The expression of transferred gene occurs only after the DNA is transported into the nucleus of a target cell. Therefore, the vectors for gene delivery must be able to overcome a number of extracellular and intracellular barriers. These include various endonucleases present in the extracellular space that can degrade the pDNA within 30 min (Kawabata et al., 1995). Another major barrier is the inability of the pDNA to cross the biological membrane due to the repulsion between the DNA and the negatively charged cell surface. Even after crossing the cell membrane, the DNA has to escape lysosomal degradation and translocate into the nucleus (Wiethoff and Middaugh, 2003). Hence, the balance between DNA protection and intracellular DNA release significantly influence transfection efficiency of chitosan-based gene delivery systems by modulating the degree of interaction between polymeric vectors and their DNA cargo (Chen et al., 2008a; Koping-Hoggard et al., 2004). However, there are no systematic studies on hydrophobic modification of chitosan to describe the optimum chain length of hydrophobic moieties to maintain the proper amphiphilicity of the polymer for improving membrane permeability of the polyplexes.

In the present report, a series of fatty acids with increasing chain length (C6-C10) were utilized to synthesize N-acyl chitosan polymers. The influence of fatty acid chain length was investigated by assessing the water solubility, particle size, zeta potential, pDNA binding affinity, pDNA release, cellular uptake, in vitro biocompatibility and transfection efficiencies.

2.2. Materials and methods

2.2.1. Materials

Chitosan (Mw ~ 50 kDa, 91% deacetylated), 3-(4,5-dimethylthiazol-2-yl)-2,5-diphenyltetrazolium bromide (MTT), and agarose were purchased from Sigma-Aldrich (St. Louis, MO, USA). Decanoic, octanoic, and hexanoic acid were procured from MP Biomedicals (Solon, OH, USA). 1-ethyl-3-(3-dimethylaminopropyl) carbodiimide hydrochloride (EDC.HCl) was obtained from Creosalus Inc (Louisville, KY, USA). DNase I was purchased from Rockland Inc (Gilbertsville, PA, USA). Hoechst 33342 dye was purchased from Anaspec (Fremont, CA, USA). pGFP and pβ-gal were purchased from Aldevron LLC (Fargo, ND, USA). Human embryonic kidney (HEK 293) cells, Eagle's minimal essential medium (EMEM), and phosphate buffered saline (PBS) were purchased from American Type Culture Collection (ATCC, Rockville, MD, USA). FuGENE HD was obtained from Roche Diagnostics (Indianapolis, IN, USA). Beta-galactosidase enzyme assay kit with reporter lysis buffer and agarose were supplied by Promega (Madison, WI, USA). All other reagents were analytical grade and used without further modification.

2.2.2. Synthesis of N-acyl chitosan

The N-acyl derivatives of chitosan (NACs) were synthesized by coupling the carboxyl group of fatty acids with amine group of chitosan in the presence of EDC (Hu et al., 2006) (Figure 5). Briefly, chitosan (1 g) was dissolved in 100 mL distilled water. Fatty acids (the charged fatty acid ratio was 20% of D-glucosamine units in chitosan) and EDC (5 mol per mol of fatty acid) were dissolved in ethanol. The chitosan solution was heated to 90°C and the fatty acid solution containing EDC was added drop wise to the chitosan solution under vigorous stirring. The reaction continued at 90°C for 12 h. After that, the reaction mixture was dialyzed using

SnakeSkinR Pleated Dialysis tubing (MWCO: 3.5 kDa, Thermo Scientific, IL, USA) against distilled water for 48 h with successive exchange of distilled water to remove the water-soluble by-products. The dialyzed suspension was then dried in a freeze dryer and washed several times with ethanol to remove the unreacted fatty acid. Finally, the precipitate was lyophilized to get the NAC polymers. The overall yield of the reaction was 88, 85 and 83% for decanoic (NAC-10), octanoic (NAC-8), and hexanoic acid (NAC-6) derivative of chitosan, respectively.

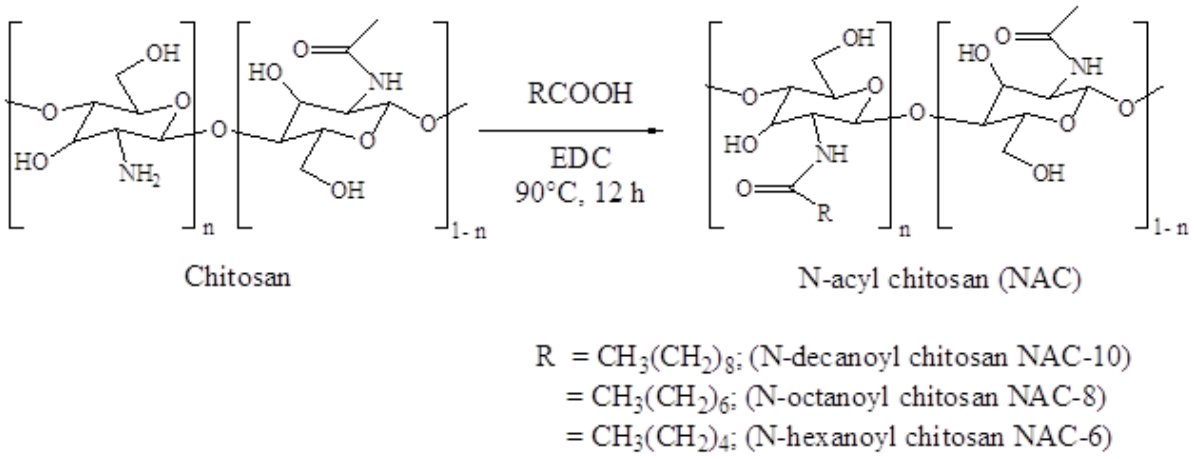

Figure 5. Schematic representation for the synthesis of N-acyl chitosan derivatives.

2.2.3. Structural characterization of N-acyl chitosan

The coupling of fatty acid on chitosan backbone was confirmed by ^{1}H NMR and FTIR spectroscopy. For ^{1}H NMR experiments, chitosan and NAC polymers were dissolved in deuterium oxide (D_2O) with 1% deuterated hydrochloric acid (DCl) and D_2O, respectively. ^{1}H NMR spectra were measured using a Mercury Varian 400 MHz spectrometer at 25°C. FTIR analyses were made using a Thermo Nicolet Nexus 470 FTIR spectrometer equipped with a N_2 purged chamber. All samples were ground with KBr powder and compressed to form pellets for the study. The degree of substitution of the polymers was determined from the elemental analysis data.

2.2.4. Determination of water solubility

The water solubility of chitosan and NAC polymers was assayed by the turbidity measurements method as a function of pH (Toh et al., 2011). Briefly, chitosan or NAC polymers were dissolved in 0.25% (v/v) acetic acid solution (2 mg/mL). The pH of the solution was adjusted by the addition of 1 N NaOH solution, and then transmittance of the solution was measured at 600 nm using a SpectraMax M5 microplate reader (Molecular Devices, CA, USA).

2.2.5. Endosomal buffering capacity

The buffer capacity of chitosan and synthesized polymers was determined by acid-base titration assay (Benns et al., 2002). Briefly, 20 mg of each sample was dissolved in 20 mL of 150 mM NaCl solution. The pH of each solution was adjusted to 10 by the addition of 0.1 N NaOH solutions. The titration was performed by stepwise addition of 20 µL of 0.1 N HCl followed by pH measurements at 25°C using a pH meter.

2.2.6. Polymer/pDNA polyplexes preparation and characterization

Chitosan and NAC polymers were dissolved into 20 mM sodium acetate buffer (pH 6.5) at different concentrations. The polymer/pDNA polyplexes of various N/P ratios (ratio of free amino groups on polymer to phosphate groups in pDNA) were prepared by drop wise addition of appropriate volume of polymeric solution into the pDNA solution (0.2 mg/mL in 20 mM sodium acetate buffer), while vortexing at high speed for 30 s. The mixture was incubated at room temperature for 30 min to achieve a stable polyplex. The average hydrodynamic diameter and zeta potential of the polyplexes were determined by DLS method using a Zetasizer Nano ZS 90 (Malvern Instruments, Malvern, UK) at 25°C. The size and zeta potential of each polyplex were measured six times. The morphology of the polyplexes was observed by DI-3100 atomic force microscope (AFM, Veeco, MN, USA) using the tapping mode. For AFM study, polyplexes were

diluted with distilled water and a small drop of the samples was placed onto a freshly cleaved mica plate, followed by air drying.

Association efficiency of pDNA was determined by centrifuging NAC/pDNA polyplexes at 30,000 × g, at 4°C for 30 min. The amount of unbound pDNA in the supernatant was measured with a SpectraMax M5 microplate reader using Hoechst dye 33342. The excitation and emission wavelengths were fixed at 350 and 450 nm, respectively. The association efficiency of different polyplexes was calculated by the following equation.

Association efficiency (%) = $(DNA_{total} - DNA_{free})/DNA_{total} \times 100$

2.2.7. Agarose gel retardation assay

The pDNA condensing capability of the polyplexes was further examined by agarose gel retardation assay at different N/P ratios. Polymer/pDNA polyplexes (containing 1 µg of pDNA) at different N/P ratios were electrophoresed on 0.8% w/v agarose gel containing 0.5 µg/mL ethidium bromide (EtBr) at 80 V for 80 min. The 0.5× Tris-acetate-ethylenediaminetetraacetic acid (TAE, Bio-Rad, CA, USA) buffer was used as a running buffer. DNA bands were visualized and photographed by a UV transilluminator (Alpha Innotech, CA, USA) at a wavelength of 254 nm.

2.2.8. Isothermal titration calorimetry (ITC) analysis

ITC was employed to determine the binding constant, enthalpy of complex formation, and the stoichiometry of binding of pDNA with chitosan based cationic polymers. Binding studies were performed using a low volume nano ITC (TA instruments, USA) with a cell volume of 190 µL at 25°C. Polymer and pDNA solution were prepared in 20 mM sodium acetate buffer at pH 6.5. Samples were degassed for 10 min prior to use. The sample cell was filled with the pDNA solution (50 µg/mL, ~ 0.1515 mM phosphate or nucleotide units) and the reference cell

with buffer solution only. The polymer solution (150 µg/mL, ~ 0.7688 mM of free amino groups) was introduced into the thermostated cell by means of a syringe which was also stirred at 250 rpm. Each titration consisted of 25 subsequent 2 µL injections each of which were 20 s in duration and were programmed to occur at 400 s intervals.

2.2.9. Protection of pDNA against nucleases

The ability of polyplexes to protect pDNA from nuclease degradation was examined by DNase I protection assay. Naked pDNA or NAC/pDNA polyplexes (20 µL equivalent to 2 µg of pDNA) were incubated with 1 unit of DNase I for 30 min at 37°C. The DNase reaction was stopped by 5 µL of 100 mM EDTA solution. Twenty microliters of heparin (5 mg/mL) was added and incubated for 2 h at room temperature to dissociate the complex. The integrity of released pDNA was evaluated by agarose gel electrophoresis as described under section 2.2.7.

2.2.10. EtBr exclusion assay

Different amount of chitosan or NAC polymers were complexed with 2 µg (20 µL of 0.1 mg/mL solution) of pDNA to obtain polyplexes of desired N/P ratios and incubated at room temperature for 30 min. The final volume of the polyplexes was adjusted to 1 mL with PBS (pH 7.4). Subsequently 0.5 µg ethidium bromide (10 µL of 0.05 mg/mL) was added and staining was completed at room temperature for 5 min. Fluorescence intensity was measured with SpectraMax M5 plate reader with the excitation wavelength at 260 nm and emission wavelength at 600 nm. Results were represented as relative fluorescence intensity where 0 suggested the existence of EtBr alone and 100% represented the fluorescence of EtBr combined with pDNA.

2.2.11. In vitro release of pDNA

A volume of 3 mL of polyplexes (containing 100 µg of pDNA) was dispersed in 30 mL of PBS (pH 7.4) and incubated at 37°C in a shaking incubator at 100 rpm. After 0, 1, 2, 4, 6, 10,

20, 30, and 48 h of incubation, 1 mL of sample was withdrawn and replaced with an equal volume of fresh buffer. The complex suspension was centrifuged at 30,000 g, at 4°C for 30 min, and the amount of free pDNA in the supernatant was quantified by spectrofluorimetry using Hoechst dye 33342. The percent of cumulative release of pDNA was calculated.

2.2.12. In vitro cytotoxicity

The cytotoxicity of polymers as well as NAC/pDNA polyplexes was evaluated by MTT assay (Lu et al., 2009). HEK 293 cells were seeded in a 96-well plate at a density of 5000 per well in 150 µL of EMEM supplemented with 10% of fetal bovine serum (FBS), and incubated at 37°C under 5% CO_2 atmosphere. The cytotoxicity of polymers was examined by determining the viability after 48 h of incubation with various concentrations of polymers (100-2000 µg/mL). Similarly, the cytotoxicity of polyplexes was evaluated at various N/P ratios (5, 10, and 20). Non treated cells were considered as control and incubated in similar conditions for same period of time. The relative cell viability was calculated by the following equation:

$$\text{Cell viability (\%)} = (OD_{sample}/OD_{control}) \times 100$$

2.2.13. Cellular uptake study

To perform the cellular uptake study the pDNA was covalently labeled with fluorescein isothiocyanate (FITC), and was allowed to form polyplexes with chitosan and NAC polymers. HEK 293 cells were seeded at a density of 5×10^4 cells per well in a 48-well plate in EMEM medium containing 10% FBS and incubated for 24 h to achieve ~ 60-70% confluency. Polyplexes containing 1 µg of pDNA were added to each well and incubated at 37°C for 4 h. The uptake process was terminated by removing the media containing pDNA/polymer polyplexes and washed with PBS. The percentages of FITC-positive cells were determined by fluorescence

activated cell sorting (FACS) analysis of the cells using a flowcytometer (Accuri Cytometer Inc., MI, USA).

2.2.14. In vitro gene transfection

Transfection assay was performed in HEK 293 cells using two different plasmids encoding for green fluorescence protein (pGFP) and β-galactosidase (pβgal) to evaluate gene transfection efficiency at the cellular and protein level, respectively. Cells were seeded at a density of 5×10^4 cells per well in a 48-well plate in EMEM medium containing 10% FBS and incubated for 24 h to achieve ~ 60-70% confluency. The culture medium was replaced with 300 µL of FBS free or 10% FBS containing EMEM medium before transfection. Polyplexes containing 1 µg of pDNA were added to each well and incubated at 37°C. After 6 h of incubation transfecting medium was replaced with 300 µL of complete growth medium and further incubated for 48 h. Non-treated cells and cells transfected with naked pDNA were used as negative control and passive control, respectively. Transfection using FuGENE HD was used as positive control and was carried out according to the manufacturer's protocol with FBS free or 10% FBS containing medium. The percentages of GFP positive cells were determined by FACS analysis of the transfected cells using a flowcytometer. The images of GFP transfected cells were taken with a FV300 confocal laser scanning microscope (Olympus, NY, USA). All transfection experiments were performed as replicates of four.

For the β-galactosidase expression, cells were washed twice with PBS (pH 7.4), and lysed using reporter lysis buffer. The β-galactosidase activity was quantified using β-galactosidase assay reagent. The total protein content of the cell lysate was analyzed using a bicinchoninic acid (BCA) assay kit. The β-galactosidase activity was expressed as milliunit of β-galactosidase/mg of the total protein.

2.2.15. Statistical analysis

Data are expressed as means ± standard deviation (SD). Statistical analyses were performed using two tailed Student's t-test and analysis of variance (ANOVA).

2.3. Results and discussion

2.3.1. Synthesis of N-acyl chitosan

The chitosan of 50 kDa molecular weight was chosen based on our preliminary studies with a series of chitosan with different molecular weight ranging from 5 to 100 kDa (maximum transfection was observed with 50 kDa chitosan, data is not shown). The coupling between chitosan and fatty acid was performed by EDC mediated reaction. The excess EDC and water soluble by-products were removed by dialysis with water, and the remaining fatty acid was removed by ethanol washing.

2.3.2. Structural characterization of N-acyl chitosan

The coupling of fatty acid on chitosan backbone was confirmed by ^{1}H NMR and FTIR spectroscopy. The ^{1}H NMR spectra of chitosan and NAC polymers are depicted in Figure 6. For chitosan, peak at 1.9 ppm revealed the three N-acetyl protons of N-acetyl glucosamine and peak at 3 ppm showed the H2 proton of N-acetyl glucosamine or glucosamine residue. The ring protons (H-3, 4, 5, 6, 6') of chitosan are considered to resonate at 3.4-3.8 ppm. The new proton peaks at 0.8 and 1.25 ppm were assigned to $–CH_3$ and $–CH_2$ of the fatty acyl residue, respectively.

FTIR spectra were also employed to confirm the coupling of fatty acid on chitosan by observing amide bond formation (Figure 7). The very weak peak at 1655 cm^{-1} for chitosan represented the carbonyl stretching of secondary amide (amide I band). The peak at 1570 cm^{-1} was ascribed to the N-H bending vibration of nonacylated α-aminoglucose primary amines (Tien

et al., 2003). After N-acyl formation, the peak at 1570 cm^{-1} almost disappeared, while very prominent peaks at 1655 and 1555 cm^{-1} were observed. The peak at 1555 cm^{-1} can be assigned to the N-H bending vibrations of the amide II band (Tien et al., 2003). The absorption peaks at 2850–2950 cm^{-1} were due to the $–CH_2$ groups, and their intensity was proportional to the acyl chain length. Hence, the FTIR results confirmed the successful synthesis of NAC polymers. The degree of fatty acid substitution was ~ 10% for all the three polymers.

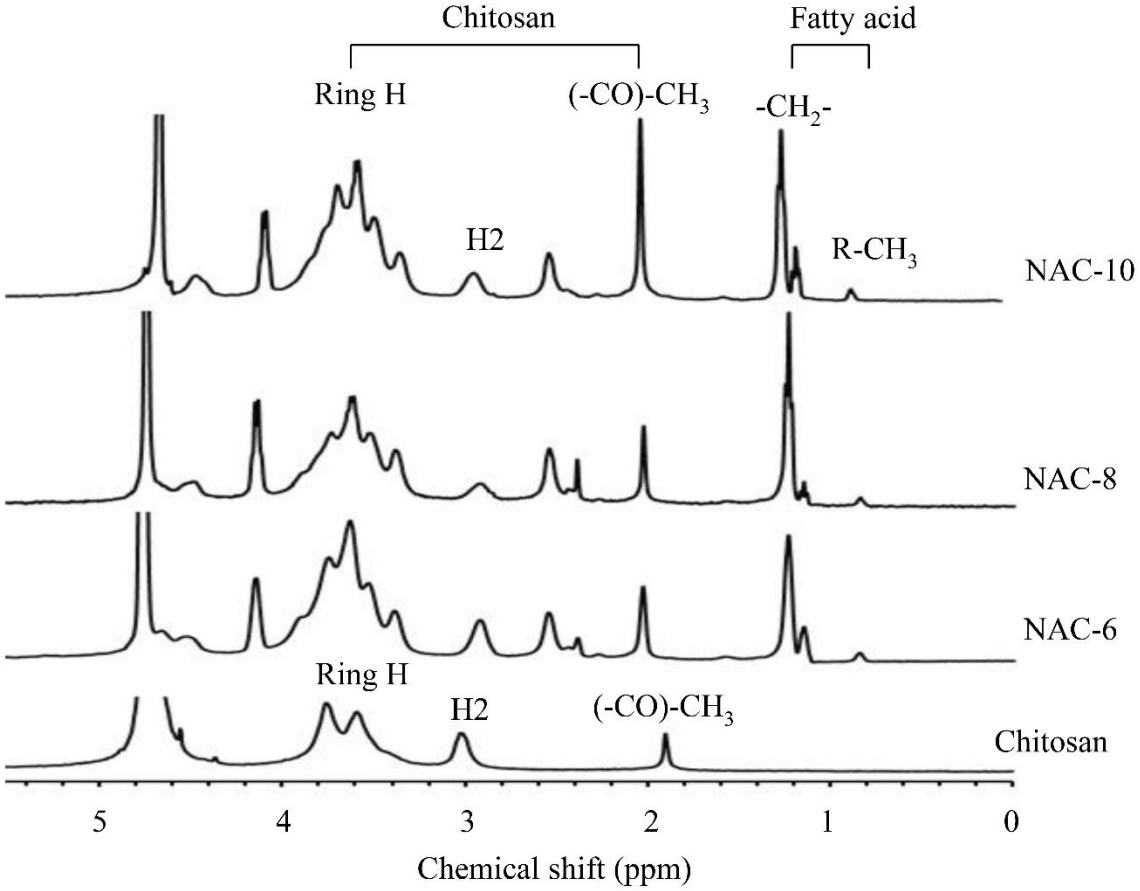

Figure 6. ^1H NMR spectra of chitosan and different NAC polymers.

2.3.3. Determination of water solubility

The water solubility of chitosan and NAC polymers were studied by measuring the transmittance at 600 nm. The cloud point pH of the polymers has been defined by Mao et al. as

the pH at which the transmittance was higher than 98% at 600 nm (Mao et al., 2004). The cloud point pH values of chitosan, NAC-6, NAC-8, and NAC-10 were 6.5, 7.54, 7.52, and 7.54, respectively. Thus, all of the NAC polymers exhibited improved water solubility at neutral pH when compared to the parent chitosan. The improved water solubility of NAC polymers is due to the disruption of H-bonded complex crystal structure of parent chitosan by the introduction of short chain hydrophobic moiety to the chitosan backbone (Pillai et al., 2009).

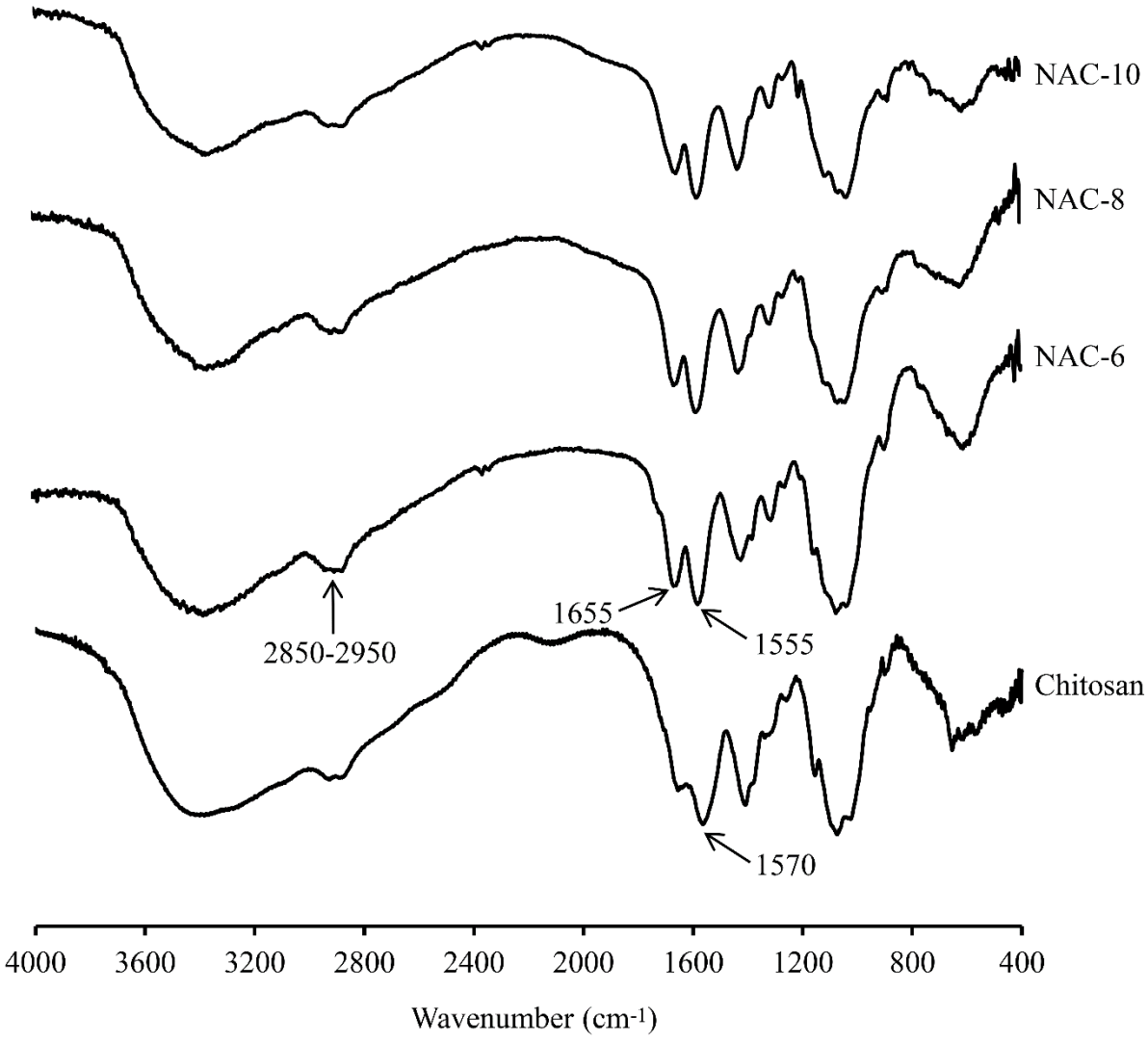

Figure 7. FTIR spectra of chitosan and different NAC polymers.

2.3.4. Endosomal buffering capacity

The buffer capacity of NAC polymers was determined by acid-base titration assay as described in previous reports (Benns et al., 2002; Lu et al., 2009). According to the proton sponge mechanism, polymers having a buffering capacity between pH 5 and 7 are hypothesized to mediate facilitated endo-lysosomal escape of their cargo due to rupture of the endocytic vesicle caused by an increased osmotic pressure (Godbey et al., 1999). As shown in Figure 8, NAC polymers exhibited very good buffer capacity in the range of pH 5 to 7.

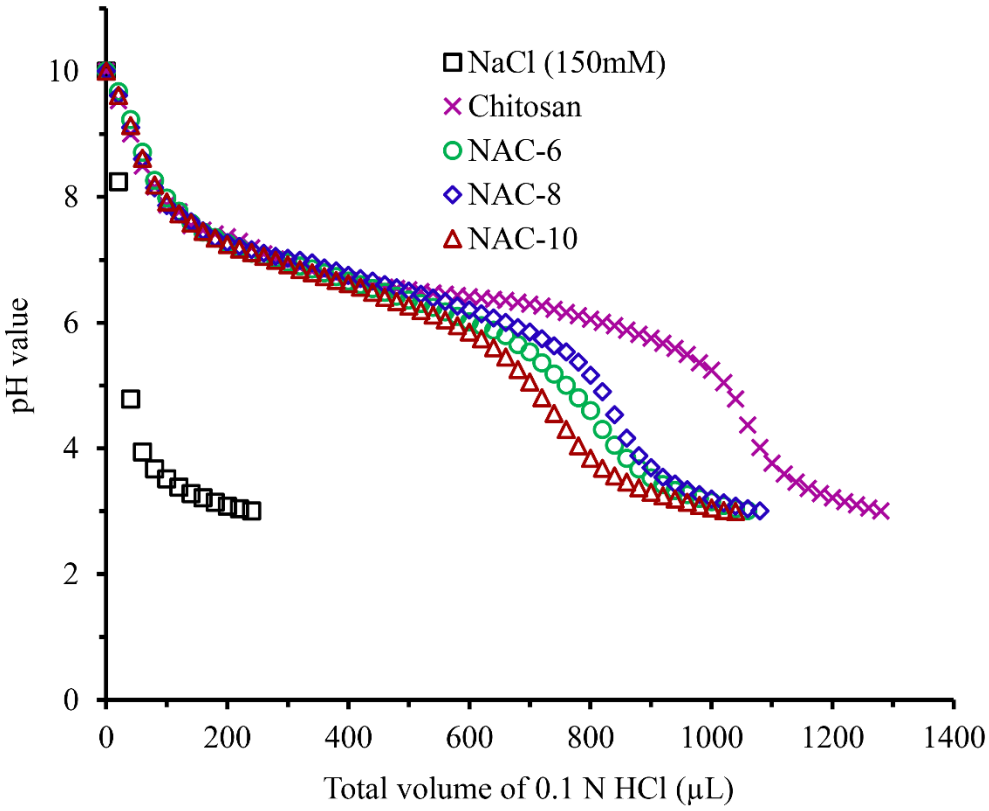

Figure 8. Endosomal buffering capacity of chitosan and different NAC polymers.

2.3.5. Characterization of polymer/pDNA polyplexes

The polymer/pDNA poyplexes were prepared in 20 mM sodium acetate buffer at pH 6.5. Due to the positive charge, these polymers effectively condensed pDNA through electrostatic

interaction to form nanoscale polyplexes. The average hydrodynamic diameter and zeta potential of polyplexes at different N/P ratios are summarized in Table 1.

Table 1. Particle sizes, zeta potentials, and association efficiencies of NAC/pDNA polyplexes in 20 mM sodium acetate buffer at pH 6.5. Data represents the mean ± SD (n = 6).

Polyplexes	N/P ratio	Particle size (nm)	PDI[a]	Zeta potential (mV)	Association efficiency (%)[b]
NAC-6/pDNA	5	308.9 ± 7.7	0.21 ± 0.02	14.3 ± 0.6	96.5±2.5
	10	248.4 ± 10.6	0.13 ± 0.03	18.2 ± 0.7	
	20	220.1 ± 1.6	0.11 ± 0.04	20.3 ± 0.8	
NAC-8/pDNA	5	339.7 ± 5.0	0.22 ± 0.02	14.8 ± 0.7	
	10	268.1 ± 7.4	0.13 ± 0.01	16.4 ± 0.9	97.8±3.5
	20	244.9 ± 4.4	0.12 ± 0.02	20.4 ± 0.5	
NAC-10/pDNA	5	342.1 ± 13.5	0.22 ± 0.05	13.3 ± 0.6	
	10	271.1 ± 5.0	0.13 ± 0.03	15.8 ± 0.4	96.2±3.1
	20	246.4 ± 5.6	0.11 ± 0.01	19.9 ± 0.9	

[a]PDI: particle dispersity index; [b]Association efficiency measured at N/P ratio of 20.

The average size of the polyplexes was in the range of 220-342 nm with a polydispersity index of 0.11-0.22. The polyplexes diameters were found to decrease with an increase in N/P ratio from 5 to 20, which was due to better condensation of pDNA by the protonated amine groups of the polymers. The polyplexes maintained a net positive charge at pH 6.5 between N/P ratios of 5 to 20. The zeta potential of the polyplexes was directly proportional to their N/P ratio. The surface morphology of the polyplexes was visualized by AFM and the polyplexes observed

were nearly spherical in shape (Figure 9). The association efficiency of the polyplexes was ~ 97% at N/P ratio of 20 (Table 1).

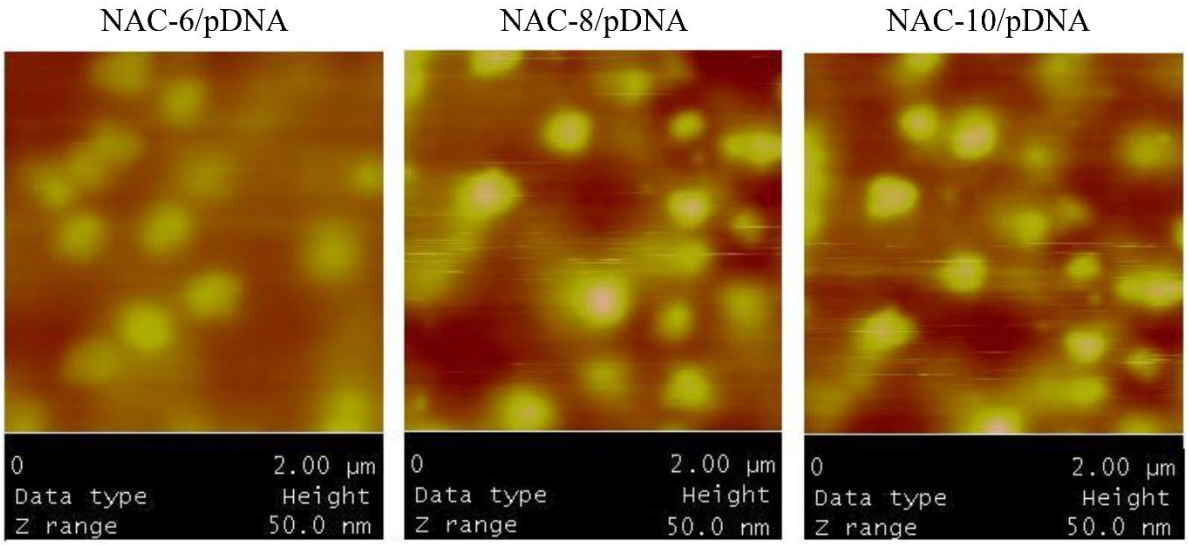

Figure 9. Morphological analysis of NAC/pDNA polyplexes using AFM at N/P ratio of 20.

2.3.6. Agarose gel retardation assay

Neutralization of negative charges on the phosphate backbone of pDNA by the positively charged polymeric nano-complexes resulted in the retardation of mobility of pDNA under the influence of an electric field. Figure 10 shows pDNA binding capacity of polyplexes at different N/P ratios. The movement of naked pDNA towards the anode was observed in the case of naked pDNA (ND). We observed only a slight retardation of mobility of pDNA at N/P ratios of 0.5 and 1. However, the complete retardation of the pDNA was observed at N/P ratios of ≥ 5, indicating the tight complexation between polymeric nanocomplexes and pDNA.

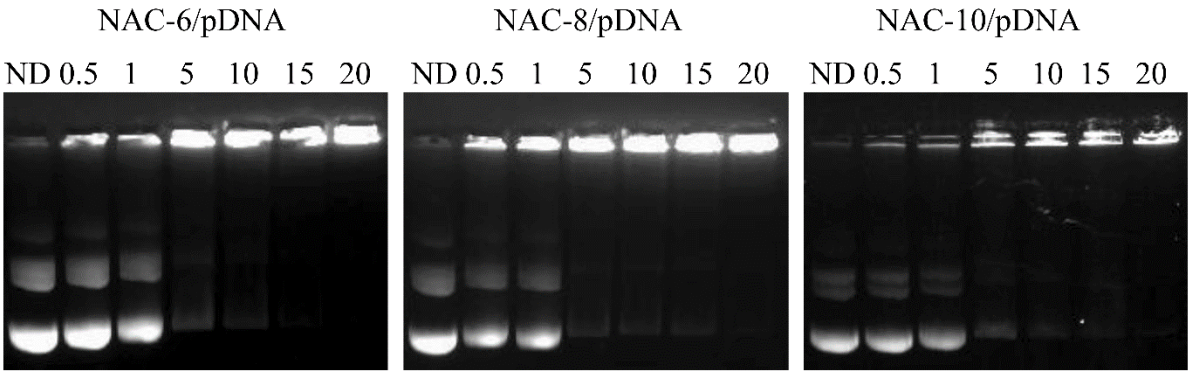

Figure 10. Agarose gel retardation assay of NAC/pDNA polyplexes at different N/P ratios.

2.3.7. ITC study

ITC was used to investigate the pDNA binding capacity of chitosan and NAC polymers. The heat change (ΔQ) per injection was represented as a function of the corresponding N/P ratio. The integrated heats of the binding of pDNA with NAC-6 polymer in 20 mM sodium acetate buffer at pH 6.5 are shown in (Figure 11). Each injection of NAC-6 polymer into the pDNA solution produced a sharp negative peak indicating an endothermic interaction. As the NAC-6 content in the cell increased, the amount of heat changes decreased indicating gradual neutralization of pDNA. The heat of dilution from titrations of polymer solution into buffer alone was subtracted to get net binding heat changes. The isotherms were fitted to an independent model using Nanoanalyze software. The thermodynamic parameters such as the pDNA binding constant, enthalpy of complex formation, and the stoichiometry of binding of pDNA with chitosan based cationic polymers are presented in Table 2. The binding affinity of NAC polymers (21.1 to 22.9) × 10^5 M^{-1} was significantly lower than the chitosan (28.8 × 10^5 M^{-1}), but it did not change significantly among the different NAC polymers with similar degrees of substitution suggesting that the fatty acid chain length had no effect on binding affinity of the polymers.

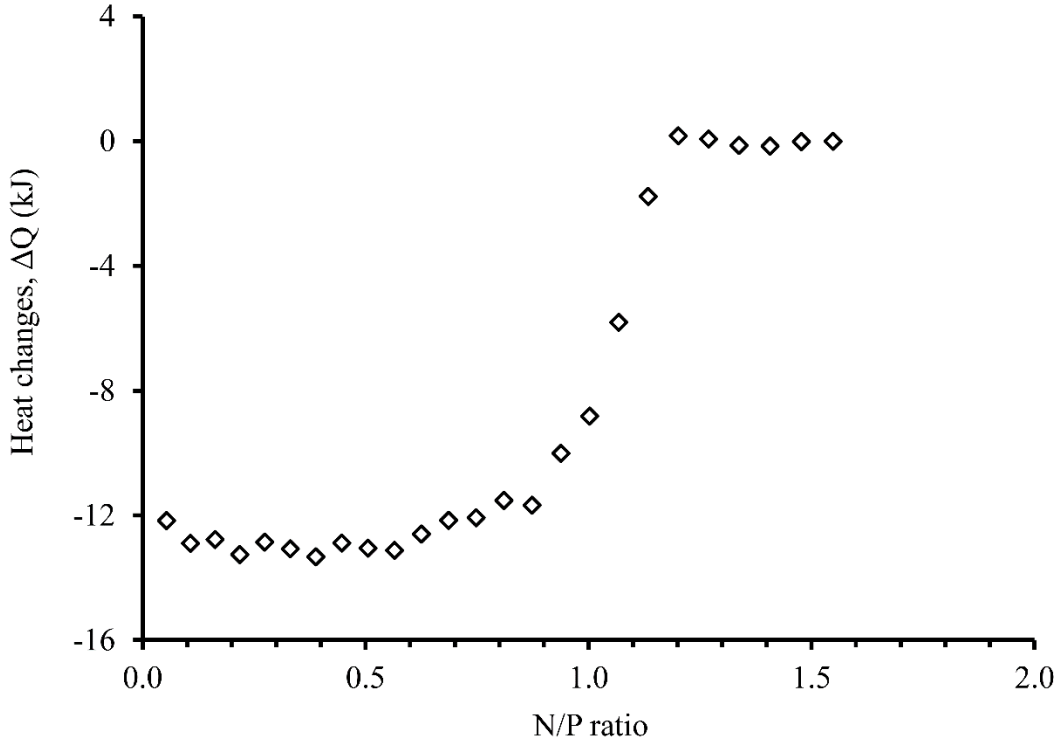

Figure 11. Integrated heats of interaction of the titration of NAC-6 into pDNA vs N/P ratios.

Table 2. Thermodynamic parameters of the binding interaction between NAC-6 polymer and pDNA in 20 mM sodium acetate buffer at pH 6.5. Data represents the mean ± SD (n = 3).

Polymer	$K \times 10^5 (M^{-1})$	n (mol)	ΔH (kJ mol^{-1})
Chitosan	28.79 ± 1.18	1.01 ± 0.02	-15.88 ± 0.52
NAC-6	21.31 ± 0.78	1.38 ± 0.02	-13.20 ± 0.25
NAC-8	22.90 ± 0.85	1.44 ± 0.03	-13.45± 0.60
NAC-10	21.15 ± 1.20	1.39 ± 0.05	-13.02 ± 0.45

2.3.8. Protection of pDNA against nucleases

The integrity of pDNA is essential for efficient gene delivery in vitro as well as in vivo, and therefore the gene delivery system should effectively protect condensed pDNA from

nuclease degradation (Katayose and Kataoka, 1998). The protective effect of polyplexes against nuclease degradation was evaluated using DNase I as a model enzyme (Figure 12). It turned out that the naked DNA was completely digested as indicated by the absence of band for DNA. All three NAC polymers exhibited distinct protective activity against DNase I at all N/P ratios tested. These results clearly indicated that NAC polymers can be used as efficient vector for transporting pDNA into the cytoplasm of cell without degradation.

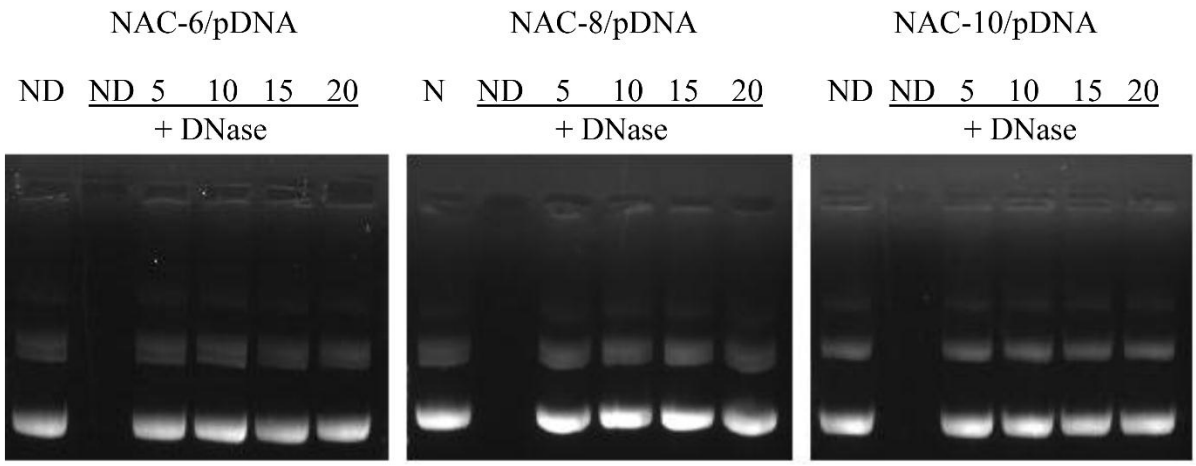

Figure 12. DNase I protection assay of NAC/pDNA polyplexes prepared at different N/P ratios.

2.3.9. EtBr exclusion assay

The binding affinity between NAC polymers and pDNA was evaluated by EtBr exclusion in PBS (pH 7.4) to correlate the pH environments in the cytoplasm and nuclei (Wang et al., 2011). It was found that the EtBr fluorescence intensity decreased with higher N/P ratio (Figure 13). At N/P ratio 20, fluorescence quenching percentages of chitosan/pDNA, NAC-6/pDNA, NAC-8/pDNA, and NAC-10/pDNA polyplexes were 90.3%, 80.2%, 79.3%, and 78.6%, respectively.

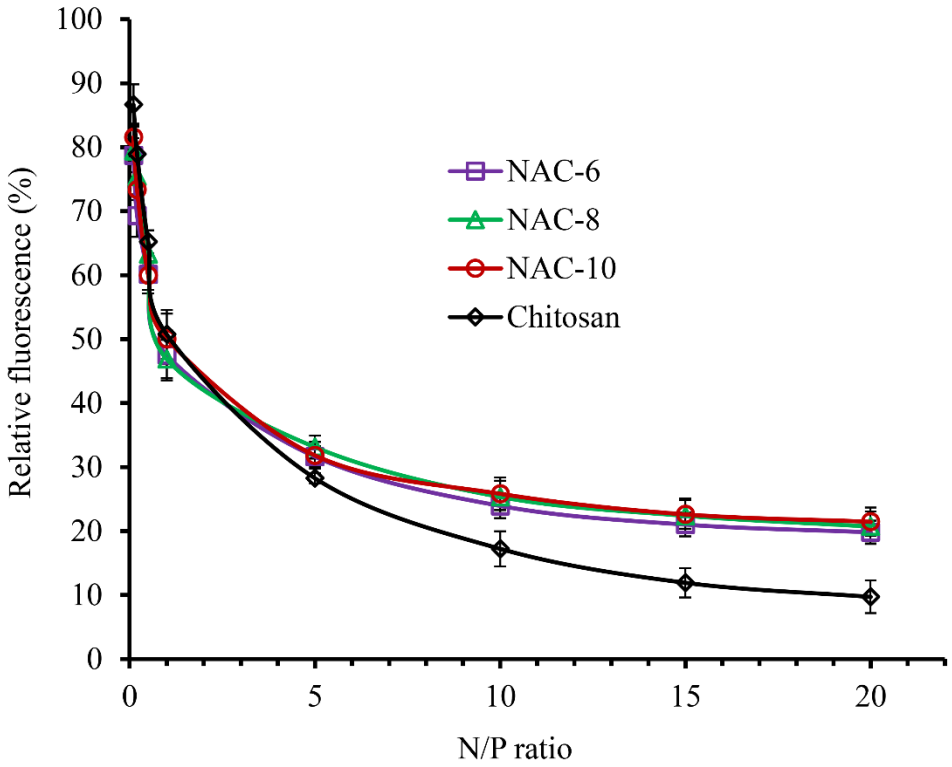

Figure 13. pDNA binding affinity of NAC polymers in PBS (pH 7.4) monitored by EtBr exclusion assay. Results are represented as relative fluorescence intensity where 0% suggests the existence of EtBr alone and 100% represents the fluorescence of EtBr combined with pDNA. Data represents the mean ± SD (n = 4).

2.3.10. In vitro release of pDNA

Figure 14 revealed the in vitro release profile of pDNA from the polyplexes prepared at N/P ratio of 20 for NAC polymers and at N/P ratio of 5 for chitosan. These N/P ratios were selected based on their transfection efficiency. For chitosan maximum transfection efficiency was achieved at N/P ratio of 5 while NAC polymers showed maximum transfection at N/P ratio of 20. The release of pDNA was slow over the period of 48 h. The cumulative release of pDNA prepared with chitosan was less than 10% at 48 h. However, there was a relatively rapid release of pDNA prepared with NAC with the cumulative release of ~ 20%, but no significant differences ($p > 0.05$) existed among the three different polyplexes. Fatty acid substitutions of chitosan facilitate the pDNA dissociation due the substitution of a fraction of free amino groups

as well as hydrophobicity-induced weakening of the electrostatic interaction between the polymer and pDNA (Wang et al., 2011).

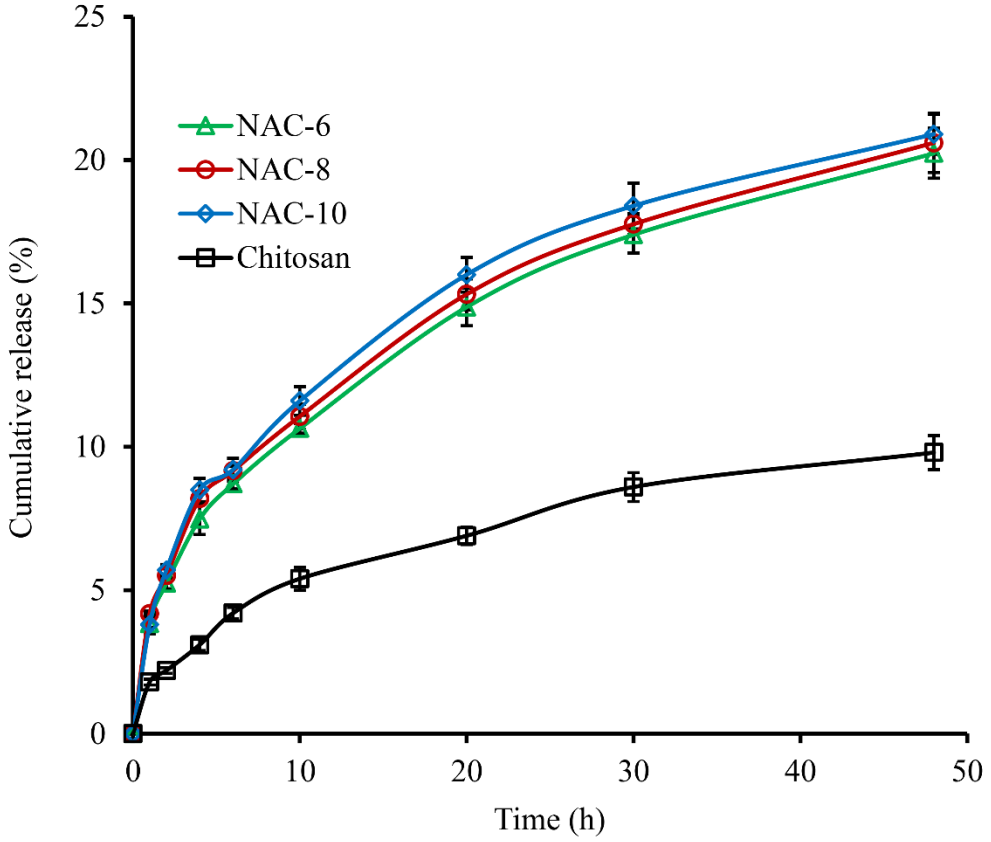

Figure 14. Cumulative pDNA release profiles of different polyplexes. NAC-6/pDNA, NAC-8/pDNA, and NAC-10/pDNA polyplexes were prepared at N/P ratio of 20 and chitosan/pDNA polyplexes was prepared at N/P ratio of 5. Polyplexes were incubated in PBS (pH 7.4) at 37°C. Data represents the mean ± SD (n = 4).

2.3.11. In vitro cytotoxicity

One important criterion of gene delivery vectors is low cytotoxicity. It has been reported that cationic agents may cause severe cytotoxicity due to interactions with cell membrane and other negatively charged cellular components or proteins (Choksakulnimitr et al., 1995; Fischer et al., 2003). It has been established that chitosan and its derivatives are less cytotoxic than other cationic polymers such as poly-lysine and polyethyleneimine. Nevertheless, their toxicity depends on the type of chitosan derivative as well as the type of cells studied (Fischer et al.,

2003; Thanou et al., 2002). In this study we used MTT assay to evaluate the toxicity of different polymers and polymer/pDNA polyplexes in HEK 293 cells. As depicted in Figure 15A, NAC polymers did not exhibit significant ($p > 0.05$) change in cell viability at the tested concentrations. Similarly, polyplexes at different N/P ratios did not alter the cell viability (Figure 15B) in comparison to the control (taken as 100% viability).

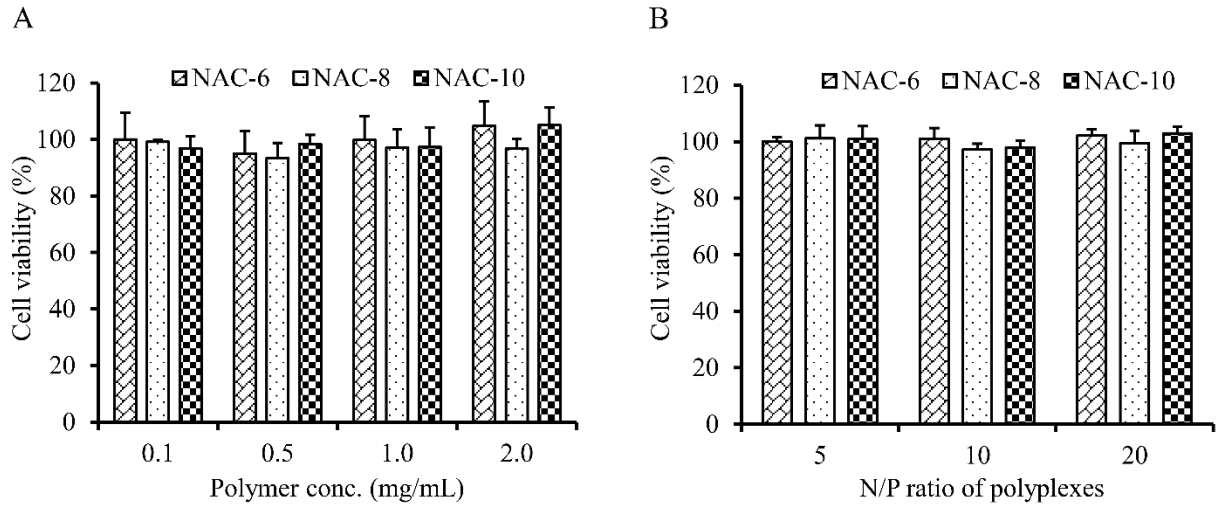

Figure 15. Cytotoxicity of (A) NAC polymers and (B) NAC/pDNA polyplexes on HEK 293 cells. Data represents the mean ± SD (n = 4).

Therefore, MTT assay results confirmed an excellent in vitro biocompatibility of the polymers as well as polyplexes, which is critical for the development of successful nonviral gene delivery systems.

2.3.12. Cellular uptake study

For chitosan/pDNA polyplexes only 15% of cells were FITC-positive while cellular uptake of different NAC/pDNA polyplexes was elevated by 5-7-fold. Since NAC polymers consist of both cationic amino groups and hydrophobic fatty acyl moieties, both charge attraction and hydrophobic interactions play an important role in the cellular uptake process by endocytosis (Piest, and Engbersen, 2010). NAC-6 polyplex exhibited highest degree of cellular uptake with

90% of cells being FITC-positive. The cellular uptake of NAC/pDNA polyplex was increased as the chain length of fatty acid substituent decreased. The uptake percentages of NAC-8/pDNA and NAC-10/pDNA polyplexes were 72% and 70%, respectively.

2.3.13. In vitro gene transfection

The transfection efficiency of polyplexes was studied in HEK 293 cells in the absence and presence of 10% FBS. To determine the transfection efficiency at cellular level, we performed FACS analysis of GFP transfected cells. The NAC-6/pGFP polyplexes exhibited about 10-fold (81.5% GFP positive cells in absence of FBS and 80.5% GFP positive cells in the presence of 10% FBS) higher transfection efficiency in comparison to chitosan/pGFP polyplexes (Figure 16A).

The transfection efficiency at protein level was evaluated by quantifying β-galactosidase activity. The amount of β-galactosidase activity was expressed in terms of milliunit of β-galactosidase/mg of the total protein. As shown in Figure 16B, NAC polymers induced a 15-25-fold elevation in the transfection efficiency as compared to chitosan in the absence and presence of 10% FBS. The transfection efficiency of the polymer increased with decreasing chain length of fatty acids and NAC-6/pβ-gal polyplex showed maximum transfection. The NAC-6/pβ-gal polyplex induced a significantly ($p < 0.001$) higher transfection in comparison to NAC-8/pβ-gal and NAC-10/pβ-gal polyplexes.

The results of the quantitative assessments were well accorded with the confocal microscope observation as depicted in Figure 17.

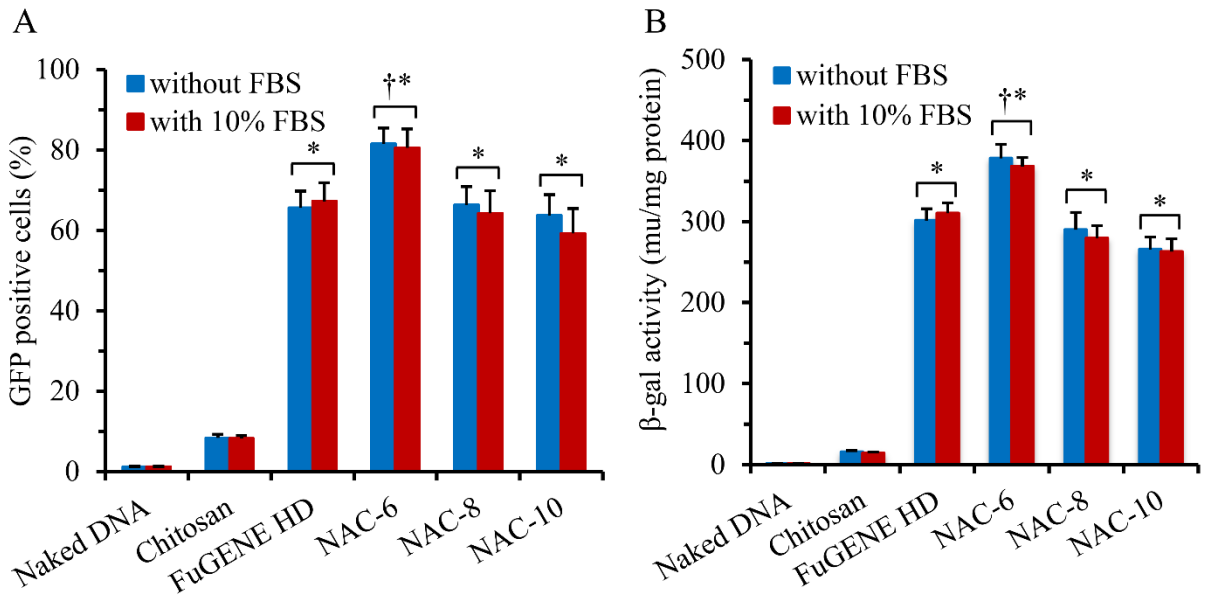

Figure 16. In vitro gene transfection efficiency of chitosan and NAC polyplexes in HEK 293 cells at N/P ratio of 5 and 20, respectively. (A) Transfection efficiency at cellular level using pGFP. (B) Transfection efficiency at protein level using pβGal. Data represents the mean ± SD (n = 4). ['*' indicates significant ($p < 0.001$) different from chitosan and '†' indicates significant ($p < 0.001$) different from FuGENE HD].

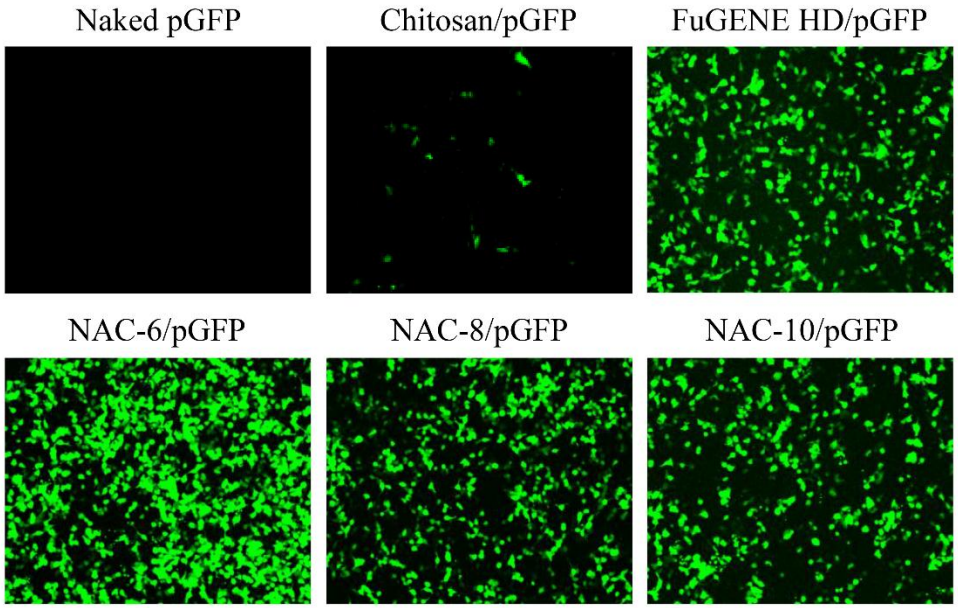

Figure 17. Confocal images of pGFP transfected HEK 293 cells (in serum free medium). Images were taken at 10× magnification after 48 h of transfection.

2.4. Conclusions

A series of N-acyl chitosan polymers were synthesized to obtain an optimum chain length of fatty acid for gene delivery application. The NAC/pDNA polyplexes exhibited suitable physicochemical properties, particle size, zeta potential, and morphology for nucleic acid delivery. The NAC polymers exhibited excellent pDNA binding ability and efficiently protected the pDNA from DNase I degradation. Polyplexes prepared with NAC polymers exerted a rapid in vitro release of condensed pDNA compared to chitosan polyplex. The polymers as well as polymer/pDNA polyplexes did not significantly ($p > 0.05$) alter the cell viability, demonstrating a prerequisite characteristic for any successful gene delivery vector. It was found that cell uptake and transfection efficiency of chitosan was increased by several fold after modification with short chain fatty acyl moiety and increased with a decrease of acyl chain length of NAC. Among the different polymeric vectors, NAC-6/pDNA polyplexes demonstrated significantly higher ($p < 0.001$) transfection efficiency in comparison to standard commercial nonviral transfecting agent FuGENE HD. Our results suggest that these novel NAC polymers hold a promising future in the area of gene delivery and can be used for both in vitro and in vivo applications.

3. SHORT CHAIN FATTY ACID CONJUGATED CHITOSAN FOR GENE DELIVERY: EFFECT OF DEGREE OF FATTY ACID SUBSTITUTION

3.1. Introduction

Development of non-toxic and competent gene delivery vectors is a crucial factor in gene therapy. A number of delivery systems have been utilized for gene transfer, which are broadly classified as viral and nonviral vectors. Although viral vectors exhibit excellent transfection efficiency and have an extensive range of cell targets, they may induce immune response and oncogenic effects which restrict their use (Ravi Kumar et al., 2004; Yamada et al., 2003). Thus, nonviral gene delivery vectors have recently gained increasing importance due to their superior safety profile in comparison to their viral counterpart.

Among nonviral vectors, chitosan has been extensively explored for gene transfer because of its excellent biocompatibility, biodegradability, and low cytotoxicity (Du et al., 2010; Gao et al., 2005; Sharma et al., 2012). Moreover, the presence of abundant primary amines and hydroxyl groups on the chitosan backbone make it amenable to easy chemical modifications (Mao et al., 2010) which further enhances its efficacy for gene delivery. The primary amines of chitosan can become positively charged at acidic pH below pKa (6.5) and are able to condense negatively charged DNA into nanoscale polyplexes through ionic interactions. The polyplexes show promise in their ability to protect DNA from nuclease degradation and delivery of condensed DNA into target cells via endocytosis (Yang et al., 2009). However, compared to the viral vector, the in vitro transfection efficiency of chitosan is still relatively low. It has been reported that the low transfection efficiency of chitosan was attributed to the poor cellular uptake and inability to release the DNA after endosomal escape due to the strong interaction between chitosan and DNA (Lu et al., 2009).

To date, several chitosan derivatives have been developed to overcome these drawbacks. It has been reported that hydrophobic modifications such as N-alkylation (Liu et al., 2003), thiolation (Lee et al., 2007), and deoxycholic acid modification (Chae et al., 2005) could facilitate intracellular DNA dissociation, alleviate serum inhibition, and provide efficient protection from enzymatic degradation (Liu et al., 2010). In addition hydrophobic modification also improves the cell membrane permeation of the polyplexes by modulating complex interactions with cells. Since the grafted polymers consist of both cationic amino groups and hydrophobic fatty acyl moieties, both charge attraction and hydrophobic interactions with the cell membrane play an important role in the endosomal uptake process which leads to favorable gene transfection (Piest and Engbersen, 2010). However, substitution of a large percentage of primary amine groups with hydrophobic residues result in unstable polyplexes leading to low levels of gene expression. Therefore, an optimum degree of substitution was required to get maximum transfection efficiency of the transferred gene.

To the best of our knowledge, there are no systematic studies about hydrophobic modification of chitosan to describe the appropriate balance between polyplex stability and intracellular DNA release. Our aim is to gain insight into the optimum degree of N-acyl substitution of chitosan to control the degree of interaction between the polymer and its pDNA cargo in order to improve membrane permeability and transfection efficiency of the polyplexes. In this study, low molecular weight chitosan was used to synthesize hexanoic acid grafted chitosan (NAC-6) copolymers with different degrees of substitution. Hexanoic acid was selected as the hydrophobic modifier based upon our previous results with a series of fatty acids ranging from hexanoic acid to decanoic acid (Layek and Singh, 2012). The influence of degree of substitution was examined in terms of physicochemical properties of the polymers, particle size

and surface charge of the polymer/pDNA polyplexes, pDNA binding strength, and in vitro pDNA release. The cellular uptake, gene transfection efficiency, and in vitro biocompatibility of the polyplexes were evaluated in HEK 293 cell lines.

3.2. Materials and methods

3.2.1. Materials

Chitosan (Mw ~ 50 kDa, 91% deacetylated), MTT, and agarose were obtained from Sigma-Aldrich (St. Louis, MO, USA). Hexanoic acid was procured from MP Biomedicals (Solon, OH, USA). EDC.HCl was purchased from Creosalus Inc (Louisville, KY, USA). DNase I was purchased from Rockland Inc (Gilbertsville, PA, USA). Hoechst 33342 dye was purchased from Anaspec (Fremont, CA, USA). pGFP and pβ-gal were purchased from Aldevron LLC (Fargo, ND, USA). HEK 293 cells, HeLa cells, Dulbecco's Modified Eagle's Medium (DMEM), and PBS were purchased from American Type Culture Collection (ATCC, Rockville, MD, USA). FuGENE HD was obtained from Roche Diagnostics (Indiapolis, IN, USA). Beta-galactosidase enzyme assay kit with reporter lysis buffer was supplied by Promega (Madison, WI, USA).

3.2.2. Synthesis of N-hexanoyl chitosan with different degrees of substitution

N-hexanoyl chitosan (NAC-6) with different degrees of fatty acid substitution were synthesized via the reaction of carboxyl group of hexanoic acid with primary amino groups of chitosan in the presence of EDC (Hu et al., 2006). Briefly, chitosan (0.5 g) was dissolved in 50 mL of distilled water. Hexanoic acid (0.1, 0.3, and 0.6 mol, respectively per mol of sugar unit of chitosan) and EDC (5 mol per mol of hexanoic acid) were dissolved in ethanol. The carboxyl group of hexanoic acid was activated by the addition of EDC solution to hexanoic acid solution. Then the activated hexanoic acid was added into chitosan solution with constant stirring and the

reaction was continued at 90°C for 12 h. The resulting NAC-6 polymers were dialyzed using dialysis tubing (MWCO: 3.5 kDa) against distilled water for two days followed by freeze-drying. The freeze dried product was dispersed in 30 mL ethanol and filtered through 0.2 µm filter to collect the precipitate. The precipitate was further washed with 20 mL ethanol thrice to remove the unreacted hexanoic acid.

3.2.3. Structural characterization of N-hexanoyl chitosan

The chemical reaction between hexanoic acid and chitosan was confirmed by FTIR and ^{1}H NMR spectroscopy. FTIR spectra were recorded using a Thermo Nicolet Nexus 470 FTIR spectrometer equipped with a nitrogen gas purged chamber. All freeze dried samples were ground with KBr powder and pressed into pellets for the study. ^{1}H NMR spectra of chitosan and NAC-6 polymers were obtained using a Mercury Varian 400 MHz spectrometer in deuterium oxide (D_2O) with 1% DCl and D_2O, respectively. The degree of substitution of the polymer was determined by elemental analysis data. The pKa of the synthesized NAC-6 polymers was determined by potentiometric titration method using Katchalsky's equation (Wang et al., 2006).

3.2.4. Endosomal buffering capacity

The endosomal buffering ability of NAC-6 polymers was determined by acid-base titration over the pH range of 10 to 3 (Lu et al., 2009). Briefly, 20 mg of each polymer was dissolved in 20 mL of 150 mM NaCl and the pH of the solution was adjusted to 10 by the addition of 0.1 N NaOH. The sample solution was then titrated with gradual addition (20 µL in each addition) of 0.1 N HCl followed by pH measurement at 25°C using a pH meter (VWR scientific model 8010, PA, USA).

3.2.5. Polymer/pDNA polyplexes preparation and characterization

The polymer/pDNA polyplexes at different N/P ratios were prepared by adding polymeric solutions to pDNA solution with gentle vortexing and incubated at room temperature for about 30 min (Layek and Singh, 2012). The N/P ratio was determined as the ratio of the number of unreacted free primary amino groups of polymer to the number of phosphate groups in pDNA. The polyplexes were prepared in 20 mM sodium acetate buffer at pH 6.5. Particle size and zeta potential of the NAC-6 nanocomplexes and NAC-6/pDNA polyplexes were measured by DLS method at 25°C on a Zetasizer Nano ZS 90. The morphology of the NAC-6 nanocomplexes and NAC-6/pDNA polyplexes was observed by AFM. The samples were placed on the surface of freshly cleaved thin mica plates (grade V-4; 15 × 15 × 0.15 mm^3) and dried under nitrogen. Images were recorded in tapping contact mode using pyramidal cantilevers at a scan rate of 1 Hz.

To determine the association efficiency, polyplexes were first centrifuged at 30000 × g for 30 min at 4°C. The amount of unbound pDNA in the supernatant solution was analyzed using Hoechst dye 33342 with a spectrofluorophotometer at excitation and emission wavelengths of 350 and 450 nm, respectively. The association efficiency of different polyplexes was calculated by the following equation.

$$\text{Association efficiency (\%)} = (pDNA_{total} - pDNA_{free})/pDNA_{total} \times 100$$

3.2.6. Agarose gel retardation assay

The complex formation of pDNA with NAC-6 polymers was studied by agarose gel retardation assay. Polyplexes (containing 1 µg of pDNA) at different N/P ratios were subjected to electrophoresis on a 0.8% (w/v) agarose gel containing 0.5 µg/mL EtBr for 80 min at 80 V in

0.5× TAE buffer. The pDNA bands were visualized and photographed using a UV transilluminator at a wavelength of 254 nm.

3.2.7. Protection of pDNA against nucleases

The pDNA protection capability of NAC-6 polymers against nuclease degradation was studied by DNase I protection assay. NAC-6/pDNA and chitosan/pDNA polyplexes containing 20 µg of pDNA were prepared at an N/P ratio of 20, followed by incubation with 5 units of DNase I at 37°C. Naked pDNA solution treated with DNase I was used as a positive control. The variation in absorbance at 260 nm was measured at 10 min intervals up to 1 h (Liu et al., 2003).

3.2.8. ITC study

ITC was employed to determine the effect of degree of hexanoic acid substitution on binding constant, enthalpy of complex formation, and the stoichiometry of binding of pDNA with different NAC-6 polymers. Binding studies were performed using a low volume nano ITC with a cell volume of 190 µL at 25°C. Samples were degassed for 10 min prior to use. The sample cell was filled with the pDNA solution (50 µg/mL ~ 0.1515 mM phosphate or nucleotide units) and the reference cell with buffer solution only. The NAC-6 solution (147-170 µg/mL, ~ 0.7688 mM of free amino groups) was introduced into the thermostatted cell by means of a syringe and stirred at 250 rpm. Each titration integrated 25 subsequent 2 µL injections programmed to proceed at 400 s intervals. The heat of dilution from titrations of polymer solution into buffer alone was subtracted to get net binding heat changes.

3.2.9. EtBr exclusion assay

NAC-6/pDNA and chitosan/pDNA polyplexes of various N/P ratios were prepared by complexing 2 µg (20 µL of 0.1 mg/mL solution) of pDNA with various amounts of polymers. The final volume of the each polyplexes was adjusted to 1 mL with the addition of PBS (pH 7.4).

Ten microliter of 0.05 mg/mL of EtBr solution was added to each polyplexes and incubated for 5 min at room temperature. Fluorescence intensity was measured with SpectraMax M5 plate reader with the excitation wavelength at 260 nm and emission wavelength at 600 nm. Results were presented as relative fluorescence intensity where 0% suggested the existence of EtBr alone and 100% represented the fluorescence of EtBr combined with pDNA.

3.2.10. In vitro release of pDNA

NAC-6/pDNA and chitosan/pDNA polyplexes (containing 100 µg of pDNA) at an N/P ratio of 20 were incubated with 30 mL of PBS (pH 7.4) at 37°C in a shaking water bath. At each time point, 1 mL of sample was withdrawn and centrifuged at 30,000 × g, for 30 min at 4°C. The amount of unbound pDNA in the supernatant was quantified by spectrofluorophotometer using Hoechst dye 33342.

3.2.11. In vitro cytotoxicity

The cytotoxicity of NAC-6 polymer as well as NAC-6/pDNA polyplexes was evaluated in vitro by MTT assay using HEK 293 and HeLa cells (Lu et al., 2009). Cells were seeded in a 96 well plate at 5×10^3 cells/well in 150 µL of DMEM/high glucose medium supplemented with 10% FBS, allowed to adhere overnight, and then the cells were incubated with various concentrations of polymers or polyplexes with different N/P ratios for 48 h. Cells treated with fresh growth medium alone were considered as control.

3.2.12. Cellular uptake study

To perform the cellular uptake study, NAC-6 polymers and FITC-labeled pDNA were allowed to form polyplexes at an N/P ratio of 20. HEK 293 cells were seeded on a 24-well plate and incubated with FITC-labeled polyplexes containing 1 µg of pDNA/well. After 4 h of uptake,

the cells were washed with PBS and the percentage of FITC-positive cells was measured using FACS analysis.

Endocytosis has been established as the primary mechanism for the uptake of nonviral gene delivery vectors into the cells (Friend et al., 1996; Zuhorn et al., 2002). There are four morphologically distinct endocytic pathways that have been identified which are clathrin-mediated endocytosis, caveolae-mediated endocytosis, macropinocytosis, and phagocytosis (Hillaireau and Couvreur, 2009). Phagocytosis is typically limited to specialized mammalian cells including macrophages, monocytes, neutrophils, and dendritic cells, whereas all other pathways occur in all cells (Conner and Schmid, 2003; Aderem and Underhill, 1999). In an effort to explore the mechanisms involved in cellular uptake, cells were pretreated with either sodium azide (10 mM) to arrest all energy dependent endocytosis, colchicine (100 μg/mL) to inhibit caveolae formation, chlorpromazine (10 μg/mL) to prevent formation of clathrin vesicles, or amioloride (50 μg/mL) to inhibit macropinocytosis in normal growth medium for 30 min before application of NAC-6/pDNA polyplexes (Nam et al., 2009; Wang et al., 2011). Following 4 h of uptake, the cells were washed with PBS and the percentage of FITC-positive cells was quantified by FACS analysis. Results were expressed as the percent relative uptake of treated cells as compared to cells without inhibitor pretreatment.

3.2.13. In vitro gene transfection

In vitro gene delivery efficacy of the NAC-6 polymers was studied in HEK 293 and HeLa cells using pGFP and pβ-gal as reporter plasmids. Cells were seeded in a 24-well plate at a density of 1×10^5 cells/well with 0.5 mL of DMEM/high glucose medium supplemented with 10% FBS and allowed to grow for 24 h to achieve ~ 60-70% confluency prior to transfection studies. The NAC-6/pGFP or NAC-6/pβ-gal polyplexes containing 1 μg of pDNA at an N/P ratio

of 20 were incubated with the cells in 10% FBS containing media at 37°C under a 5% CO_2 humidified atmosphere for 4 h. Then, the transfecting media was replaced with fresh media and the cells were incubated up to 48 h. The transfection efficiency was evaluated by measuring the percentage of GFP positive cells, as determined by FACS analysis. The images of GFP positive cells were photographed with a FV300 confocal laser scanning microscope at 10× magnification. For the β-galactosidase transfection studies, transfected cells were washed twice with PBS (pH 7.4) and lysed using 1× reporter lysis buffer. The β-galactosidase enzyme activity was quantified using β-galactosidase assay kit. The total amount of protein content of the cell lysate was measured using BCA assay reagent. The β-galactosidase activity was stated as milliunit of β-galactosidase/mg of the total protein.

3.3. Results and discussion

3.3.1. Synthesis of N-hexanoyl chitosan with different degrees of substitution

The NAC-6 polymers with different degrees of hexanoic acid substitution were prepared by carbodiimide mediated coupling of free amino groups of chitosan and carboxyl groups of fatty acid. The excess carbodiimide and water soluble by-products were eliminated by dialysis with water, and the unreacted fatty acid was removed by ethanol washing.

3.3.2. Structural characterization of N-hexanoyl chitosan

The structures of the NAC-6 polymers were confirmed by FTIR (Figure 18) and ^{1}H NMR (Figure 19) spectroscopy. The peaks at 1640 cm^{-1} and 1540 cm^{-1} under FTIR spectrum can be ascribed to the carbonyl stretching of secondary amides (amide I band) and N–H bending vibrations of the amide II band, respectively (Tien et al., 2003). After haxanoic acid grafting, the peaks at 1640 cm^{-1} (indicating formation of amide bonds) and 2820–2920 cm^{-1} were intensified. The peaks at 2820–2920 cm^{-1} were due to the acyl chain (–CH_2 groups) and their intensities were

proportional to the degree of hexanoic acid substitutions. On the other hand, no absorption peak of the carboxyl groups of hexanoic acid (1700 cm^{-1}) was found in the FTIR spectra of NAC-6, thereby suggesting grafting of hexanoic acid moiety onto the chitosan backbone.

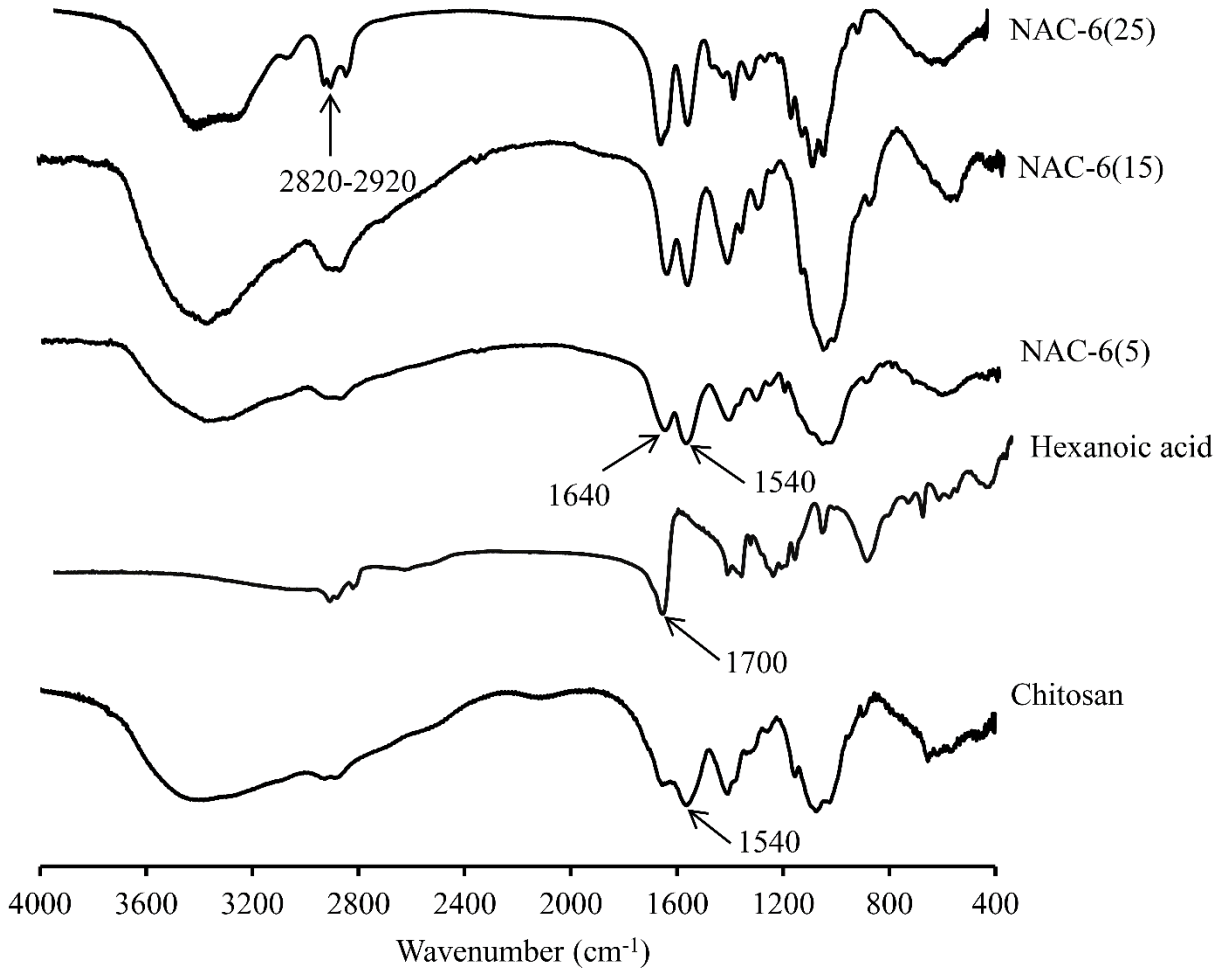

Figure 18. FTIR spectra of chitosan, hexanoic acid, NAC-6(5), NAC-6(15), and NAC-6(25).

The ^{1}H NMR spectra of chitosan and NAC-6 polymers are depicted in Figure 19. For chitosan, peak at 1.8 ppm revealed the three N-acetyl protons of N-acetyl glucosamine and peak at 2.9 ppm showed the H2 proton of N-acetyl glucosamine or glucosamine residue. The ring protons (H-3, 4, 5, 6, 6') of chitosan are considered to resonate at 3.4-3.8 ppm. In comparison, NAC polymers displayed the new peak at 0.8 ppm, which was assigned to the methyl protons of

hexanoic acid. The peak at 1.2 ppm was assigned to the methylene protons of hexanoic acid. The degree of hexanoic acid substitution was estimated by elemental analysis and was found to be 5.5%, NAC-6(5); 15.2%, NAC-6(15); and 24.6%, NAC-6(25), respectively.

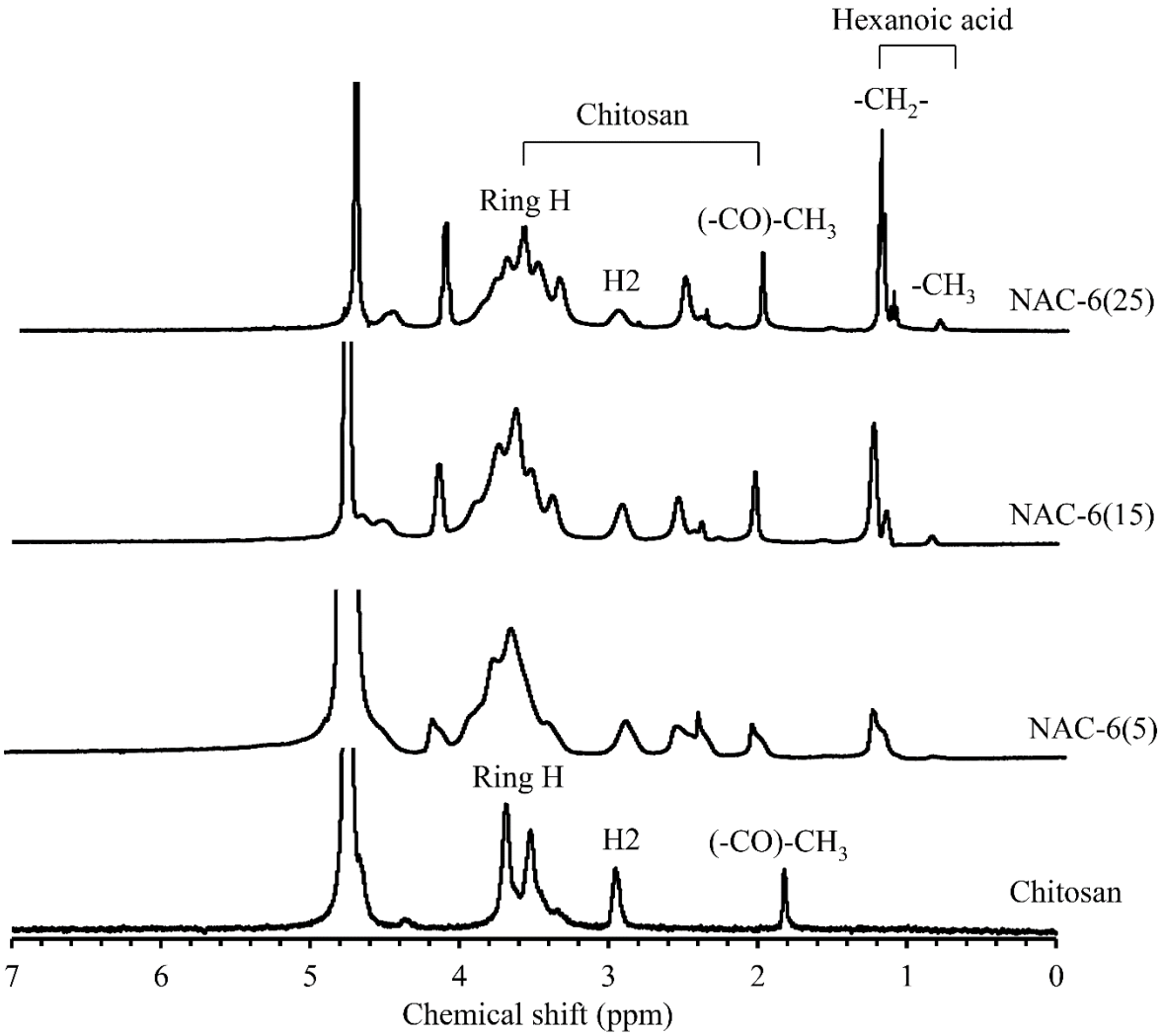

Figure 19. ^{1}H NMR spectra of chitosan and different NAC-6 polymers.

The pKa of NAC-6 polymers was determined by potentiometric titration method. The pKa of NAC-6 polymers with 5.5%, 15.2%, and 24.6% substitution was 6.75, 6.82, and 6.95, respectively, which increased with increasing degree of substitution. Chitosan with lower degree of hexanoic acid substitution carried a slightly increased surface charge density and thus acquired lower pKa values owing to an increased surface potential (Filion et al., 2007). These

results were well accorded with the previously reported data (Domard, 1987; Wang et al., 2006; Toh et al., 2011).

3.3.3. Endosomal buffering capacity

A good gene delivery system should be capable of protecting its cargo from endolysosomal degradation. The onset and extent of endolysosomal escaping capacity of a cationic polymer is correlated with the buffering ability in the pH range of 5 to 7 (Godbey et al., 1999). The buffer capacity causes an increase in endosomal osmotic pressure that results in the disruption of endocytic vesicles and subsequent release of polyplexes into the cytoplasm to improve overall gene transfection efficiency (Behr, 1997; Varkouhi et al., 2011). The results of acid-base titration (Figure 20) indicated good buffering capacity of NAC-6 polymers between pH 5 to 7 when the substitution degree was up to 15%. NAC-6(25) showed poor buffering ability due to the least fraction of available free amines when compared to NAC-6(15) and NAC-6(5). These results clearly indicate the improved endolysomal escaping capacity of NAC-6(5) and NAC-6(15) polymers over NAC-6(25).

3.3.4. Characterization of polymer/pDNA polyplexes

Particle size and surface charge of polyplexes are known to be the critical parameters that govern the polyplexes' cellular uptake and interaction with cell membranes (Choosakoonkriang et al., 2003). Generally, small particles within size ranges of 50 to several hundred nanometers are suitable for cellular internalization via endocytosis (Liu and Reineke, 2005). The volume average hydrodynamic diameter and zeta potential of the NAC-6 nanocomplexes and NAC-6/pDNA polyplexes at different N/P ratios are shown in Table 3. The size of the NAC-6 nanocomplexes slightly increased upon addition of pDNA while the N/P ratio was 5. Thereafter, the size of the polyplexes showed a tendency to decrease with the increasing N/P ratio indicating

formation of more compact polyplexes caused by the presence of a higher density of protonated amines surrounding the polyplexes. At a particular N/P ratio, the size of the polyplexes increased as the degree of substitution increased from 5 to 25% indicating formation of less compact polyplexes.

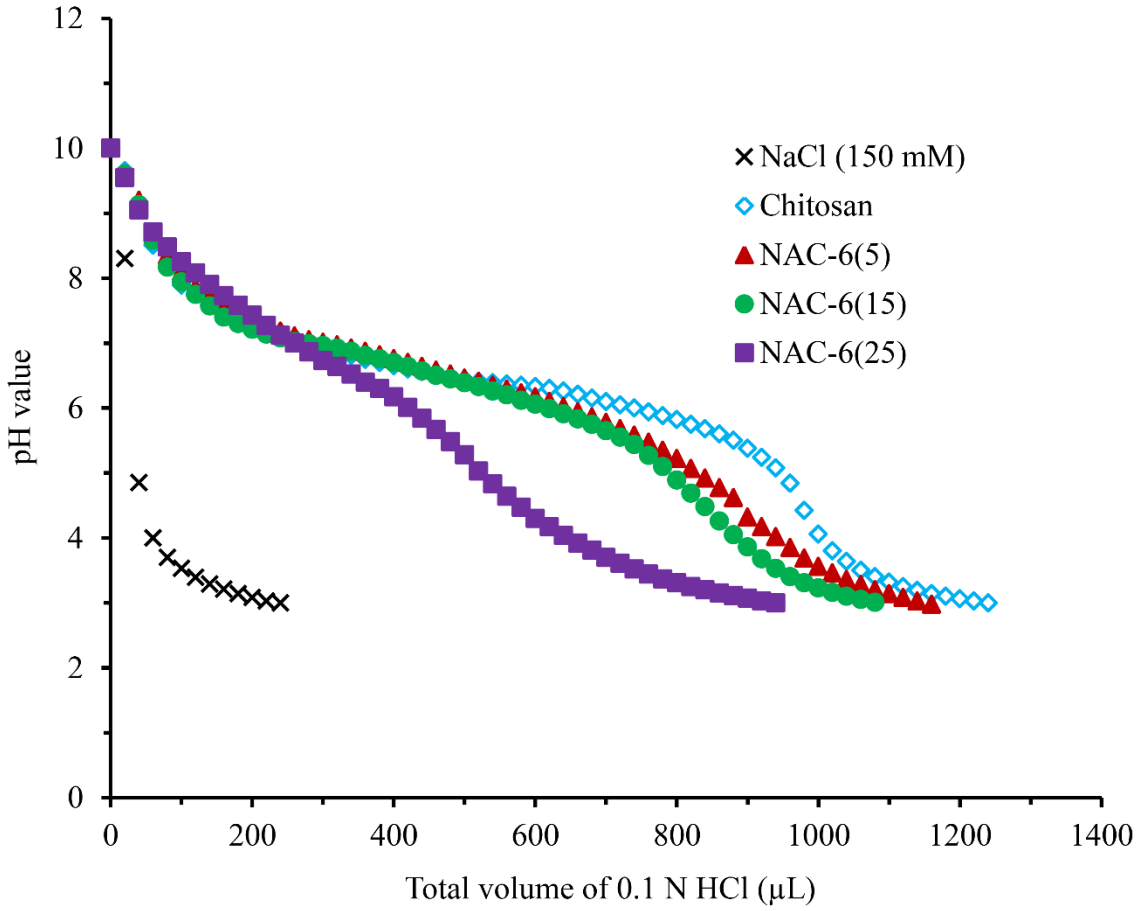

Figure 20. Endosomal buffering capacity of chitosan and different NAC-6 polymers.

At pH 6.5, NAC-6 nanocomplexes maintained stable positive charge (Table 3) thus effectively condensing the negatively charged pDNA through electrostatic interaction to form nanosized polyplexes. After making NAC-6/pDNA polyplexes, the zeta potential of the NAC-6 nanocomplexes decreased due to neutralization of the positive charge of NAC-6 polymers by the negative charge of pDNA phosphate groups in the said polyplexes. We observed that the zeta

potential of the polyplexes changed from 10.3 to 20.5 mV when the N/P ratio increased from 5 to 20. Moreover, at a fixed N/P ratio, the zeta potential of NAC-6(25)/pDNA polyplexes was lower than that of NAC-6(5)/pDNA and NAC-6(15)/pDNA polyplexes.

Table 3. Particle sizes and zeta potentials of NAC-6 nanocomplexes and their corresponding pDNA polyplexes. Association efficiencies of NAC-6/pDNA polyplexes at pH 6.5. Data represents the mean ± SD (n = 6).

Sample	Particle size (nm)		Zeta potential (mV)			
	Nanocomplex[a]	Polyplex	Nanocomplex[a]	Polyplex	N/P ratio	Association efficiency (%)[b]
NAC-6(5)	252.6 ± 8.9	280.5 ± 6.4	25.5 ± 1.0	14.2 ± 0.5	5	
		240.9 ± 5.5		16.1 ± 0.3	10	
		210.3 ± 6.3		20.5 ± 0.9	20	96.8 ± 2.2
NAC-6(15)	301.2 ± 9.3	336.8 ± 3.9	24.5 ± 0.7	14.1 ± 0.5	5	
		274.4 ± 7.9		17.7 ± 0.4	10	
		251.8 ± 5.2		20.1 ± 0.5	20	90.6 ± 2.9
NAC-6(25)	321.1 ± 6.5	377.0 ± 6.1	18.3 ± 1.5	10.3 ± 0.2	5	
		314.4 ± 4.2		13.3 ± 0.4	10	
		298.6 ± 8.6		14.9 ± 0.7	20	82.5 ± 4.7
Chitosan	-	262.5 ± 5.6	40.8 ± 1.7	23.1 ± 1.2	5	
		247.7 ± 8.1		26.0 ± 1.1	10	
		225.6 ± 4.3		27.6 ± 0.8	20	98.8 ± 2.5

[a]Nanocomplexes were prepared at a concentration of 200 µg/mL; [b]Association efficiency measured at N/P ratio of 20.

The surface morphology of the NAC-6 nanocomplexes and NAC-6/pDNA polyplexes was visualized by AFM. The polyplexes were nearly spherical in shape (Figure 21). Furthermore, upon addition of pDNA, no apparent change in the surface morphology was observed, suggesting that the NAC-6 was able to form a compact complex with the pDNA. The association efficiencies of the NAC-6/pDNA polyplexes at the N/P ratio of 20 were decreased significantly ($p < 0.05$) as the degree of hexanoic acid substitution of the polymer increased.

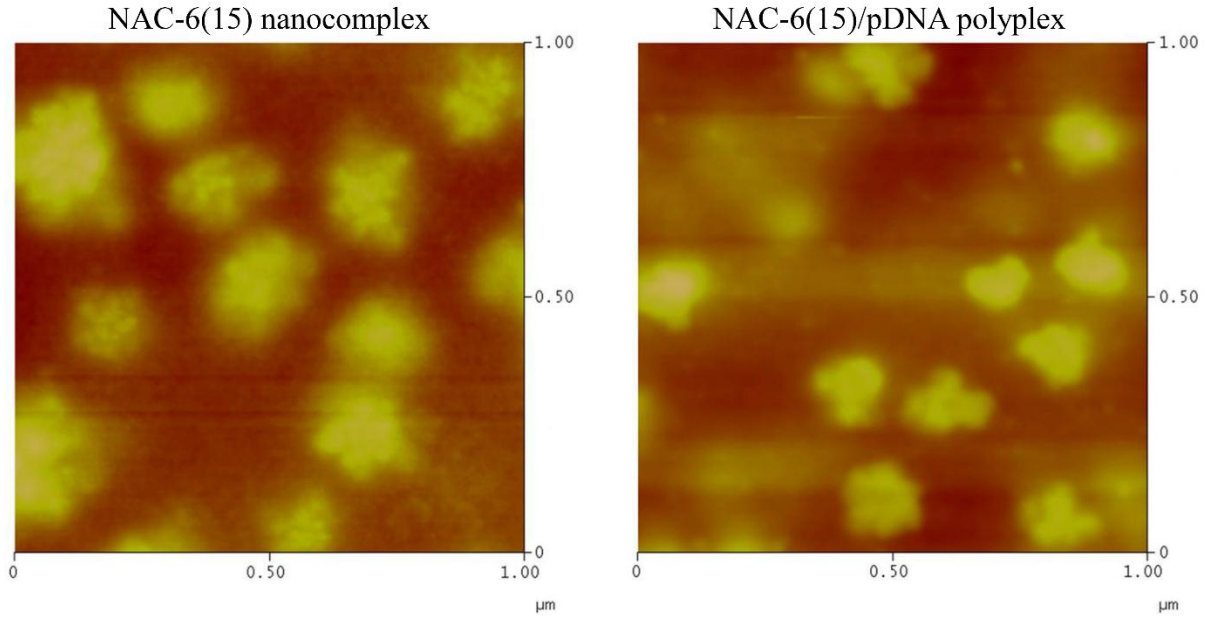

Figure 21. Morphological analysis of (A) NAC-6(15) nanocomplex and NAC-6(15)/pDNA polyplex at N/P ratio of 20.

3.3.5. Agarose gel retardation assay

To transport pDNA to cells, the cationic polymer vectors should be able to complex pDNA through electrostatic interaction. The electrophoretic band of pDNA on agarose gel can be used to characterize the formation of stable polyplexes since the partial or complete charge neutralization of pDNA by the vector results in complete retardation of pDNA migration toward the anode (Zelikin et al., 2002). Figure 22 shows the effect of charge ratio on pDNA condensing capacity of NAC-6(5), NAC-6(15), and NAC-6(25) from the agarose gel electrophoresis assay.

The presence of partially dissociated pDNA at the N/P ratio of 1 suggested the formation of physically unstable complexes. When the N/P ratios of the polyplexes increased to ≥ 2, migration of pDNA was completely prevented, indicating tight complex formation between NAC-6 nanocomplexes and pDNA.

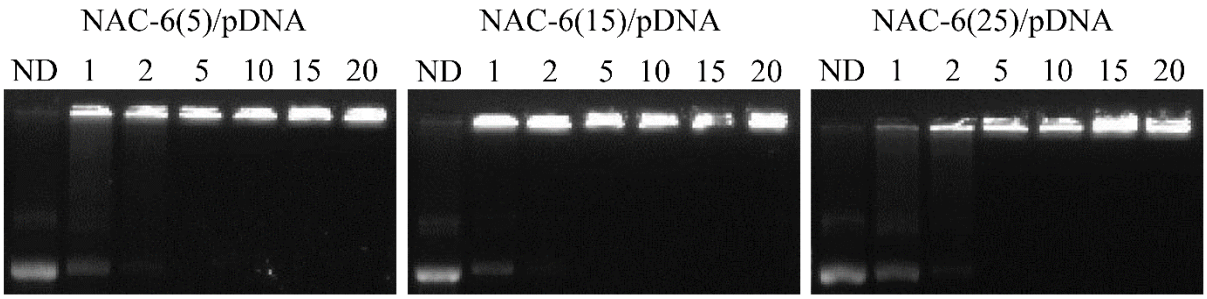

Figure 22. Agarose gel retardation assay to test pDNA binding capacity of NAC-6/pDNA polyplexes at different N/P ratios.

3.3.6. Protection of pDNA against nucleases

The integrity of pDNA is an essential parameter to ensure its desired function in vitro and in vivo, and therefore the gene delivery vector should efficiently protect condensed pDNA from endonuclease degradation (Katayose and Kataoka, 1998). The effect of NAC-6 polymer on protection of pDNA from nuclease degradation was examined using DNase I enzyme. The naked pDNA was vulnerable to enzymatic degradation as observed by rapid increase of absorbance at 260 nm while chitosan/pDNA polyplexes could prevent the degradation of pDNA to great extent (Figure 23). Additionally, NAC-6 polymers demonstrated a significantly higher pDNA protection ability than chitosan/pDNA nanocomplex after 60 min of co-incubation with DNase I, suggesting that the hexanoic acid substitution was advantageous for DNase I protection. The higher degree of hexanoic acid grafting of chitosan was thought to be providing better shielding of enzymatic digestion sites by hydrophobic interactions (Wang et al., 2011) as well as lowering the permeability of DNase I (Liu and Yao, 2002). These results demonstrate that the NAC-6

polymers have great potential to provide pDNA stability for an extensive period of time in a nuclease rich environment and therefore can be used as efficient nonviral vectors for transporting pDNA into the cytoplasm of a cell without degradation which contributes to the higher transfection efficiency of NAC-6/pDNA polyplexes.

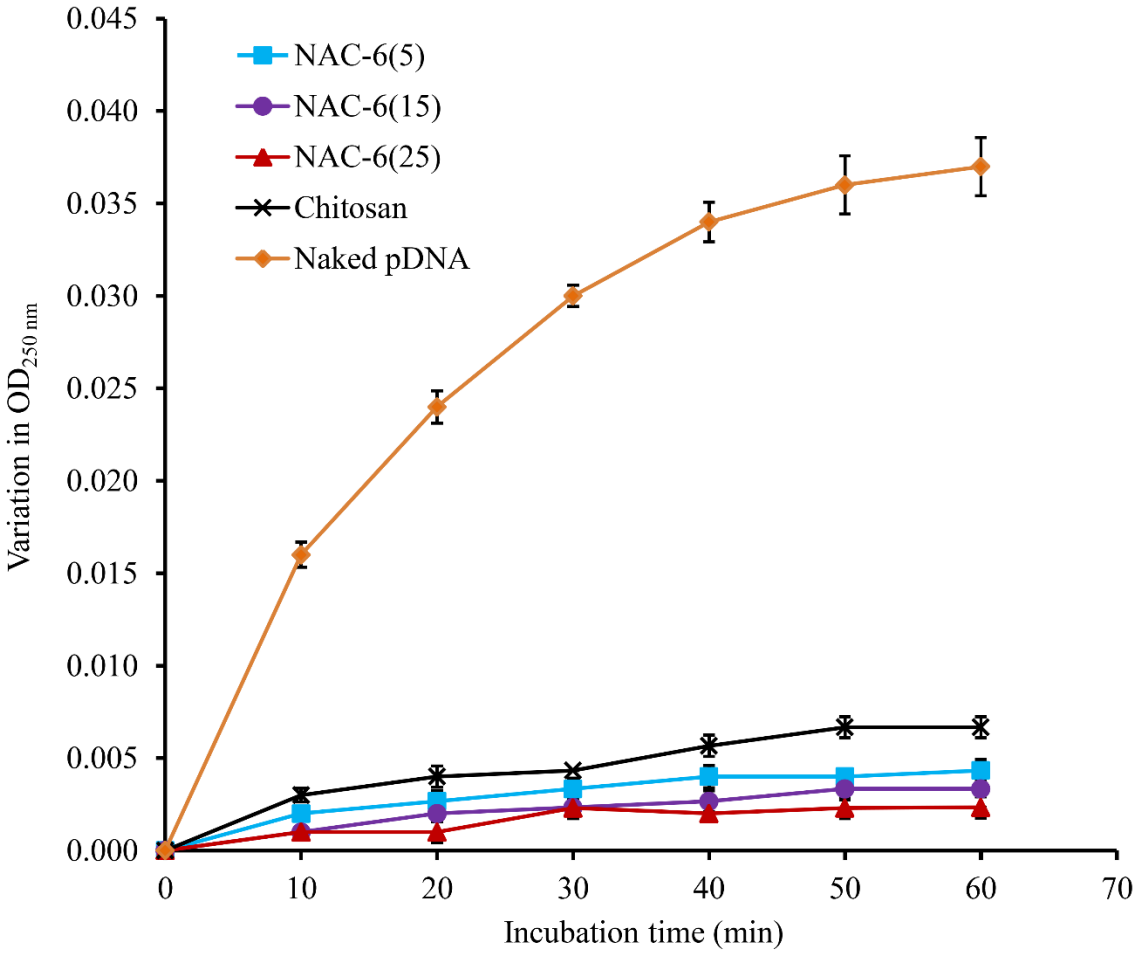

Figure 23. DNase I protection assay measured by the variation in $OD_{260\ nm}$. Chitosan/pDNA and different NAC-6/pDNA polyplexes were prepared at the N/P ratio of 20. Data represents the mean ± SD (n = 4).

3.3.7. ITC study

The strong ionic interaction of chitosan with pDNA remained a major rate limiting step for the effective intracellular release of pDNA, which is critical for transcription and translation of the transferred pDNA (Lu et al., 2009). The ITC experiment was employed to quantitatively

measure the pDNA binding affinity of NAC-6 polymers with varying degrees of hexanoic acid substitution. The integrated heats of the binding of pDNA with NAC-6 polymers in different buffers at pH 6.5 and 7.4 are shown in Figure 24. Each injection of NAC-6 polymer into the pDNA solution produced a sharp negative peak indicating an endothermic interaction. As the NAC-6 content in the cell increased, the amount of heat changes decreased indicating gradual neutralization of pDNA. The thermodynamic parameters including binding constant (K), enthalpy of complex formation (Q), and the stoichiometry of binding (n) of pDNA with NAC-6 are represented in Tables 4 and 5.

The results of the ITC experiments clearly highlighted the decreased pDNA binding affinity of NAC-6 polymer with the increased degree of hexanoic acid substitution as indicated by lower binding constant (K). At pH 6.5, the binding affinity of NAC-6(25) polymer was reduced to approximately 1/5 as compared to chitosan. Therefore, the higher degree of hexanoic acid substitution may result in enhanced dissociation of polyplexes inside the cells (Gabrielson and Pack, 2006). We observed a reduced binding affinity of NAC-6 polymers at a higher pH of 7.4 as compared to pH 6.5, which was due to the deprotonation of cationic NAC-6 polymers; as a result the electrostatic interaction between NAC-6 polymer and pDNA was eventually attenuated. The calorimetric titration of chitosan at pH 7.4 was not evaluated due to insolubility of chitosan at neutral or basic pH. The pDNA has a constant negative charge over the pH ranges we studied because the pKa of its phosphate groups is about 1 (Ma et al., 2009). Hence, changes in the solution pH will only affect the degree of ionization of NAC-6 polymer affecting the binding constant and other thermal parameters of the NAC-6 polymers.

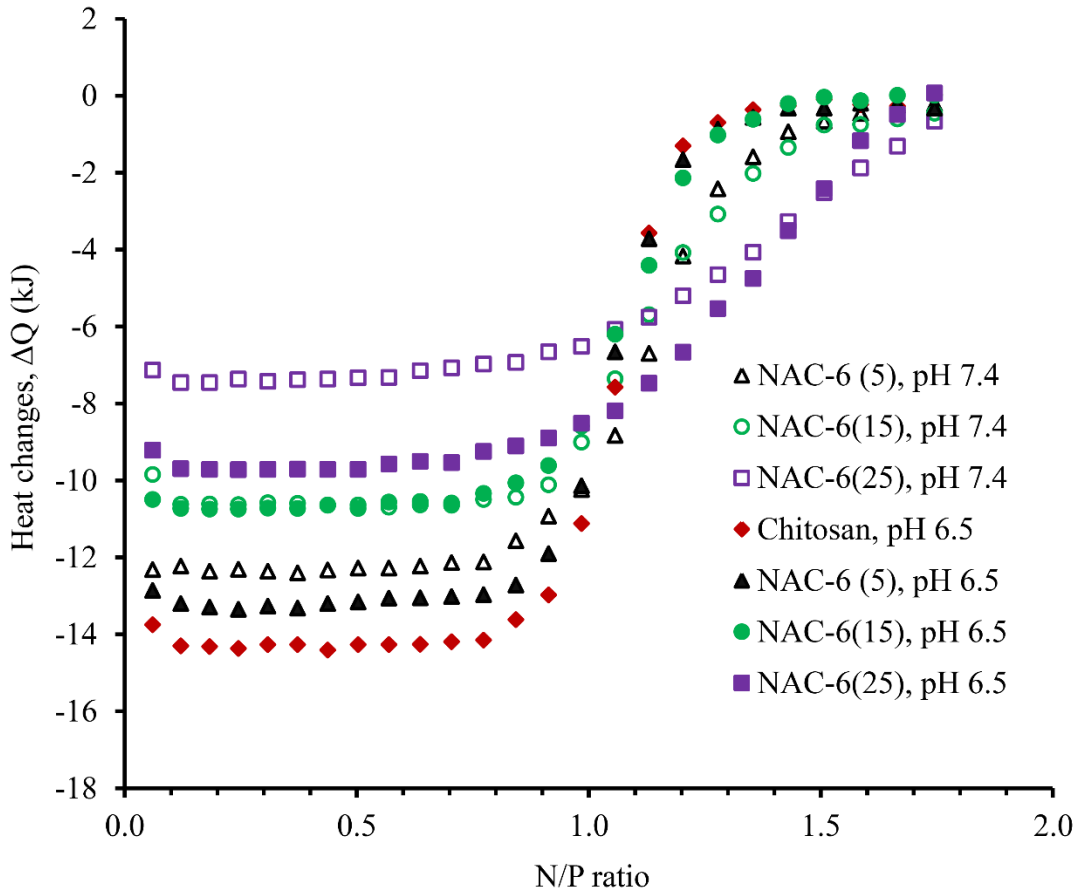

Figure 24. Integrated heats of interaction of the titrations of different NAC-6 polymers into pDNA vs N/P ratios.

Table 4. Thermodynamic parameters of the binding interaction between polymer and pDNA in 20 mM sodium acetate buffer at pH 6.5. Data represents the mean ± SD (n = 3).

Polymer	K $\times 10^5 (M^{-1})$	n (mol)	ΔH (kJ mol^{-1})
Chitosan	29.16 ± 1.16	1.02 ± 0.01	-9.35 ± 0.41
NAC-6(5)	22.12 ± 1.37	1.03 ± 0.02	-8.68 ± 0.17
NAC-6(15)	16.46 ± 1.12	1.06 ± 0.02	-7.02 ± 0.21
NAC-6(25)	5.94 ± 0.42	1.30 ± 0.03	-6.35 ± 0.22

Table 5. Thermodynamic parameters of the binding interaction between polymer and pDNA in 5 mM phosphate buffer at pH 7.4. Data represents the mean ± SD (n = 3).

Polymer	$K \times 10^5 (M^{-1})$	n (mol)	ΔH (kJ mol^{-1})
NAC-6(5)	11.12 ± 0.36	1.11 ± 0.05	-8.13 ± 0.35
NAC-6(15)	8.13 ± 0.34	1.13 ± 0.03	-7.08 ± 0.43
NAC-6(25)	3.45 ± 0.13	1.36 ± 0.05	-4.89 ± 0.34

3.3.8. EtBr exclusion assay

After the polyplexes enter the cytoplasm, a very strong binding affinity between pDNA and its vectors creates a problem in unpacking of pDNA cargoes, and thereby hinders gene expression (Chen et al., 2008b; Strand et al., 2010). The binding affinity between NAC-6 nanocomplexes and pDNA was evaluated by EtBr exclusion in PBS (pH 7.4) to correlate with the existing pH environments in the cytoplasm and nuclei. EtBr is a cationic intercalating agent, whose fluorescent intensity increased by almost 20-fold after binding with DNA. The electrostatic interaction between NAC-6 nanocomplexes and pDNA causes the exclusion of EtBr from DNA double helix to solution, resulting in decay of EtBr fluorescence. The lesser extent of fluorescence quenching indicates the higher fraction of EtBr remained bound to DNA. As demonstrated in Figure 25, a positive correlation of higher EtBr fluorescence quenching with higher charge ratio was observed**.** At an N/P ratio 20, compared to chitosan/pDNA polyplexes of which 90.3% of fluorescence was quenched, the quenching percentages of NAC-6(5)/pDNA, NAC-6(15)/pDNA, and NAC-6(25)/pDNA polyplexes were 83.9%, 79.1%, and 59.3%, respectively, indicating a decreased binding affinity for pDNA as hexanoic acid substitution increased. Hexanoic acid substitutions of chitosan assist the pDNA dissociation from the

polyplexes due to a decrease in charge density of resulting NAC-6 polymers as well as hydrophobicity-induced weakening of the electrostatic interaction between the NAC-6 and pDNA. Our observation supports the earlier study reported by Liu et al. (2003).

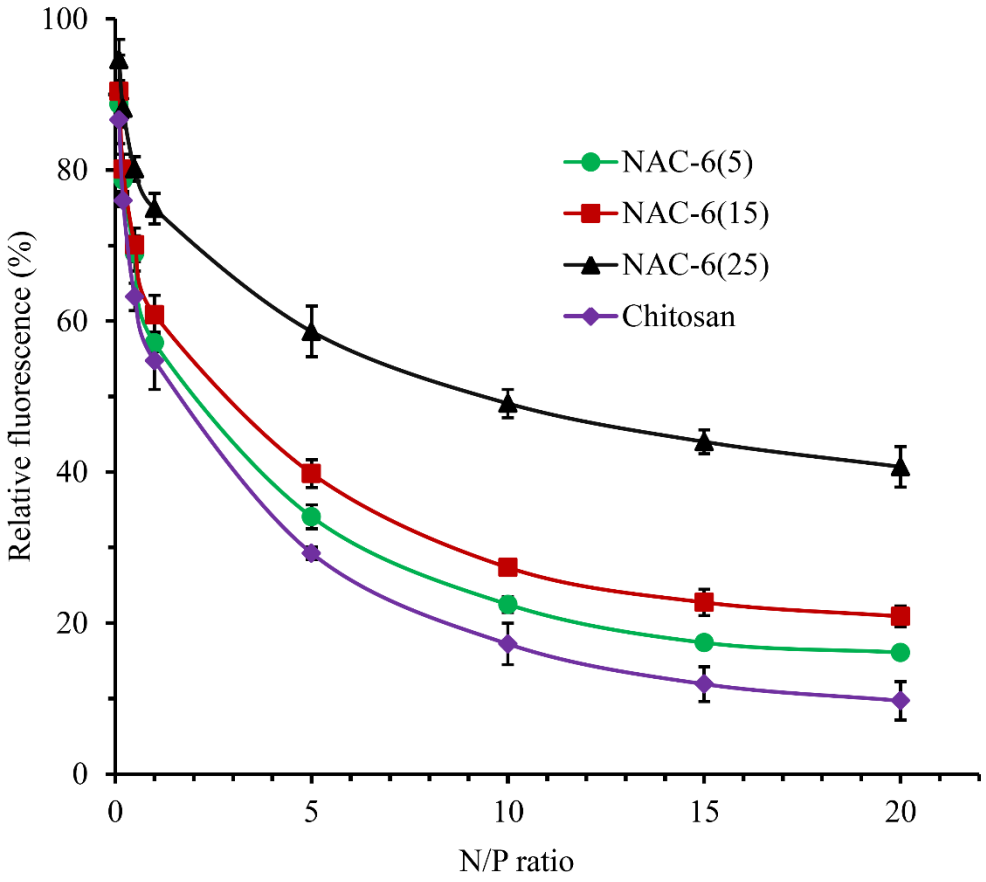

Figure 25. pDNA binding strength in PBS (pH 7.4) monitored by EtBr exclusion assay. Results are represented as relative fluorescence intensity where 0% suggests the existence of EtBr alone and 100% represents the fluorescence of EtBr combined with pDNA. Data represents the mean ± SD (n = 4).

3.3.9. In vitro release of pDNA

The formation of stable polyplexes is a prerequisite for efficient gene delivery which provides protection of pDNA from extracellular nucleases, followed by endolysosomal escape. On the other hand, nuclear transportation and gene expression are not achieved unless pDNA is released from the NAC-6/pDNA polyplexes once inside the cell (Schaffer et al., 2000). Thus, the

proper balance between polyplex stability and the intracellular unpacking of pDNA from these polyplexes has to be fine-tuned to achieve high levels gene expression (Köping-Höggård et al., 2004; Chen et al., 2008b). Figure 26 revealed the cumulative release profile of pDNA from polyplexes in PBS (pH 7.4). After 48 h, about 9.6% of the condensed pDNA was released from chitosan/pDNA polyplexes while the cumulative release from NAC-6(5)/pDNA, NAC-6(15)/pDNA, and NAC-6(25)/pDNA polyplexes were increased to 17%, 29%, and 38.9%, respectively. Therefore, a positive correlation of higher degree of hexanoic acid substitution with increased pDNA release was evident, which suggested the reduction in pDNA binding capacity (Wang et al., 2011). The outcome of in vitro release profile was well accorded with the results of the ITC experiment and EtBr assay.

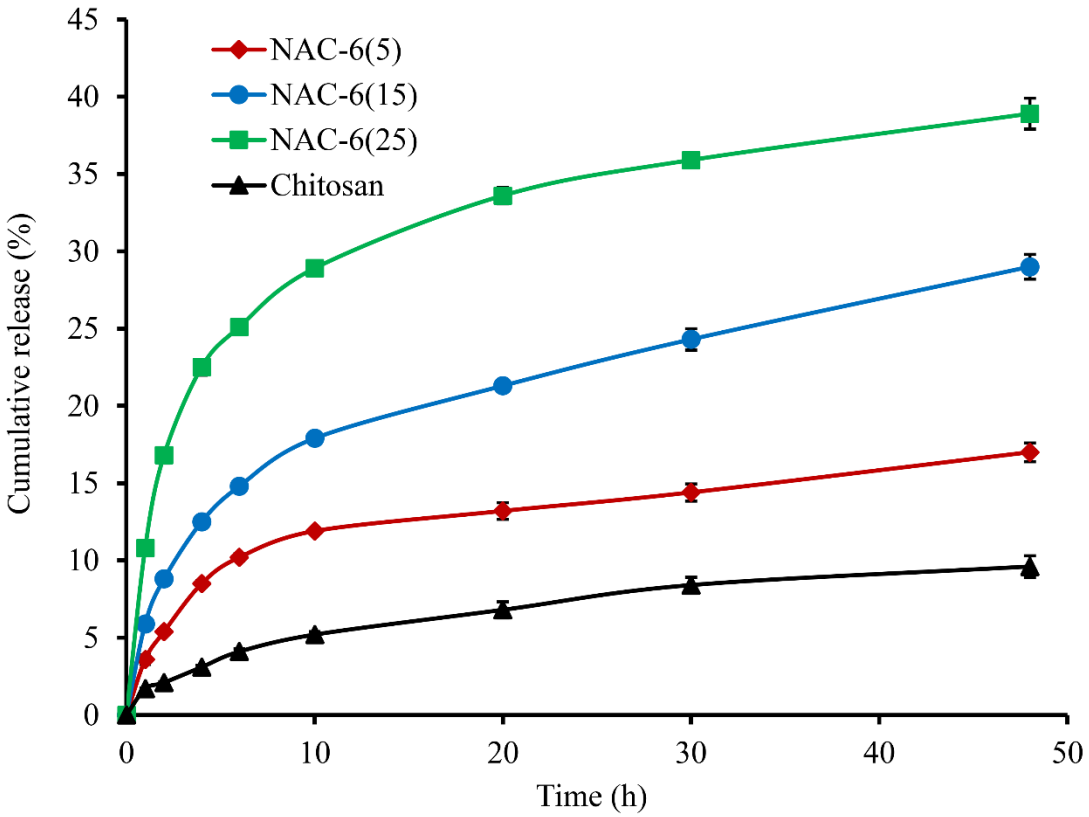

Figure 26. Cumulative pDNA release profiles of different polyplexes. Polyplexes were prepared at the N/P ratio of 20 and were incubated in PBS (pH 7.4) at 37°C. Data represents the mean ± SD (n = 4).

3.3.10. In vitro cytotoxicity

One important criterion of gene delivery vectors is low cytotoxicity. The cationic polymers are reported to have some inherent cytotoxicity due to interactions with cell membranes and negatively charged intracellular components (Choksakulnimitr et al., 1995; Fischer et al., 2003). Numerous studies have emphasized the relatively nontoxic nature of chitosan-based derivatives over other cationic polymers such as poly-lysine and polyethyleneimine (Duceppe and Tabrizian, 2010; Rudzinski and Aminabhavi, 2010). Nevertheless, their toxicity depends on the type of chitosan derivative as well as the type of cells studied (Fischer et al., 2003). As depicted in Figure 27**,** NAC-6 polymers did not alter the cell viability up to the concentration of 2 mg/mL which was 50-fold higher than the maximum polymer concentration used for in vitro transfection studies. Moreover, the degree of hexanoic acid substitution did not alter the viability of either HEK 293 or HeLa cells. Similarly, NAC-6/pDNA polyplexes at different N/P ratios did not affect the cell viability in comparison to the control (considered as 100% viability). Therefore, results of MTT assay confirmed the nontoxic nature of NAC-6 polymers as well as NAC-6/pDNA polyplexes under the experimental conditions. This finding clearly suggests that NAC-6 polymers could be used as suitable nonviral vector for repeated administration of large quantities of genes of interest.

3.3.11. Cellular uptake study

Since the target site for therapeutic genes are typically localized inside the nucleus, the capability of the polymer/pDNA polyplexes to cross the cell membrane is critical for efficient gene expression (Gao et al., 2009; Wang et al., 2011). The uptake of chitosan/pDNA and NAC-6/pDNA polyplexes by HEK 293 cells were quantitatively measured by FACS analysis.

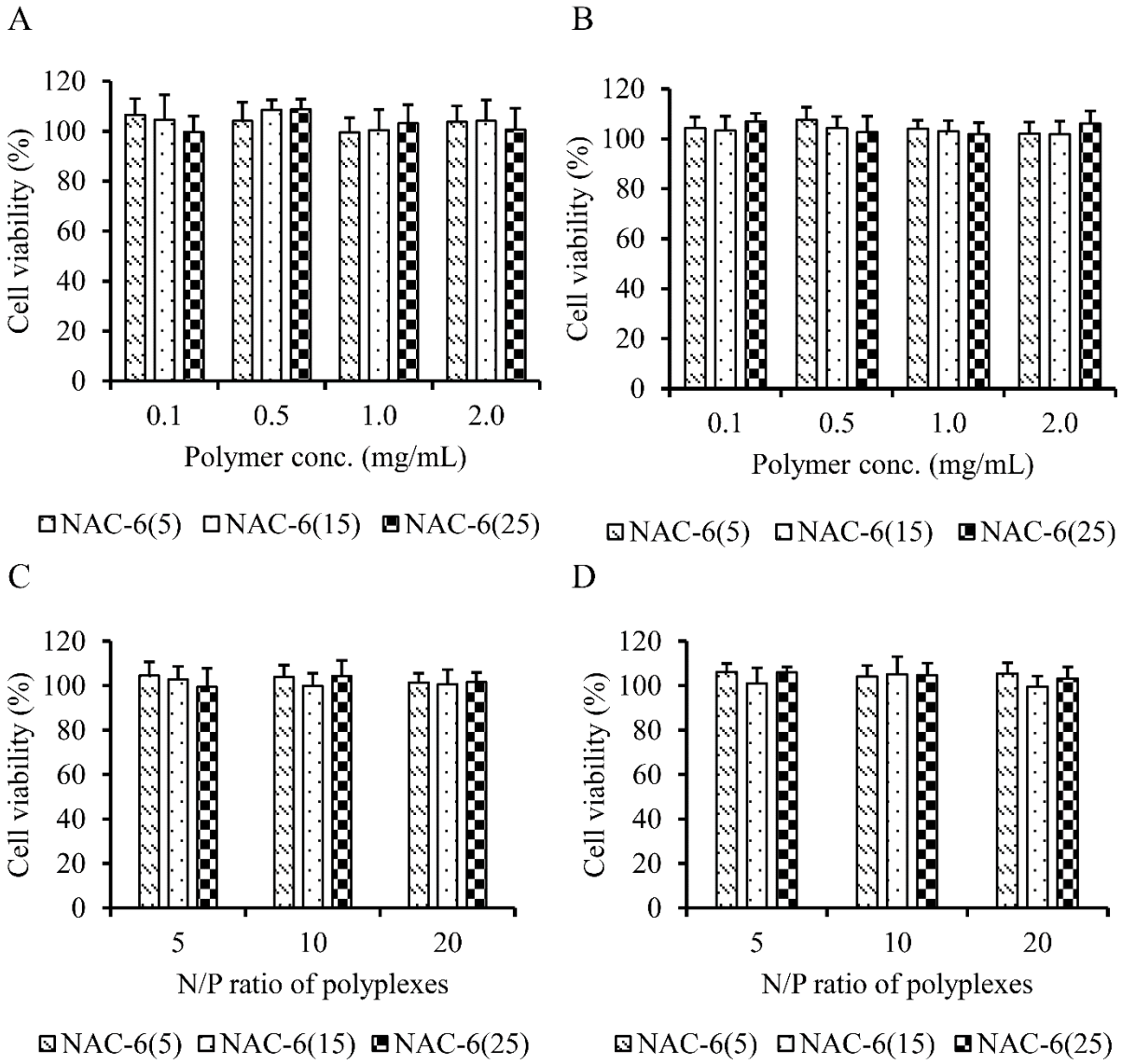

Figure 27. Cytotoxicity of (A, B) NAC-6 polymers and (C, D) NAC-6/pDNA polyplexes on HEK 293 cells (A, C) and HeLa cells (B, D). Data represents the mean ± SD (n = 4).

For chitosan/pDNA polyplexes, we found only 14.5% FITC-positive cells while cellular uptake was elevated by 2 to 7-fold for NAC-6/pDNA polyplexes (Figure 28A). Increasing hexanoic acid substitution from 5 to 15 % enhanced the cell uptake from 45.6% to 99.1%. In contrary, a 3.2-fold cellular uptake reduction was evident for NAC-6(25)/pDNA polyplexes as compared to NAC-6(15)/pDNA polyplexes. Increased hydrophobicity of NAC-6 polymers by

hexanoic acid substitution to a certain extent (up to 15%) might be favorable for cellular uptake by endocytosis process (Liu et al., 2010). In contrast, substitution of a large fraction of free amino groups of chitosan with hexanoic acid could result in formation of loosely compact, large polyplexes with less cationic charge which facilitate premature release of pDNA followed by reduction in uptake by endocytosis. Thus, the design of chitosan derivatives with the proper degree of hydrophobic substitution is important for enhanced cellular uptake of polyplexes.

As depicted in Figure 28B, pretreatment with sodium azide induced remarkable decrease in uptake (~ 80%) compared to uptake by control cells. The striking reduction of cellular uptake with sodium azide pretreatment indicated that an energy-dependent internalization process contributed to 80% of the cellular uptake, while the remaining 20% might be derived from diffusion or physical adsorption of the polyplexes (Wang et al., 2011).

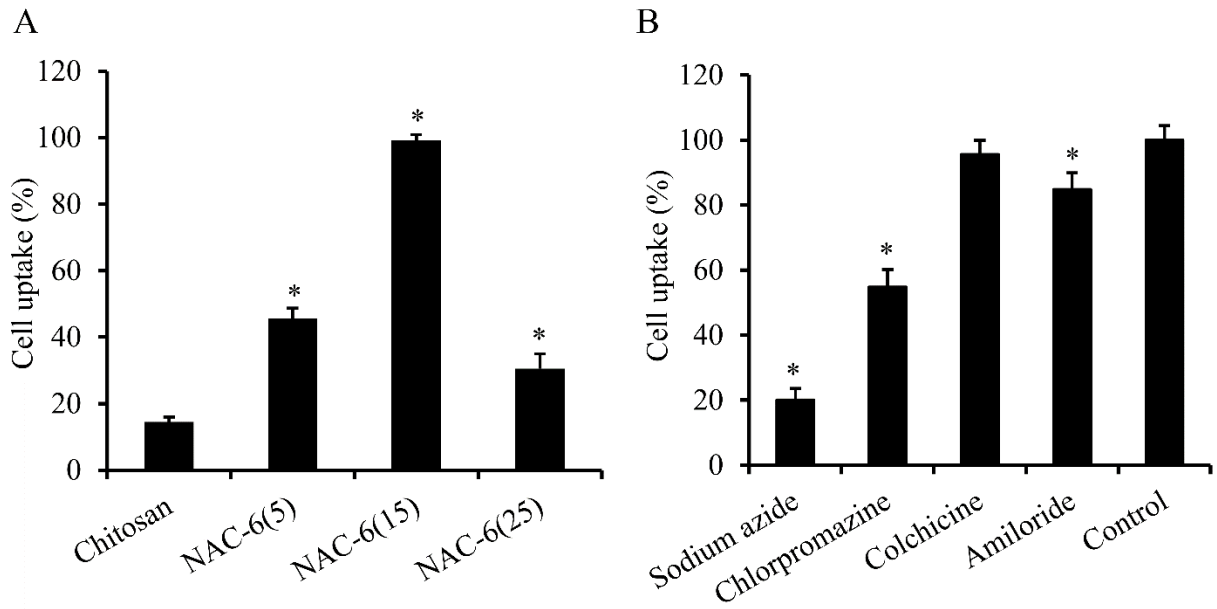

Figure 28. (A) Cellular uptake of chitosan/pDNA and NAC-6/pDNA polyplexes in HEK 293 cells. Cells were incubated with different polyplexes at 37°C for 4 h. Data represents the mean ± SD (n = 4) [‘*’ indicates significantly ($p < 0.05$) higher than chitosan]. (B) The effect of inhibitors on the uptake of NAC-6(15)/pDNA polyplexes. The uptake percentage in control cells was set as 100%. Data represents the mean ± SD (n = 4). [‘*’ indicates significantly ($p < 0.05$) lower than control].

When HEK 293 cells were pre-incubated with chlorpromazine and then treated with NAC-6/pDNA polyplexes, the uptake of polyplexes was reduced by approximately 45.2% indicating the association of a clathrin-mediated process in polyplex internalization. Similarly, when cells were pre-treated with amiloride, a selective inhibitor of the Na^+/H^+ exchange required for macropinocytosis, the polyplex uptake reduced by 15% compared to cells not treated with amiloride. The negligible inhibition (i.e., 4.4%) induced by colchicine is against the caveolin-mediated endocytosis in polyplex uptake. Taken together, the cellular uptake mechanism studies suggest that the internalization of NAC-6/pDNA polyplex is mediated by more than one endocytosis pathway including both clathrin-mediated endocytosis (major pathway) as well as macropinocytosis (minor pathway).

3.3.12. In vitro gene transfection

A desirable level of gene expression is the key consideration in the design of a suitable gene delivery vector. All gene transfection studies were performed in the presence of 10% FBS containing medium. To compare the gene transfer capacity of different NAC-6 polymers, transfection experiments were performed on HEK 293 and HeLa cells using pGFP and pβ-gal as reporter genes. As illustrated in Figure 29, a clear dependence of transfection efficiency on degree of hexanoic acid substitution was observed. The transfection efficiency was improved when the substitution degree increased, reached the peak value at about 15%, and then decreased at higher substitution of 25%. In HEK 293 cells, the NAC-6(15)/pGFP polyplexes at an N/P ratio of 20 exhibited the optimum level of transfection with 95.3% of GFP positive cells, which was 13.2-fold higher compared to the chitosan/pGFP polyplexes and 1.33-fold higher than the transfection efficiency mediated by the FuGENE HD (Figure 29A).

The transfection efficiency of NAC-6 polymers was also evaluated in terms of β-galactisidase activity (Figure 29B). The results of quantitative analysis were in the agreement with the confocal images of GFP transfected cells (Figure 30). The trend of transfection efficiency of NAC-6 polymers was further confirmed in HeLa cells. However, the overall in vitro gene transfection efficiency in HeLa cells [i.e., 64.5% of GFP positive cells for NAC-6(15)] was much lower than that in HEK 293 cells, which was attributed to the fact that transfection efficiency of the NAC-6 polymers is cell line dependent as described by previous reports (Lu et al., 2009; Mao et al., 2001).

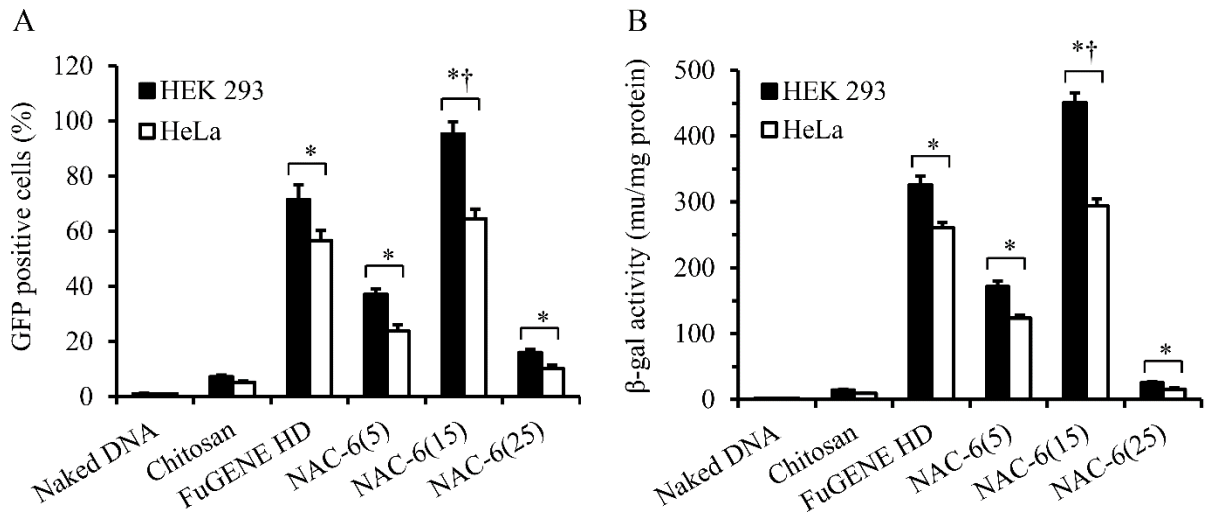

Figure 29. In vitro transfection efficiency of chitosan and NAC-6 polyplexes in HEK 293 and HeLa cells at N/P ratio of 20. (A) Transfection efficiency at cellular level using pGFP plasmid. (B) Transfection efficiency at protein level using pβ-gal plasmid. Data represents the mean ± SD (n = 4). ['*' indicates significantly ($p < 0.05$) greater than chitosan; '†' indicates significantly ($p < 0.05$) higher than FuGENE HD].

In vitro assessment of all NAC-6 polymers and NAC-6/pDNA polyplexes demonstrated that higher transfection activity of NAC-6(5) and NAC-6(15) were correlated with the increased pDNA release from polyplexes as a result of decreased interaction between NAC-6 nanocomplexes and pDNA, enhanced stability of polyplexes in 10% FBS containing medium, and improved cell uptake. Thus, the NAC-6(5) and NAC-6(15) exhibited an overall

improvement in gene transfection efficiency as compared with chitosan, which was achieved by finding the appropriate balance between polyplex stability and timely pDNA release. However, despite faster pDNA release, NAC-6(25)/pDNA polyplexes showed lower transfection efficiency as compared to NAC-6(15)/pDNA and NAC-6(5)/pDNA polyplexes, which might be explained by poor buffering capacity of NAC-6(25) polymer, weaker binding affinity between pDNA and polymer resulting in premature pDNA release, and reduced cell uptake.

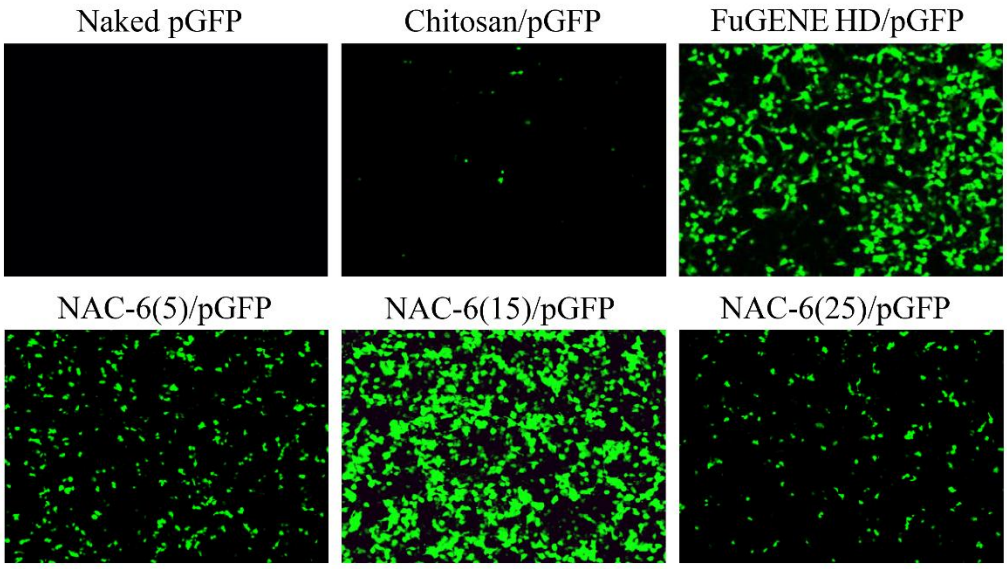

Figure 30. Confocal images of GFP transfected HEK 293 cells. Images were taken at 10× magnification after 48 h of transfection.

3.4. Conclusions

In summary, a series of hexanoic acid grafted chitosan with variable degree of amino substitutions was synthesized as a promising nonviral gene delivery vector. We demonstrated that the degree of hexanoic acid substitution greatly affected the pDNA binding, polyplex stability, cellular uptake, polyplex unpacking, and transfection efficiency. The synthesized graft polymers as well as polymer/pDNA polyplexes were nontoxic under experimental conditions. We found that the intermediate level of hydrophobic modification of chitosan with NAC-6(15)

was favorable for pDNA delivery as suggested by multi-fold improvement in cellular internalization and transgene expression compared to chitosan. Therefore, our results can serve as guide for the design of novel N-acyl derivatives of chitosan as safe and effective nonviral gene delivery vectors.

4. AMINO ACID CONGUGATED CHITOSAN FOR GENE DELIVERY: EFFECT OF AMINO ACID HYDROPHOBICITY

4.1. Introduction

Gene therapy has emerged as a powerful tool to treat many innate or acquired diseases by delivering missing genes, replacing defective genes, or silencing undesired gene expression. Large size, high anionic charge density, and susceptibility toward nuclease degradation are considerable barriers to efficient delivery of DNA into the targeted cells. Recombinant viruses have served as efficient transfection vectors in many experimental studies (Carrillo-Carrasco et al., 2010; Kay et al., 2001; Vigna and Naldini, 2000). However, issues of carcinogenicity, immunogenicity, and inflammation, as well as restrictions in nucleic acid cargo size impose serious concerns for clinical applications of viral vectors (Check, 2005; Hacein-Bey-Abina et al., 2003; Raper et al., 2003; Thomas et al., 2003). The challenges confronted with viral vectors have accelerated the search for alternative, nonviral vectors (Needham et al., 2012; Pack et al., 2005). One of the promising contenders as a nonviral vector is chitosan, a natural copolymer of randomly distributed N-acetyl-D-glucosamine and β-(1, 4)-linked D-glucosamine derived from partial deacetylation of chitin. The last decade has witnessed an increasing interest in chitosan-based vectors due to their availability, biocompatibility, biodegradability, low cytotoxicity, ease of chemical modification, and high cationic charge density (Du et al., 2010; Lee et al., 1998; Malmo et al., 2011). However, the gene transfection efficiency of unmodified chitosan is too low for practical application. Studies have demonstrated that the strong ionic interactions between chitosan and DNA have possibly prevented the unpacking of condensed DNA from chitosan and ultimately reduced gene expression (Hoggard et al., 2004). Moreover, the poor cellular uptake of

chitosan/DNA polyplexes has a negative impact on the transfection efficiency (Layek and Singh, 2012).

To address these issues, various chemical modifications have been executed on chitosan through easily modifiable primary amine and hydroxyl groups. Among them, hydrophobic modifications of chitosan have displayed promising results. Incorporation of hydrophobic units into cationic polymers enhances their adsorption to the lipophilic cell membranes and facilitates adsorption-mediated endocytosis of the polymer/pDNA polyplexes (Wong et al., 2007). Furthermore, hydrophobic modification of cationic polymers have shown facilitated dissociation of polymer/DNA which enhances the release of DNA that would otherwise remain strongly bound through ionic interactions between phosphate groups of DNA and cationic units of polymers (Gabrielson and Pack, 2006). These unique advantages of hydrophobic modification may lead to a superior transfection efficiency for chitosan over other polymeric systems using ionic interactions alone. With this object, chitosan has been modified with numerous hydrophobic moieties such as alkyl (Liu et al., 2003), acyl (Hu et al., 2006), cholesterol (Son et al., 2004), deoxycholic acid (Lee et al., 2005), 5β-cholanic acid (Yoo et al., 2005), and urocanic acid (Kim et al., 2003).

Chitosan-peptide derivatives have recently received increasing interest in drug and gene delivery applications because of their distinct benefits of enhanced cell adsorption as well as excellent safety profile (Casettari et al., 2012). However, the transfection potential of hydrophobic amino acid modified chitosan has yet to be explored. The grafting of a hydrophobic amino acid to chitosan would result in amphiphilic derivatives, which promote the formation of nanoscale micellar structures in aqueous environments and enhance membrane permeability of the polymer/pDNA polyplexes (Yuan et al., 2011). The objective of this study was to investigate

the gene transfection performance of hydrophobic amino acid modified chitosan and to evaluate the influence of hydrophobicity of an amino acid pendant on the different steps of the gene delivery process. To accomplish our goal, low molecular weight chitosan was modified with L-alanine, L-valine, L-leucine, L-isoleucine, and L-phenylalanine with the relative hydrophobicity indices of 41, 76, 97, 99, and 100, respectively (Monera et al., 1995). The graft polymers were characterized and their complexation with pDNA, in vitro pDNA release rate, cellular uptake, in vitro transfection efficiency, cytotoxicity, and blood compatibility were investigated.

4.2. Materials and methods

4.2.1. Materials

Chitosan (Mw ~ 50 kDa, 91% deacetylated), N-Acetyl-L-alanine, N-Acetyl-L-valine, N-Acetyl-L-leucine, N-Acetyl-L-isoleucine, N-Acetyl-L-phenylalanine, MTT, and FITC were purchased from Sigma-Aldrich (St. Louis, MO, USA). EDC.HCl was obtained from Creosalus Inc (Louisville, KY, USA). DNase I was procured from Rockland Inc (Gilbertsville, PA, USA). N-hydroxysuccinimide (NHS) and heparin sodium were purchased from Alfa Aesar (Ward Hill, MA, USA). pβ-gal and pGFP were from Aldevron LLC (Fargo, ND, USA). HEK 293 cell lines, PBS, and DMEM were obtained from American Type Culture Collection (ATCC, Rockville, MD, USA). FuGENE HD was purchased from Roche Diagnostics (Indianapolis, IN, USA). Agarose and β-galactosidase enzyme assay kit were purchased from Promega (Madison, WI, USA). All other chemicals were of analytical grade and used without further modification.

4.2.2. Synthesis of amino acids grafted chitosan (AGC)

AGC polymers were synthesized by the reaction of the free carboxyl group of amino acids with the free primary amine groups of chitosan in presence of EDC/NHS (Figure 31) (Yoksan and Akashi, 2009). Chitosan (0.6 g) was dissolved in 50 mL acidified distilled water at

pH 5.0. N-acetyl amino acid (0.3 mol/mol of D-glucosamine of chitosan) and EDC (3 mol/mol of amino acid) were dissolved in ethanol and stirred for 1 h followed by the addition of NHS (3 mol/mol of amino acid). The mixture of amino acid solution containing EDC and NHS was added drop wise to the chitosan solution under constant stirring and the reaction was continued at room temperature for 24 h. The reaction mixture was then refluxed with 1 N hydrochloric acid for 0.5 h to remove the N-acetyl protecting groups of amino acids (Goswami et al., 2005). Then the solution was cooled to room temperature, and neutralized with 1 N NaOH. Finally, the resulting polymer was dialyzed using dialysis membrane (MWCO: 6-8 kDa) against distilled water for 48 h followed by freeze-drying.

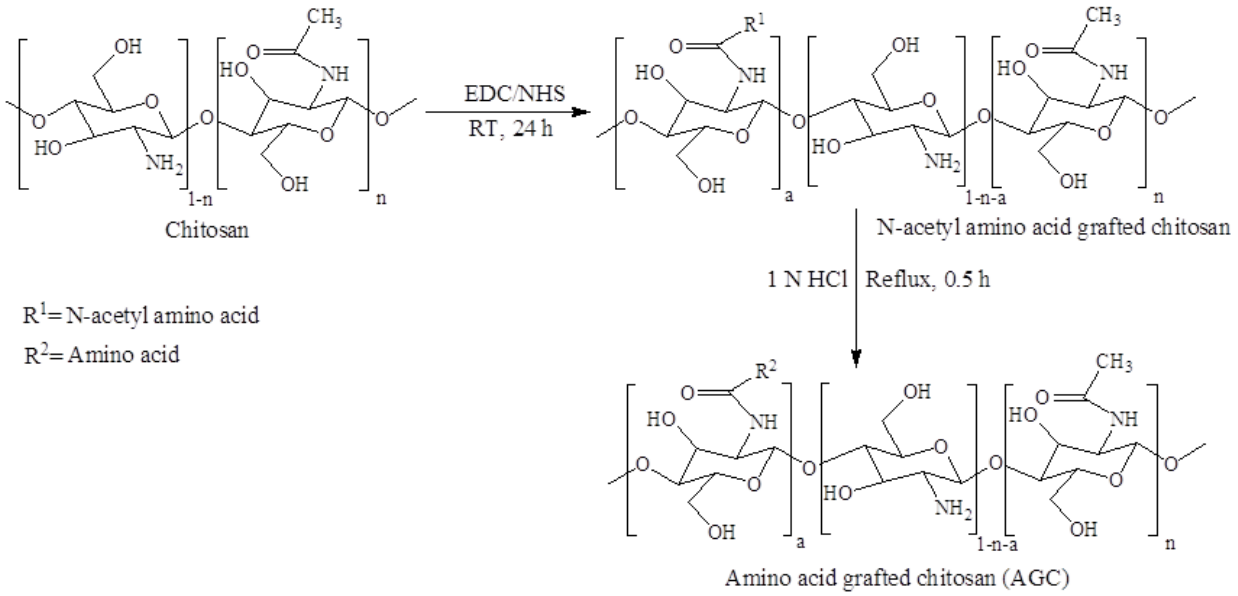

Figure 31. Schematic representation for the synthesis of AGC polymers.

4.2.3. Structural characterization of AGC polymers

The chemical structure of polymers was confirmed by ^{1}H NMR. For the ^{1}H NMR study, chitosan and AGC polymers were dissolved at a concentration of 1 mg/mL in deuterated water with 1% DCl. The ^{1}H NMR spectra were examined using a Mercury Varian 400 MHz spectrometer at 25°C.

4.2.4. Endosomal buffering capacity

The endosomal buffering capacity of AGC polymers was determined by simple acid-base titration as reported by Benns et al. (2002). Briefly, 20 mg of AGC polymer was dissolved in 20 mL of 150 mM NaCl and the solution was set to pH 10 by the addition of 0.1 N NaOH. The titration was accomplished by stepwise addition of 20 µL of 0.1M HCl followed by pH measurement at 25°C using a pH meter. The buffering capacities of chitosan and the AGC polymers were calculated using the following equation (Piest and Engbersen, 2010):

$$\text{Buffering capacity (\%)} = (\Delta V_{pol} - \Delta V_{NaCl}) \times 0.1\ M/N \times 100$$

where ΔV_{pol} and ΔV_{NaCl} are the volumes of 0.1 M HCl required to change the pH from 7.4 to 5.1 in polymer solution and 150 mM NaCl solution, respectively. The value of ΔV_{NaCl} was found to be negligible within this pH range. N is the total amount (mmol) of protonable amine groups in each titration.

4.2.5. Determination of critical micelle concentration (CMC)

The CMC of the AGC polymers was determined by fluorescence measurement using pyrene probe method (Ye et al., 2008). The fluorescence emission spectrums of pyrene with varying concentrations of polymer ranging from 5-1000 µg/mL were taken with a Fluoromax-4 spectrofluorometer (Horiba Jobin Yvon, NJ, USA) at 25°C. The experimental concentration of pyrene was maintained at 0.6 µM. The excitation wavelength (λ_{ex}) was 336 nm and emissions were recorded between 360-450 nm. Both the excitation and emission slit widths were fixed at 2 nm. The ratio of the fluorescence intensities of peak I (372 nm) to peak III (395 nm) of pyrene was also calculated.

4.2.6. Polymer/pDNA polyplexes preparation and characterization

The polymer/pDNA polyplexes of desired weight ratios were prepared by mixing varying concentrations of polymeric solutions with 0.1 mg/mL of pDNA solution while gently vortexing and then incubated for 30 min at room temperature. The polyplexes were made in 20 mM sodium acetate/acetic acid buffer at pH 6.5. The volume average hydrodynamic diameters and zeta potentials of the polymer/pDNA polyplexes at different weight ratios were measured by DLS method using Zetasizer Nano ZS at 25°C. The pDNA concentration of each sample was kept at 10 µg/mL.

4.2.7. Agarose gel retardation assay

The association of pDNA with AGC polymers was monitored by agarose gel electrophoresis. The polyplexes containing 1 µg of pDNA at different weight ratios were loaded on to 0.8% (w/v) agarose gel stained with EtBr (0.5 µg/mL) and electrophoresed at 80 V in 0.5× TAE buffer for 80 min. The resulting pDNA migration patterns were visualized and recorded using a UV transilluminator at 254 nm.

4.2.8. Protection of pDNA against nucleases

The stability of AGC/pDNA polyplexes against nuclease degradation was monitored by DNase I protection assay (Layek and Singh, 2012). AGC/pDNA polyplexes, containing 2 µg of pDNA in 20 µL of DNase reaction buffer, were incubated at 37°C under shaking at 50 rpm for 60 min with 1 unit of DNase I. Naked pDNA with DNase I served as a positive control. After incubation, the DNase reaction was stopped by adding 5 µL of an aqueous EDTA (100 mM) solution. Subsequently, 20 µL of heparin solution (5 mg/mL) was added to each sample and incubated at 37°C for 2 h to release pDNA from the complex. To confirm the integrity, released pDNA was subjected to electrophoresis on 0.8% (w/v) agarose gel.

4.2.9. In vitro release of pDNA

AGC/pDNA and chitosan/pDNA polyplexes, containing 50 µg of pDNA at weight ratio of 40, were dispersed in 20 mL of PBS (pH 7.4). The polyplex suspension was incubated at 37°C in a reciprocal shaking water bath at 50 rpm. At different time points, 0.5 mL of suspension was centrifuged at 30,000 × *g*, 4°C for 30 min. The amount of unbound pDNA in the supernatant was quantified by spectrofluorimeter after staining with Hoechst dye 33342.

4.2.10. Fluorescence labeling of AGC polymers

FITC-labeled AGC polymers were synthesized by the reaction between free primary amino groups of AGC and the isothiocyanate group of FITC (Ge et al., 2009). Briefly, 10 mg of AGC polymer was dissolved in 5 mL of distilled water. FITC (1 mg) was dissolved in 1 mL of dehydrated methanol. The methanolic solution of FITC was added drop wise to the AGC solution with moderate stirring and the reaction was continued overnight in the dark at room temperature. The FITC-labeled AGC polymers were precipitated using 0.1 M NaOH and washed five times with dehydrated methanol to remove unreacted FITC. Finally, the FITC-labeled AGC polymer was dissolved in 20 mL of water and dialyzed using a dialysis membrane against distilled water for 48 h, followed by lyophilization.

4.2.11. Blood compatibility study

Hemolytic activity as well as morphological analysis of rat erythrocytes was performed in vitro to estimate the blood compatibility of AGC polymers (Zhou et al., 2012). The erythrocytes were harvested from freshly withdrawn blood from Sprague-Dawley rats followed by centrifugation at 1500 rpm for 10 min using Microfuge 18 centrifuge (Beckman Coulter, CA, USA) and washed three times with PBS. The pelleted erythrocytes were resuspended in PBS to a concentration of 5×10^9 cells/mL. Then, 100 µL of this cell suspension was incubated with 900

µL of the solution of AGC polymers, with varying concentrations, at 37°C for 1 h. Cells treated with PBS and 1% Triton X-100 were used as negative and positive control, respectively. After incubation, the cell suspension was centrifuged at 1500 rpm for 10 min using Microfuge 18 centrifuge and the supernatant solution was used to measure the absorbance of the released hemoglobin using a SpectraMax M5 plate reader at 540 nm. The percent hemolysis was calculated by the following equation:

$$\text{Hemolysis (\%)} = (A - A_0)/(A_{100} - A_0) \times 100$$

where A, A_0 and A_{100} correspond to the absorbance of polymer sample, negative, and positive control, respectively.

The morphology of the erythrocytes, incubated with different AGC polymers as mentioned above, was observed using an Olympus DP72 microscope at 40× magnification.

4.2.12. In vitro cytotoxicity

The cytotoxicity of AGC polymers as well as AGC/pDNA polyplexes was assessed by MTT assay (Lu et al., 2009). HEK 293 cells were plated onto a 96-well plate at 1×10^4 cells/well in 150 µL DMEM culture medium containing 10% FBS and allowed to adhere overnight. The next day, the growth medium was removed and the cells were washed with PBS. The cells were then incubated with different concentrations (100-1000 µg/mL) of polymers or AGC/pDNA polyplexes at various weight ratios (5, 10, 20, 30, 40, and 50) for 48 h. After treatment, polymer or AGC/pDNA polyplex solution was removed and the cells were incubated with 100 µL of MTT (1 mg/mL) solution for another 3 h under the same conditions. Then, the MTT containing culture medium was discarded and formazan crystals produced by live cells were dissolved in 150 µL of dimethyl sulfoxide. Finally, the absorbance at 570 nm was determined using a microplate reader. Non treated cells were considered as control and incubated in similar

conditions for the same period of time. The relative cell viability (%) was calculated by the following equation.

$$\text{Cell viability (\%)} = (OD_{sample}/OD_{control}) \times 100$$

4.2.13. Cellular uptake

To evaluate the cellular uptake, FITC-labeled AGC polymers and pDNA were allowed to form stable polyplexes at the weight ratio of 40. The weight ratio 40 was selected based on the size of the polyplexes. HEK 293 cells were seeded onto 6-well plate and transfected with FITC-AGC/pDNA polyplexes containing 4 µg of pDNA/well. After 4 h of transfection at 37°C, cell uptake was terminated by removing polyplex containing culture medium and washing the cells several times with PBS. FITC-positive HEK 293 cells were visualized by an Olympus FV300 confocal microscope and quantitatively determined by flowcytometer.

4.2.14. In vitro gene transfection

In vitro gene transfection efficacy of AGC polymers was evaluated in HEK 293 cells using pβ-gal and pGFP as model plasmids. To simulate the physiological conditions, gene transfection experiments were carried out in the presence of 10% FBS containing growth medium. Cells were plated onto a 24-well plate at a density of 1×10^5 cells/well with 0.5 mL of DMEM/high glucose medium for 24 h to achieve ~ 60-70% confluency prior to transfection. Following this, the pβ-gal or pGFP polyplexes containing 1 µg of pDNA at various weight ratios were incubated with the cells. FuGENE HD was used as positive control and the transfection assay was carried out according to the manufacturer's protocol. After 4 h of incubation, the transfecting media was replaced with fresh complete media and the cells were incubated for another 48 h. For the GFP transfection studies, the percentage of GFP transfected cells was determined by FACS analysis. GFP positive cells were also visualized and photographed with a

FV300 confocal laser scanning microscope at 20× magnification. To assay the β-galactosidase expression, the growth medium was removed and the cells were washed with PBS. After thorough lysis of the cells with reporter lysis buffer, the β-galactosidase enzyme activity was measured using β-galactosidase assay kit at 450 nm. The total protein per milligram of the cell lysate was determined by micro BCA assay.

4.3. Results and discussion

4.3.1. Synthesis of AGC polymers

The AGC polymers were synthesized by EDC/NHS mediated coupling reaction between chitosan and amino acid. L-alanine, L-valine, L-leucine, L-isoleucine, and L-phenylalanine were used to obtain AGC-A, AGC-V, AGC-L, AGC-I, and AGC-F graft polymers, respectively. We used N-acetyl amino acids in order to prevent self-association of amino acids molecules during the coupling reaction. The excess coupling reagents and unreacted amino acid were eliminated by dialysis with distilled water.

4.3.2. Structural characterization of AGC polymers

The chemical reaction between the chitosan and amino acids was confirmed by ^{1}H NMR (Figure 32) spectroscopy. For chitosan, the peak at 2.0 ppm was assigned to the three acetyl protons of N-acetyl glucosamine and the peak at 3.15 ppm revealed the H2 proton of the glucosamine or N-acetyl glucosamine residue. The ring protons (H-3, 4, 5, 6, 6') of chitosan appeared between 3.6-4.0 ppm. After coupling with amino acids, the new peaks at 0.9 (except for AGC-A and AGC-F) and 1.1 ppm confirmed the successful grafting of amino acid molecules on the chitosan backbone. The phenyl ring protons of AGC-F appeared between 7.2-7.4 ppm. The degree of amino acid substitution was ~ 15% as determined by the elemental analysis.

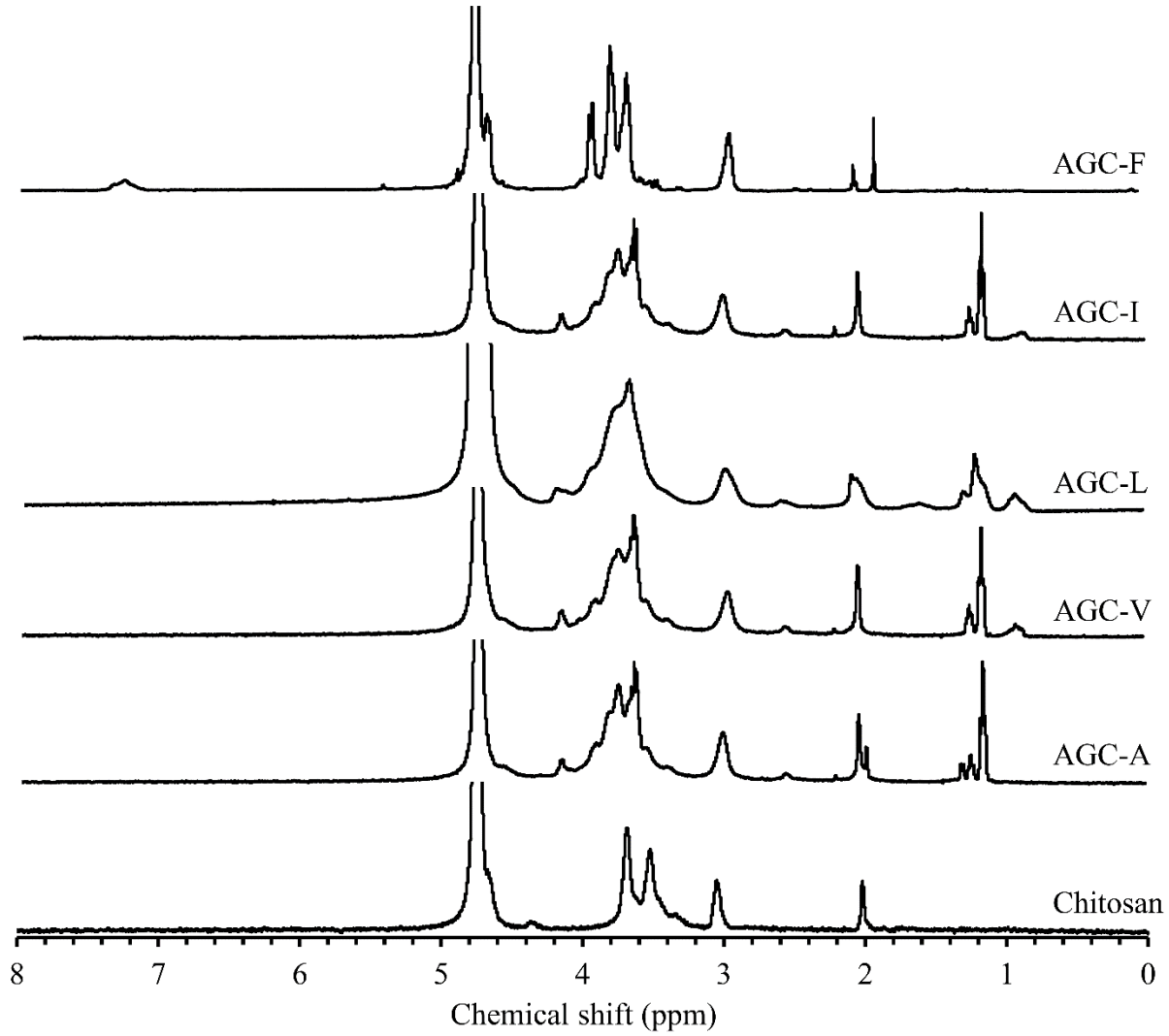

Figure 32. ^{1}H NMR spectra of chitosan and different AGC polymers.

4.3.3. Endosomal buffering capacity

A good nonviral gene delivery vector should escape the endolysosomal degradation pathway (Mansouri et al., 2004). The buffering capacity of a cationic polymer is an important feature that can facilitate the endolysosomal escape of polyplexes via the proton-sponge mechanism to mediate enhanced gene expression (Tang and Szoka, 1997).The buffering capacity of each AGC polymer was calculated as the percentage of amine groups that become protonated between pH 7.4 to 5.1. As shown in Figure 33, AGC polymers exhibited comparable buffering

capacity as that of unmodified chitosan. The buffering capacity of chitosan, AGC-A, AGC-V, AGC-L, AGC-I, and AGC-F were 75.1%, 70.8%, 65.2%, 69.5%, 70.5%, and 68.0%, respectively.

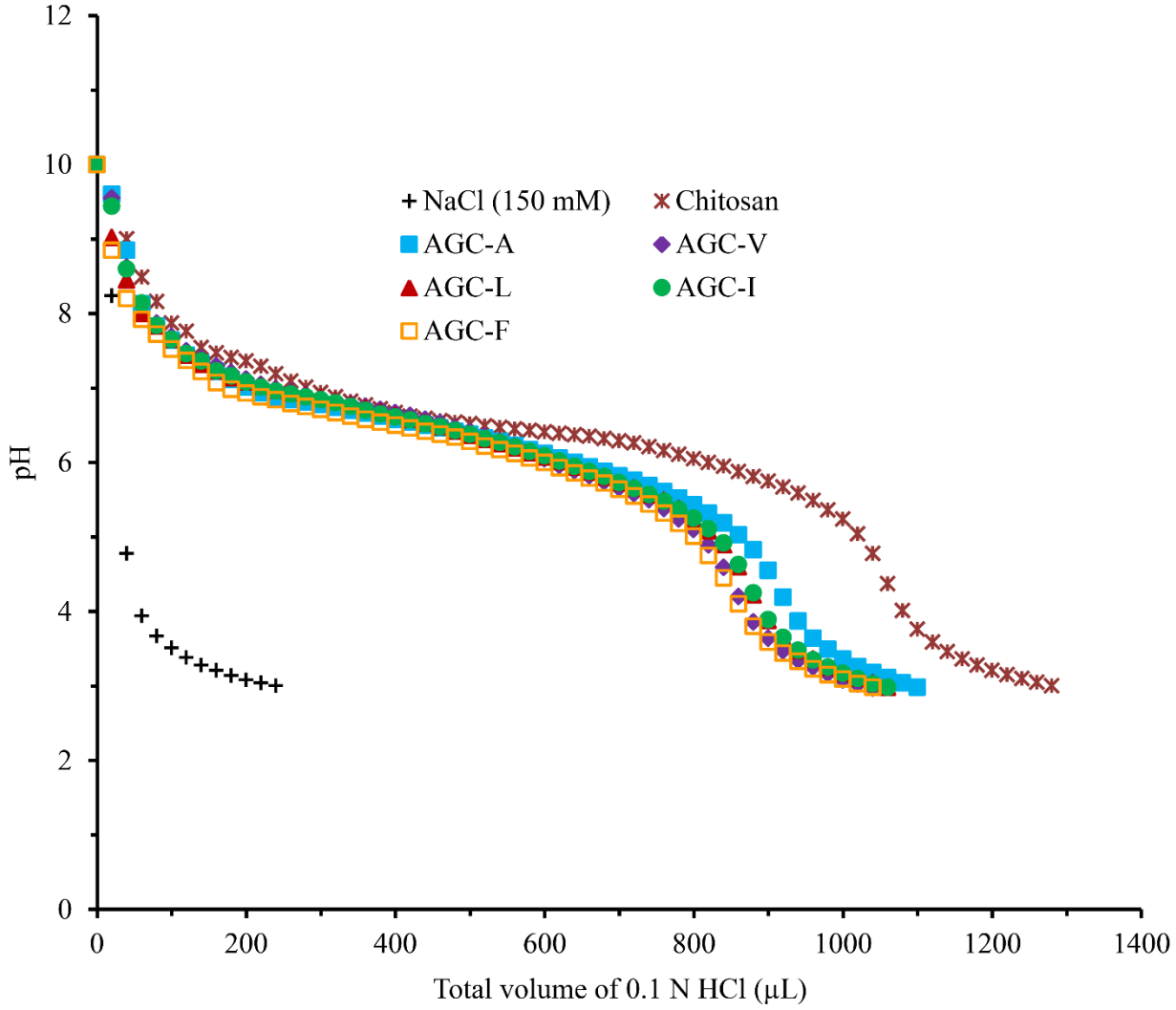

Figure 33. Endosomal buffering capacity of chitosan and different AGC polymers.

4.3.4. Determination of CMC

The CMC of AGC polymers in aqueous media was examined by dye solubilization method using pyrene as a fluorescent molecular probe. The CMC values of AGC-A, AGC-V,

AGC-L, AGC-I, and AGC-F were 160, 110, 90, 90, and 70 µg/mL, respectively, and decreased with increasing hydrophobicity of the amino acid substituent.

4.3.5. Characterization of AGC/pDNA polyplexes

Appropriate particle size and positive zeta potential of polyplexes are important for cellular uptake and efficient gene transfection. Previous study reported that cells usually uptake complexes within the size range of 50 to several hundred nanometers (Liu and Reineke, 2005). The mean diameter of AGC/pDNA polyplexes as a function of weight ratio was demonstrated in Figure 34A. At a weight ratio of 1, AGC polymers formed large particles due to the inadequate cationic charge for pDNA condensation. The particle size was found to decrease with the increasing polymer/pDNA weight ratio, indicating better condensation of pDNA because of the higher amount of available protonated amine of AGC. There is no appreciable decrease in particle size above weight ratio of 40. At the weight ratio of 40, AGC/pDNA polplexes had particle size ranging from 160.8 to 181.7 nm with a narrow polydispersity index of 0.11-0.19. As demonstrated in Figure 34B, at weight ratio of 1, AGC/pDNA polyplexes had nearly neutral surface charge. When the AGC/pDNA weight ratio increased to 5, the zeta potential of the polyplexes was found to have increased sharply. Zeta potential further increased with the increasing weight ratio of AGC/pDNA polyplexes. Thus, the results of DLS study demonstrated the formation of nanosized polyplexes with net cationic surface charge.

4.3.6. Agarose gel retardation assay

The formation of stable polyplexes between AGC polymers and pDNA was examined by agarose gel retardation assay. Naked pDNA was used as a positive control. As shown in Figure 35A, the presence of partially dissociated pDNA in lane b indicated the formation of physically unstable polyplexes at weight ratio of 0.2. When the polymer/pDNA weight ratios increased to ≥

5, migration of pDNA was completely retarded, indicating tight complex formation between AGC polymers and pDNA.

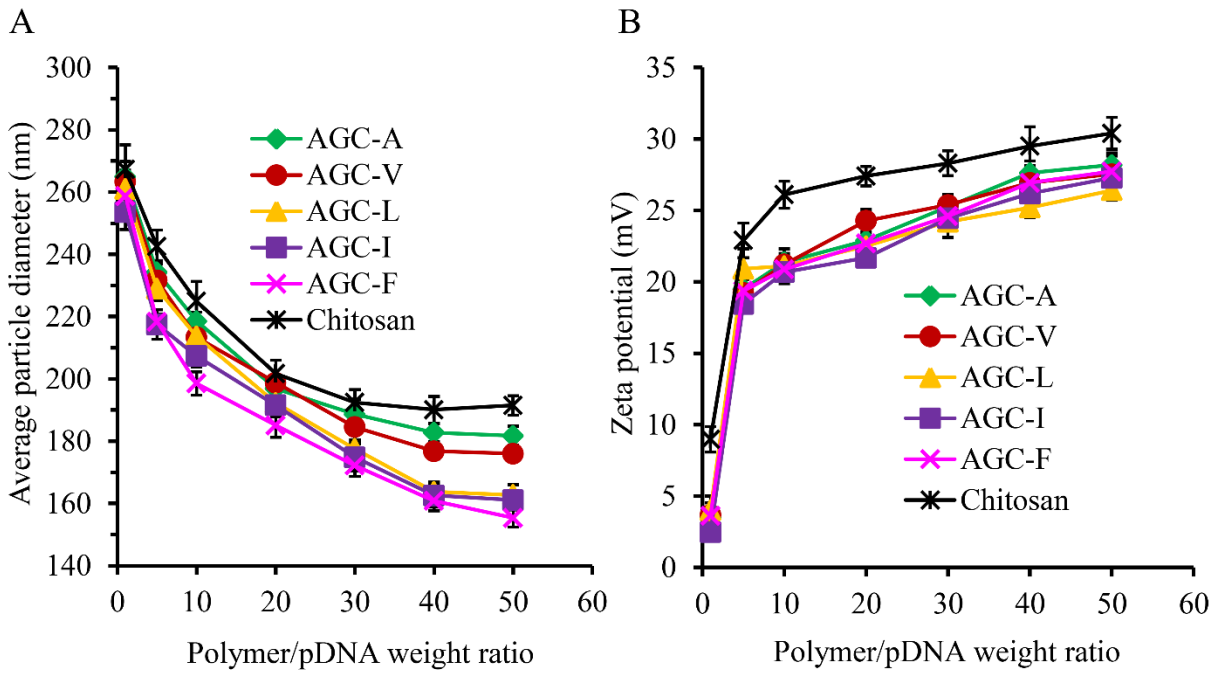

Figure 34. (A) Average particle sizes and (B) zeta potentials of AGC/pDNA and chitosan/pDNA polyplexes prepared at various weight ratios. Data represents the mean ± SD (n = 6).

4.3.7. Protection of pDNA against nucleases

The integrity of pDNA is critical to ensure its desired function in vitro and in vivo. Therefore, the gene delivery system should efficiently protect condensed pDNA from enzymatic degradation (Katayose and Kataoka, 1998). The effect of AGC polymers on protection of pDNA against nuclease degradation was monitored using DNase I as a model enzyme. As shown in Figure 35B, the naked pDNA was vulnerable to enzymatic degradation as evidenced by the absence of band for pDNA. In contrast, chitosan/pDNA and AGC/pDNA polyplexes displayed distinct protection of condensed pDNA from DNase I at all weight ratios (5, 10, 20, 30, 40, and 50) investigated. These results clearly suggest that AGC polymers could be used as efficient gene carriers for transporting pDNA inside the cells without enzymatic degradation.

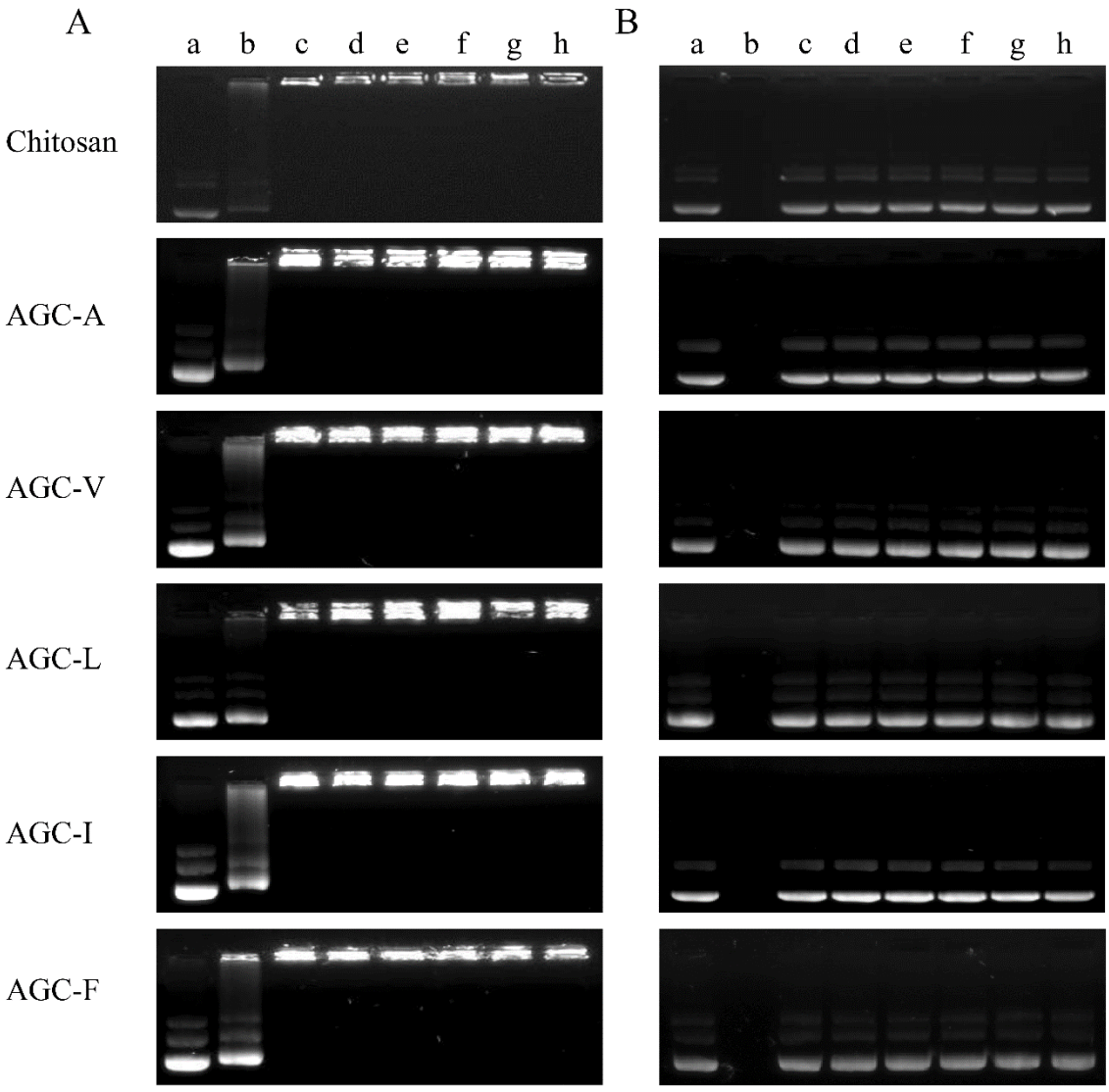

Figure 35. (A) Agarose gel retardation assay of chitosan/pDNA and AGC/pDNA polyplexes at different weight ratios. Lane a: naked DNA; Lanes b-h: polymer/pDNA polyplexes at the weight ratios of 0.2, 5, 10, 20, 30, 40, and 50, respectively. (B) DNase I protection assay of chitosan/pDNA and AGC/pDNA polyplexes prepared at different weight ratios. Lane a: naked DNA; Lane b: naked DNA + DNase I; Lanes c-h: polymer/pDNA polyplexes (at the weight ratios of 5, 10, 20, 30, 40, and 50, respectively) + DNase I.

4.3.8. In vitro release of pDNA

Though the formation of a stable complex is an important criterion to provide efficient protection of condensed pDNA from extracellular nucleases and endolysosomal degradation, nuclear localization and gene expression are not attained unless the condensed pDNA is released

from the polyplexes (Schaffer et al., 2000). Therefore, the balance between the polyplex stability and intracellular pDNA release needs to be fine-tuned to maximize gene expression (Chen et al., 2008b). Incorporation of hydrophobic or hydrophilic segments to the polymeric backbone has appeared as an effective strategy to reduce polymer/pDNA binding force (Pack et al., 2005). Figure 36 shows the cumulative in vitro release profile of pDNA from polyplexes prepared at a weight ratio of 40. PBS at pH 7.4 was used as the release medium to simulate the existing pH environments of the cytoplasm and nuclei. After a 48 h time period, the cumulative release percentages from AGC-A/pDNA, AGC-V/pDNA, AGC-L/pDNA, AGC-I/pDNA, and AGC-F/pDNA polyplexes were increased to 18.8, 21.9, 25.3, 25.7%, and 27.1%, respectively as compared to chitosan/pDNA polyplexes from which only 9.1% of condensed pDNA was released. These results clearly indicate that hydrophobic amino acid substitution facilitated the dissociation of pDNA from the polyplexes owing to the hydrophobicity-induced weakening of the electrostatic interaction between pDNA and its carrier (Liu et al., 2003). In addition, a positive correlation of increased hydrophobicity of amino acid substituent with increased pDNA release was observed, which is in accordance with the existing literature (Layek and Singh, 2012). Therefore, the enhanced pDNA release rate combined with excellent DNA protection of AGC polymers render them suitable as an efficient gene delivery vector.

4.3.9. Blood compatibility study

The nonspecific interactions of cationic polymers with blood components are considered a serious limitation to the in vivo application of cationic delivery systems (Yang et al., 2012). These interactions may result in significant decrease in half-life, targetability of the polyplexes, and reproducibility of the medication (Kainthan et al., 2006). The hemocompatibility of the

cationic AGC polymers was evaluated by spectrophotometric measurement of hemoglobin release from erythrocytes after treatment with different concentrations of polymers.

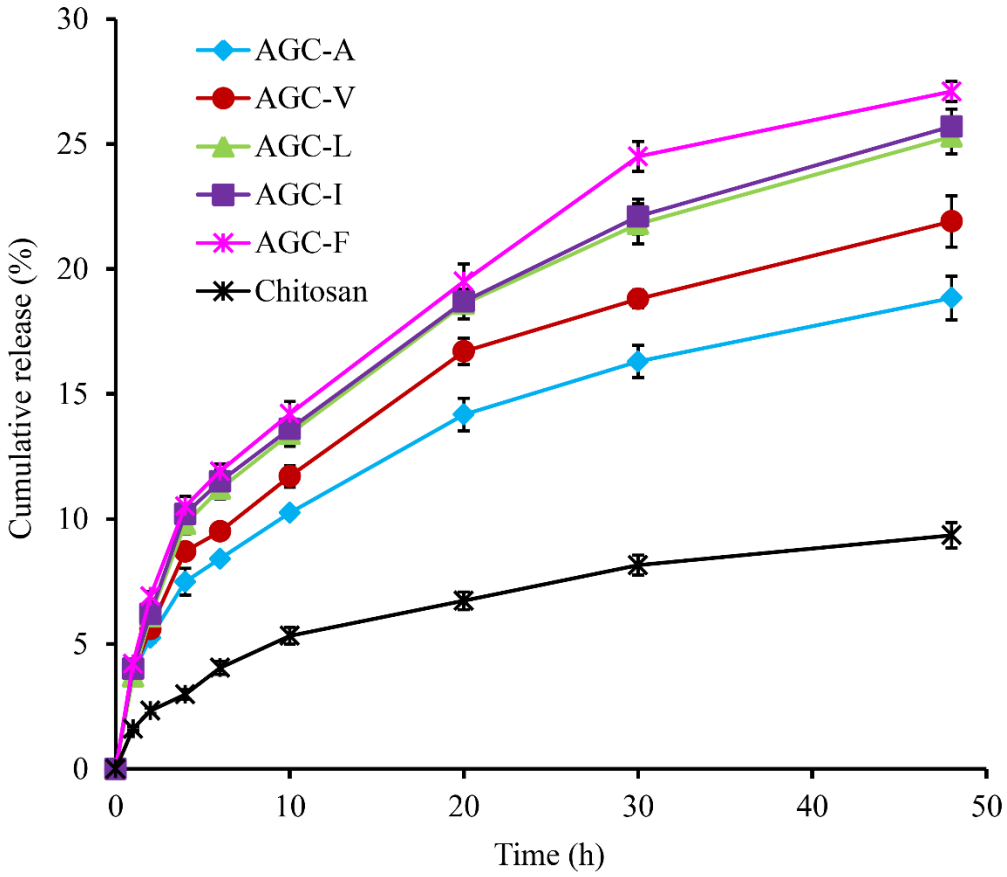

Figure 36. Cumulative pDNA release profiles of different polyplexes. AGC/pDNA and chitosan/pDNA polyplexes were prepared at the weight ratio of 40 and were incubated in PBS (pH 7.4) at 37°C in a reciprocal shaking water bath at 100 rpm. Data represents the mean ± SD (n = 4).

As revealed in Figure 37A, no indication of hemolysis was observed with various AGC polymers, suggesting that the graft polymers did not disrupt the integrity of erythrocyte membrane. The visual observation of the hemolytic phenomenon (Figure 37B) was consistent with the quantitative spectrophotometric measurement. The detailed morphological changes of treated erythrocytes were analyzed by light microscopy at 40× magnification. As shown in

Figure 38, the erythrocytes treated with PBS and different AGC polymers appeared as normal cells with biconcave shape and smooth surfaces. On the contrary, erythrocytes treated with 1% Triton X-100 were completely disrupted, showing significant release of hemoglobin and a large amount of erythrocyte debris. The results of optical morphological study were in accordance with the quantitative hemolysis assay, suggesting no negative effects of cationic AGC polymers on the erythrocyte membranes.

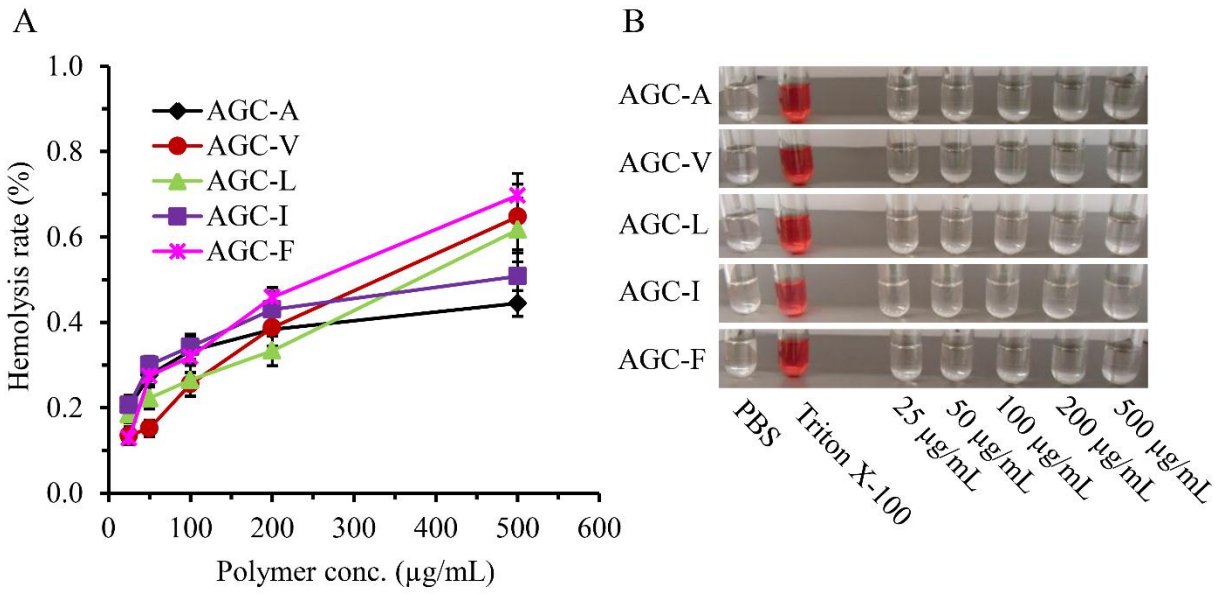

Figure 37. (A) Hemolytic activity of AGC polymers at different concentrations. Hemolytic activity of 1% (v/v) Triton X-100 was set as 100%. Data represents the mean ± SD (n = 4). (B) Visual observation of hemolysis caused by the AGC polymers at different concentrations.

4.3.10. In vitro cytotoxicity

The cationic polymers are reported to comprise some inherent cytotoxicity due to interactions with negatively charged cellular components, proteins, and blood components (Fischer et al., 2003). However, numerous studies have accentuated on the relatively nontoxic character of chitosan-based derivatives (Duceppe and Tabrizian, 2010; Rudzinski and Aminabhavi, 2010).

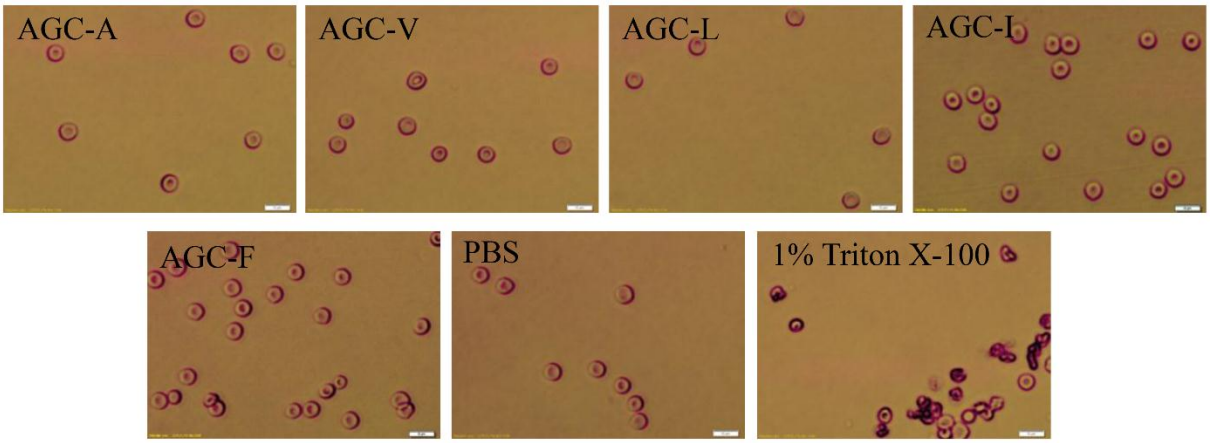

Figure 38. Light microscopic images of rat erythrocytes treated with AGC polymers (500 µg/mL), 1× PBS, and 1% (v/v) Triton X-100. Images were taken at 40× magnification using Olympus DP72 microscope.

As depicted in Figure 39A, AGC polymers did not exerted any noticeable cytotoxicity in HEK 293 cells at concentration below 1 mg/mL, which was 20-fold greater than the maximum polymer concentration used in transfection studies. Moreover, the chain lengths of amino acid substituent did not affect the cell viability. Similarly, AGC/pDNA polyplexes at different weight ratios did not alter the cell viability (Figure 39B) in comparison to control (considered as 100% viability). Thus, the results of MTT assay clearly demonstrate the non toxic nature of the polymers as well as the polyplexes under experimental conditions. This finding suggests that AGC polymers could be used as suitable gene delivery carrier for repetitive administration of large doses of genes of interest.

4.3.11. Cellular uptake

As the site of action for therapeutic genes are usually situated inside the nucleus, the capability of the polyplexes to cross the cell membranes is crucial for effective gene expression. The cell uptake of AGC/pDNA polyplexes by HEK 293 cells was visualized by confocal microscopy as shown in Figure 40. The confocal microscopy results demonstrated that after 4 h of incubation, the FITC-labeled polyplexes were found to be internalized into the cells. Both the

fluorescence intensity and number of FITC-positive cells were increased notably with the increasing hydrophobicity of amino acid substituent.

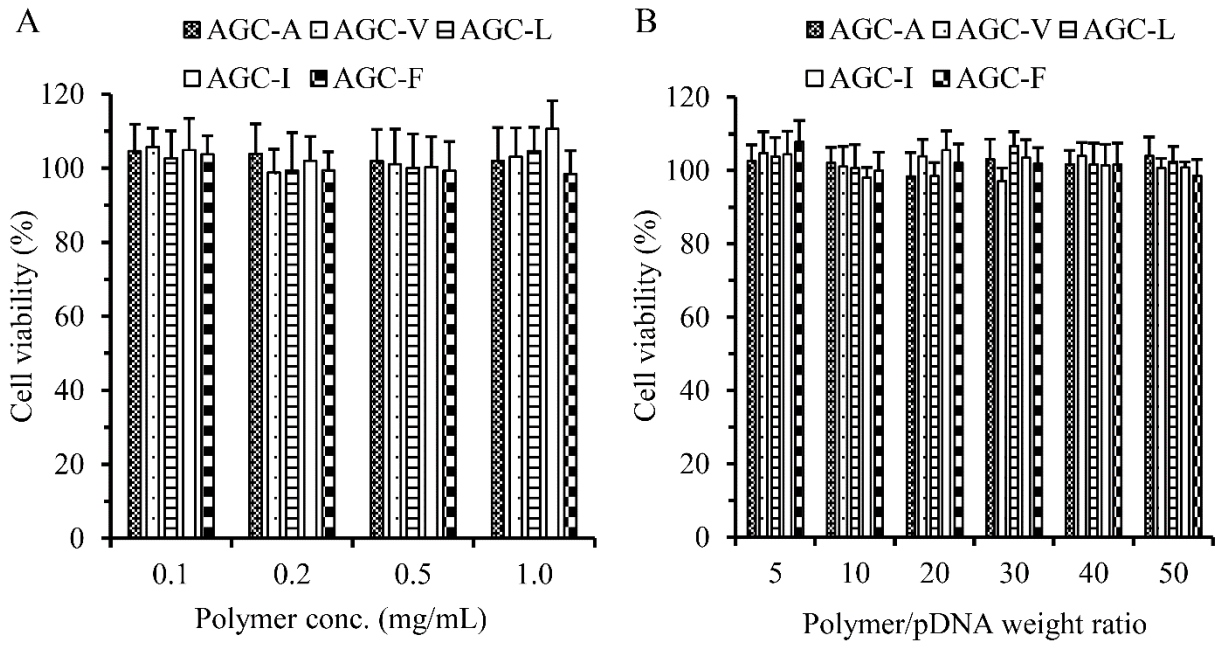

Figure 39. In vitro cytotoxicity of (A) AGC polymers and (B) AGC/pDNA polyplexes in HEK 293 cells. Data represents the mean ± SD (n = 4).

The cell uptake of different polyplexes was also quantitatively measured by FACS analysis. As shown in Figure 41, only 18.3% of FITC-positive cells were mediated by chitosan/pDNA polyplexes while the uptake percentages were elevated by 4-6-fold for AGC/pDNA polyplexes. Since AGC polymers contain both cationic amine groups and hydrophobic amino acids on their backbone, both charge attraction and hydrophobic interactions facilitate the endocytosis mediated uptake process (Piest and Engbersen, 2010). The uptake percentages of AGC-A/pDNA, AGC-V/pDNA, AGC-L/pDNA, AGC-I/pDNA, and AGC-F/pDNA polyplexes were 62.6%, 84.6%, 97.9%, 98.3%, and 99%, respectively. The improved cellular uptake of AGC-L/pDNA, AGC-I/pDNA, and AGC-F/pDNA polyplexes over other

vectors might be attributed to the smaller particle size and better amphiphilicity of the corresponding polymers.

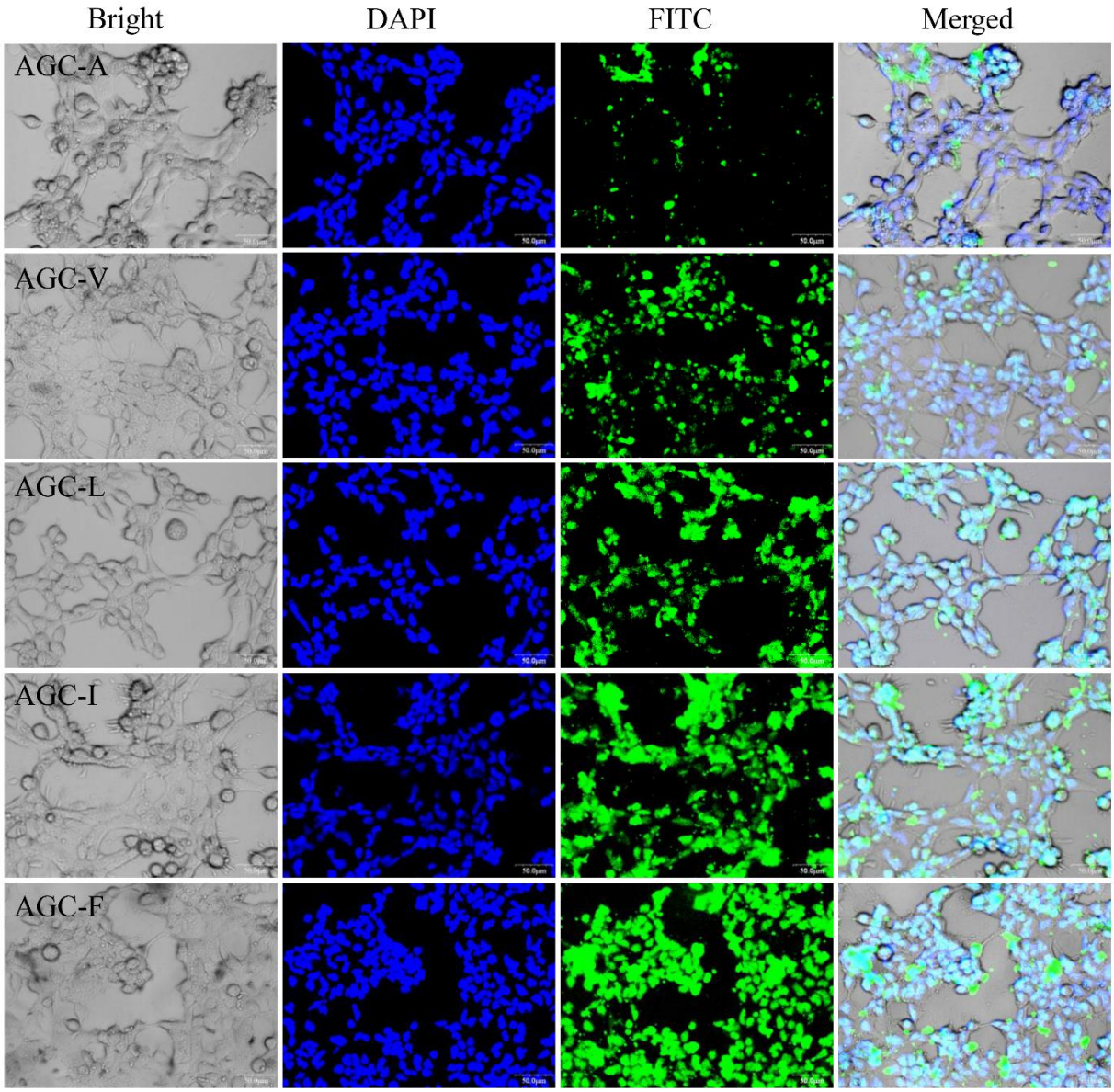

Figure 40. Cellular uptake of FITC-labeled AGC/pDNA polyplexes in HEK 293 cells. Cells were incubated with different polyplexes at 37°C for 4 h. The nuclei of the cells were stained with DAPI. The merged image shows an overlap of the nuclei (blue) and polyplexes (green) within the cells after uptake of polyplexes by HEK 293 cells.

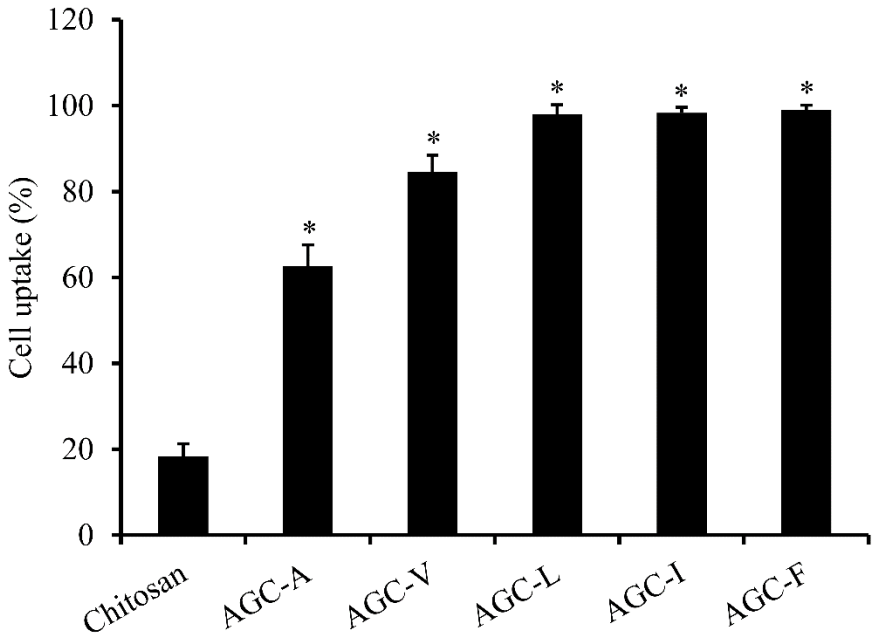

Figure 41. Cellular uptake of chitosan/pDNA and AGC/pDNA polyplexes in HEK 293 cells. Cells were incubated with different polyplexes at 37°C for 4 h. Data represents the mean ± SD (n = 4) ['*' indicates significantly ($p < 0.05$) higher than chitosan].

4.3.12. In vitro gene transfection

A desirable degree of gene expression is the central issue in the design of a suitable gene delivery vector (Wang et al., 2011). To address whether modification of chitosan with hydrophobic amino acids could enhance its gene delivery efficacy, we compared the gene transfection of AGC/pDNA polyplexes with that of chitosan/pDNA polyplexes in HEK 293 cells. As shown in Figure 42, gene transfection ability of the AGC polymers were significantly ($p < 0.05$) higher than chitosan at all weight ratios investigated. Moreover, transfection efficiency of the AGC polymers depended substantially on polymer to pDNA weight ratio. At weight ratio of 5, AGC polymers exhibited low gene transfer capacity. However, the transfection potential of the polyplexes increased with the increasing weight ratios; the optimum weight ratio was found to be 40. The gene transfer capacity of the graft polymers also increased with the increasing hydrophobicity of the amino acid residue (Figure 43). At the weight ratio of 40, AGC-F/pGFP

polyplexes demonstrated the highest level of transfection efficiency with ~ 83% of GFP positive cells which was better than FuGENE HD having only ~ 69% of GFP transfected cells.

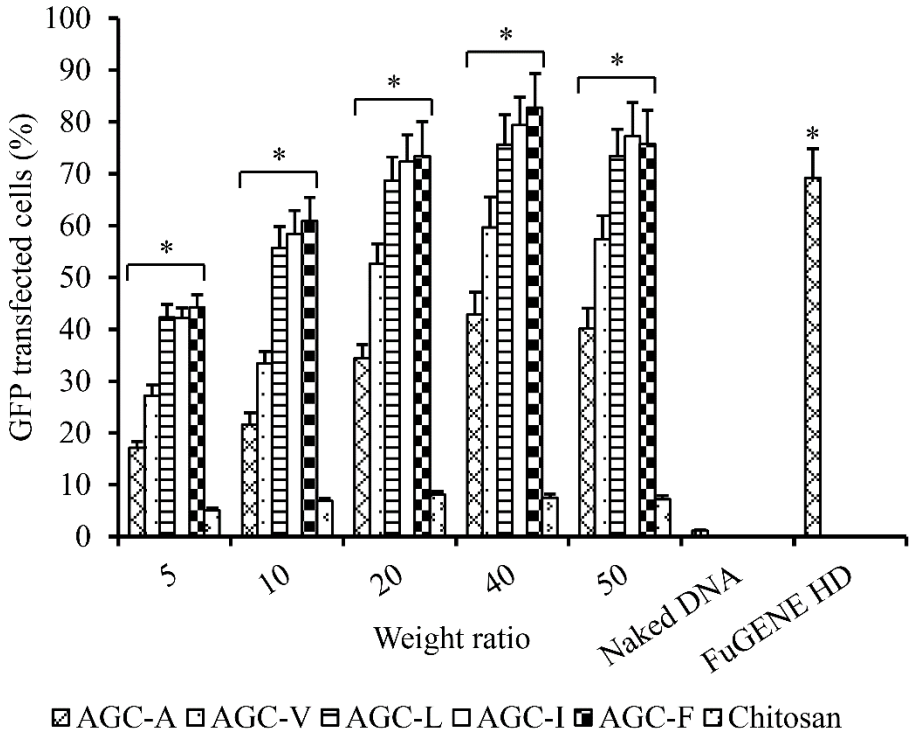

Figure 42. Transfection efficiency of chitosan/pGFP and AGC/pGFP polyplexes at cellular level using pGFP. GFP positive HEK 293 cells were quantified by FACS analysis after 48 h of transfection. Data represents the mean ± SD (n = 4). ['*' indicates significantly ($p < 0.05$) higher than chitosan].

The transfection efficiency of AGC polymers at the protein level was determined by quantifying the β-galactosidase activity. As depicted in Figure. 44, AGC polymers induced a 13-30-fold enhancement in gene transfection efficiency of low molecular weight chitosan. Additionally, the β-galactosidase expression was varied among different AGC polyplexes which was in accordance with the outcome of FACS analysis data.

The transfection efficiency of different AGC/pGFP polyplexes was also investigated by confocal microscopy. Figure 45 shows the typical confocal images of HEK 293 cells transfected by the chitosan/pGFP polyplex, AGC/pGFP polyplex, and FuGENE HD/pGFP complex. GFP

expression could not be observed when the transfection was carried out by naked pGFP (data not shown). Intense fluorescence signal was detected when the transfections were performed by AGC polymers and FuGENE HD. In addition, the fluorescence intensity of AGC-F/pGFP appeared to be higher than that of all other formulations. The enhanced transfection efficiency of AGC polymers is likely related to the increased cellular uptake and better unpacking of condensed pDNA. The higher transfection efficiency of the polyplexes at weight ratio of 40 could be explained by the formation of smaller particle size with higher surface charge which leads to increased endocytosis of the polyplexes as well as the facilitated endolysosomal escape of polyplexes by larger amount of free cationic polymer (Thibault et al., 2011).

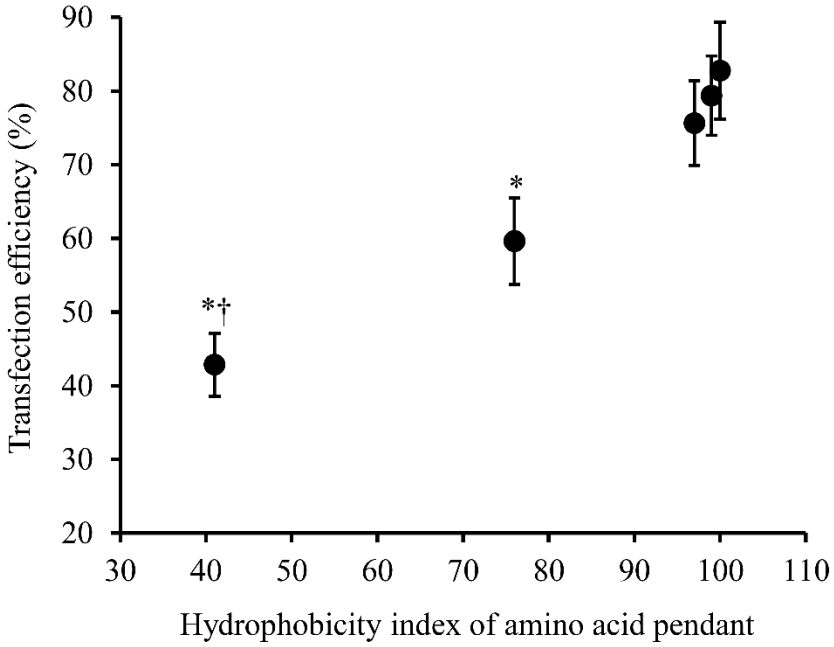

Figure 43. Effect of hydrophobicity index of amino acid pendant on the transfection efficiency of AGC/pGFP polyplexes at the weight ratio of 40. Data represents the mean ± SD (n = 4). ['*' indicates significantly ($p < 0.05$) different from AGC-L/pGFP, AGC-I/pGFP, and AGC-F/pGFP; '†' indicates significantly ($p < 0.05$) different from AGC-V/pGFP].

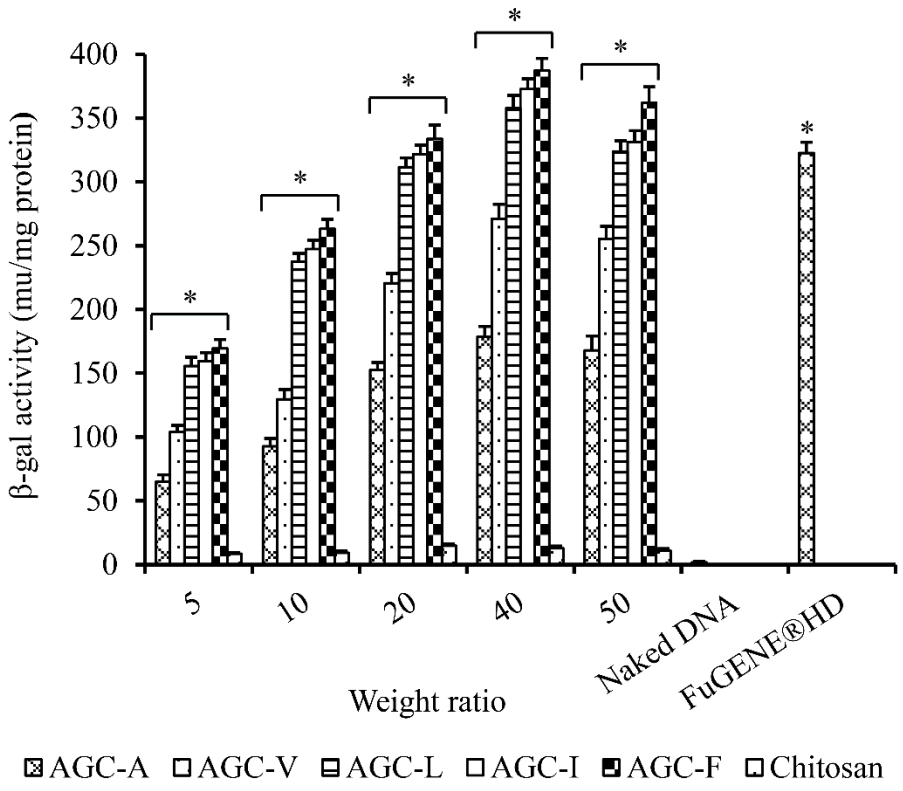

Figure 44. Transfection efficiency of chitosan/pGFP and AGC/pGFP polyplexes at protein level using pβgal. Data represents the mean ± SD (n = 4). ['*' indicates significantly ($p < 0.05$) higher than chitosan].

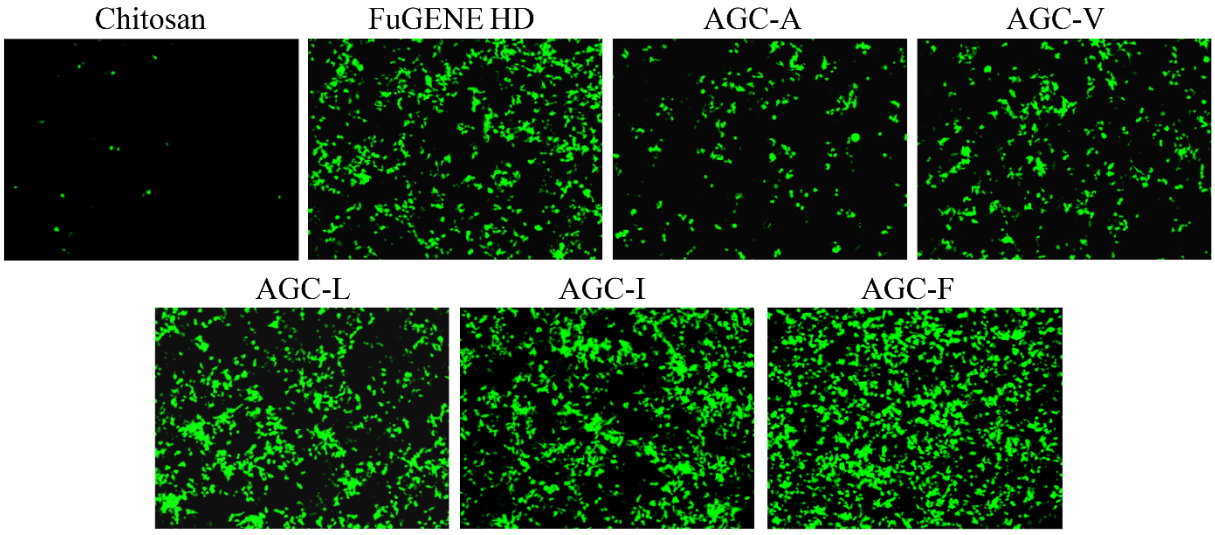

Figure 45. Confocal microscopic images of pGFP positive HEK 293 cells after 48 h of transfection. Images were taken at 10× magnification.

4.4. Conclusions

In this report, a series of amino acid grafted chitosan based polymers was synthesized as promising nonviral gene delivery vectors. These polymers exhibited efficient pDNA binding and protection ability. Hydrophobicity of amino acid substituent affected the particle size, cellular uptake, and in vitro pDNA release rate. The transfection efficiencies of AGC/pDNA polyplexes increased significantly with the increasing hydrophobicity of amino acid substituent. In addition, AGC polymers exhibited excellent blood compatibility and no cytotoxicity under experimental conditions. Therefore, amino acid conjugated chitosan possesses great potential as a nonviral vector for gene therapy.

5. HYDROPHOBICALLY MODIFIED MANNOSYLATED CHITOSAN FOR TARGETED DNA VACCINE DELIVERY TO ANTIGEN PRESENTING CELLS

5.1. Introduction

DNA vaccines have great potential in prevention and treatment of cancers and infectious diseases. Several advantages are associated with DNA immunization including no risk of reversion to pathogenicity, low cost, and stability in comparison with conventional live-attenuated, killed, or protein subunit-based vaccines (Medi et al., 2005). More importantly, DNA vaccines use host cells as bioreactors for the synthesis of antigenic proteins in vivo (Tang et al., 1992). The endogenously produced antigens can utilize both major histocompatibility complex (MHC) class I and II pathways for antigen presentation (Leitner et al., 2000) and thereby induce strong and long lasting humoral and cytotoxic T-lymphocytes (CTL) mediated immunity (Donnelly et al., 1997). The antibodies act by neutralizing the microorganisms, whereas the cytotoxic T lymphocytes act by killing infected cells (Ulmer et al., 1996). Hence, the DNA vaccines can be potentially useful for both prophylactic and therapeutic purposes (Huebener et al., 2008).

The limitations associated with most DNA delivery vectors impede successful development of DNA vaccines (Lu et al., 2008). Thus, the design of an efficient DNA delivery vector is of paramount importance in the overall process of DNA vaccine development. Recombinant viruses have been proven as excellent gene delivery vectors in numerous in vitro experiments; however, this approach is restricted by their inherent immunogenicity and severe toxicity in clinical trials (Glover et al., 2005). Therefore, research on novel nonviral synthetic DNA delivery vectors has gained an unprecedented relevance because of their good safety

profile, ease of synthetic procedure, and capability of delivering large fragment of DNA into the targeted cells (Mintzer and Simanek, 2009).

A number of nonviral vectors have been developed for DNA delivery that utilized a wide range of materials such as cationic liposomes (Chan et al., 2012; Gopal et al., 2011), peptides (Prata et al., 2008), and different cationic polymers (Du et al., 2012; Mintzer and Simanek, 2009). Among these, chitosan has been extensively studied in virtue of its inherent biocompatibility, biodegradability, and low cytotoxicity in comparison to other cationic polymers (Guliyeva et al., 2006; Kang et al., 2009; Lee et al., 2005). Moreover, the positive surface charge and presence of easily modifiable primary amines and hydroxyl groups on the chitosan backbone make it an attractive tool for DNA delivery. However, the poor transfection efficiency of chitosan is resulting in expression of a clinically inadequate level of desired therapeutics. The low transfection efficiency of chitosan-based delivery systems is primarily attributed to their poor cellular uptake and incomplete dissociation of DNA within cells due to strong ionic interaction (Lu et al., 2009). Recent studies have demonstrated that, grafting of hydrophobic molecules on chitosan backbone diminished the net positive charge density on chitosan which facilitates the intracellular dissociation of polymer/pDNA polyplexes (Kim et al., 2007). In addition, this modification also greatly improved the cellular uptake and in vitro gene transfection efficacy of chitosan by increasing the adsorption mediated endocytosis process (Wong et al., 2007).

Another major shortcoming of chitosan-based DNA delivery systems is its poor cell specificity. The efficient delivery of antigen-encoded DNA into specific cells is of utmost importance to successful DNA vaccine development (Sun et al., 2012). Hence, there is tremendous prospect for developing DNA vaccines that efficiently target professional APCs with

a DNA delivery vector. The APCs such as macrophages and dendritic cells play a crucial role as effector cells in the initiation of immune responses to foreign antigens. These cells are highly efficient in internalizing and processing of antigens for presentation to T-lymphocytes (Abbas et al., 1994). The additional co-stimulatory signals are then produced by the APCs leading to proliferation and differentiation of lymphocytes. It has been reported that MR is abundantly expressed on the surface of APCs (Kim et al., 2006). Therefore, mannose could be conjugated to the drug and gene delivery system to trigger the MR-mediated endocytosis, which would increase the efficacy of desired DNA vaccine.

In this study, we have taken a dual approach to improve the cell specificity and overall gene transfection efficiency of low molecular weight chitosan. Initially, chitosan was modified with hydrophobic moieties such as L-phenylalanine and N-hexanoic acid to enhance the adsorptive endocytosis and unpacking of vector/pDNA polyplexes (Layek and Singh, 2013a, Layek and Singh, 2013b). In the second step, hydrophobically modified chitosan was conjugated with α-D-mannopyranosylphenyl isothiocyanate to impart cell specificity to the polymeric DNA vector. To the best of our knowledge this is the first study that combines the benefits of hydrophobic modification along with receptor targeting to deliver DNA into APCs. The physicochemical properties of hydrophobically modified mannosylated chitosan and its complex with pDNA were characterized. The cytotoxicity, cellular uptake, APC targeting ability, and in vitro gene transfection efficiency were also investigated. The in vivo DNA vaccine delivery efficiency of the polymers was evaluated by comparing the cellular and humoral immune responses induced by the different formulations.

5.2. Materials and methods

5.2.1. Materials

Chitosan (Mw ~ 50 kDa, 91% deacetylated), N-acetyl-L-phenylalanine, FITC, α-D-mannopyranosylphenyl isothiocyanate, and MTT were purchased from Sigma-Aldrich (St. Louis, MO, USA). Hexanoic acid was procured from MP Biomedicals (Solon, OH, USA). EDC.HCl was procured from Creosalus Inc (Louisville, KY, USA). DNase I enzyme was obtained from Rockland Inc (Gilbertsville, PA, USA). pGFP, HBsAg, and HBsAg encoding plasmid DNA (pHBsAg) were purchased from Aldevron LLC (Fargo, ND, USA). Murine macrophage (RAW 264.7) cells and DMEM were obtained from American Type Culture Collection (ATCC, Rockville, MD, USA). FuGENE HD was obtained from Roche Diagnostics (Indiapolis, IN, USA). C57Bl/6 bone marrow derived adherent DC cells (DC 2.4) was kindly provided by Dr. Kenneth Rock (Dana Farber Cancer Institute, Boston, MA). Female Balb/c mice of 6 weeks old were purchased from Harlan Laboratories (Indiapolis, IN, USA). Low melting point agarose was purchased from Promega (Madison, WI, USA). All other chemicals were obtained commercially and used without further modification.

5.2.2. Synthesis of hydrophobically modified mannosylated chitosan

The AGC-F was synthesized by carbodiimide mediated coupling reaction between the carboxyl group of N-acetyl-L-phenylalanine and primary amines of chitosan as described in section (4.2.2). In the second step, AGC-F was mannosylated by the thiourea reaction between isothiocyanate groups of α-D-mannopyranosylphenyl isothiocyanate and primary amino groups of AGC-F. Briefly, AGC-F dissolved in distilled water was mixed with α-D-mannopyranosylphenyl isothiocyanate (0.07 mol/mol of sugar unit of AGC-F) in dimethyl sulfoxide. The reaction proceeded for 24 h at room temperature with constant stirring. Finally,

the resulting graft polymer was dialyzed against distilled water for 48 h followed by lyophilization. Similarly, NAC-6(15) polymer was mannosylated to get NAC-6(15)-Man. The synthetic scheme of mannosylated polymer is shown in Figure 46.

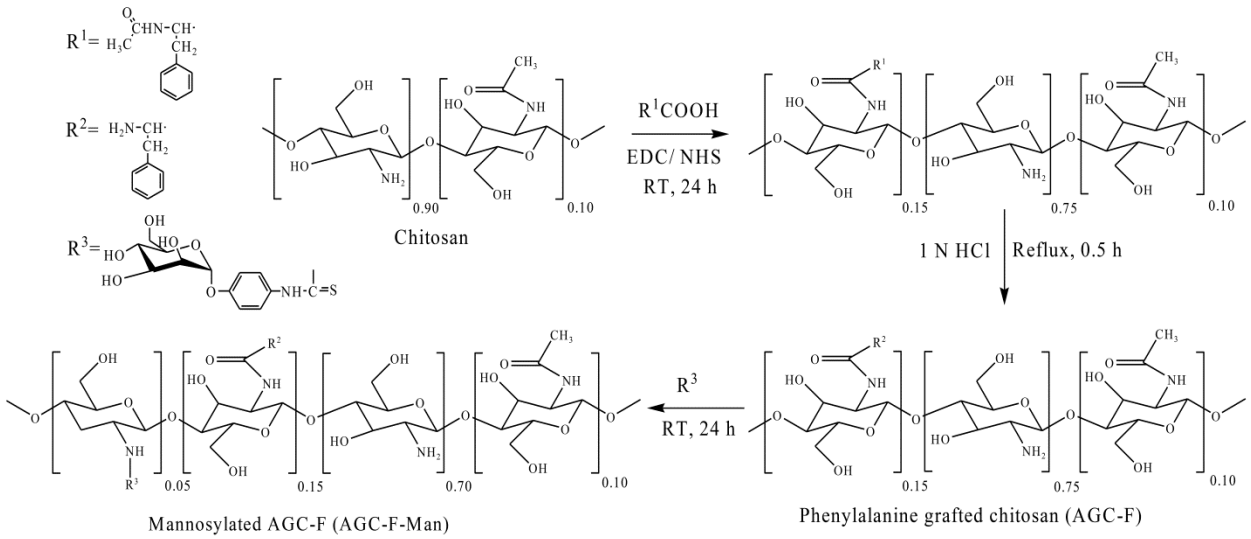

Figure 46. Schematic representation for the synthesis of mannosylated AGC-F (AGC-F-Man).

5.2.3. Characterization of mannosylated polymers

The chemical structure of polymers was confirmed by ^{1}H NMR. For ^{1}H NMR experiments, chitosan and mannosylated polymers were dissolved in D_2O and were analyzed in a Mercury Varian 400 MHz spectrometer at 25°C.

5.2.4. Polymer/pDNA polyplexes preparation and characterization

Mannosylated polymers were dissolved in 20 mM sodium acetate buffer with different concentrations at pH 6.5. The polymer/pDNA complexes of desired weight ratios were prepared by adding polymer solution to pDNA solution (100 µg/mL in 20 mM sodium acetate buffer, pH 6.5) while gently vortexing for 10 s and subsequently incubated at room temperature for 30 min. The pDNA and polymer solutions were made in sodium acetate buffer at pH 6.5. The particle size and zeta potentials of the different polyplexes were determined by DLS method using Zetasizer Nano ZS-90 at 25°C. The light scattering measurements were performed at a 90°

scattering angle with a laser wavelength of 633 nm. The final pDNA concentration of each sample was maintained at 10 µg/mL.

5.2.5. DNA binding assay

The pDNA binding ability of graft polymers was evaluated by agarose gel retardation assay with the pGFP. The polymer/pDNA polyplexes at different weight ratios were prepared by mixing 1 µg of the pGFP with various amounts of polymers. The polyplexes were then mixed with 6× gel loading dye (New England BioLabs, MA, USA) and subjected to electrophoresis on to a 0.8% (w/v) agarose gel containing 0.5 µg/mL EtBr at a constant voltage of 80 V for 80 min in 0.5× TAE buffer. The migration of pDNA bands were visualized and photographed with a UV transilluminator at a wavelength of 254 nm.

5.2.6. Protection of pDNA against nucleases

Resistance to nuclease degradation was determined by DNase I protection assay. The polymer/pDNA polyplexes at various weight ratios were incubated with DNase I (1 unit per 2 µg of pDNA) enzyme in 1× DNase reaction buffer at 37°C for 60 min. The free pDNA incubated with DNase I under similar conditions served as a positive control. After incubation, 5 µL of 100 mM EDTA was added to each sample to inactivate DNase I. Subsequently, 20 µL of 5 mg/mL heparin solution was added to all samples and incubated at room temperature for 1 h. The integrity of released pDNA was analyzed by agarose gel retardation assay.

5.2.7. In vitro release study

Polyplexes containing 50 µg of pDNA at weight the ratio of 40 were dispersed in 20 mL of phosphate buffered saline at pH 7.4. The release study was performed at 37°C temperature in a reciprocal shaking water bath at 50 rpm. At predetermined time points, 0.5 mL of sample was

withdrawn and centrifuged at 30,000 × *g*, 4°C for 30 min. The amount of released pDNA was quantified by fluorospectrophotometry after staining with Hoechst dye 33342.

5.2.8. In vitro cytotoxicity

In vitro cytotoxicity of graft polymers as well as polymer/pDNA polyplexes was evaluated by MTT assay in RAW 264.7 cell line. Cells were plated onto a 96-well plate at a density of 1×10^4 cells/well in 150 µL DMEM medium supplemented with 10% FBS and allowed to adhere overnight. The growth medium was then replaced with fresh culture medium containing different concentrations (100-1000 µg/mL) of polymers or polyplexes having 0.2 µg of pDNA at different weight ratios (5, 10, 20, 30, 40, and 50) for 48 h. Cells treated with 10% FBS containing growth media served as negative control. After treatment, polymer or polymer/pDNA polyplex solution was removed and the cells were incubated with 100 µL of MTT solution (1 mg/mL) in FBS free DMEM medium for another 3 h. Then the medium of each well was discarded and formazan crystals produced by proliferating cells were dissolved in 150 µL of dimethyl sulfoxide. Using a microplate reader, the absorbance of each sample was measured at 570 nm. The relative cell viability was calculated by the following equation:

$$\text{Cell viability (\%)} = (OD_{sample} / OD_{control}) \times 100$$

5.2.9. Cellular uptake study

RAW 264.7 cells were seeded in 6-well plate at a density of 4×10^5 cells/well and incubated overnight for attachment. To perform uptake process, FITC-labeled polymer/pDNA polyplex containing 4 µg of pDNA at an optimized weight ratio of 40 were added to each well. After 4 h of incubation at 37°C, the uptake process was terminated by discarding the polyplex containing growth medium and washing the cells three times with PBS. In order to visualize cell

uptake process, the FITC-positive cells were further incubated with 2.5 µg/mL of DAPI for 20 min to stain the nuclei and photographed with a FV300 confocal laser microscope.

5.2.10. In vitro competition assay

For competitive inhibition assays, cells and FITC-labeled polyplexes were prepared as mentioned above. To block the binding of mannosylated polyplexes to mannose receptor, RAW 264.7 cells were pre-incubated for 20 min prior to uptake study with 20 mM of D-mannose. Subsequently, cells were incubated with FITC-labeled polyplexes for 4 h at 37°C. After rinsing the cells thrice with PBS, the FITC-positive cells were monitored by confocal microscopy.

5.2.11. In vitro gene transfection

In vitro transfection efficiency of graft polymers was evaluated in RAW 264.7 and DC 2.4 cells using pGFP and pβ-gal as model plasmids. Cells were seeded onto a 24-well plate at a density of 1×10^5 cells/well in 0.5 mL DMEM supplemented with 10% FBS and allowed to grow 24 h to achieve ~ 60-70% confluency before transfection study. Subsequently, the cells were rinsed with PBS and incubated with polyplexes containing 1 µg of pDNA at different weight ratios. After 4 h of incubation, the transfecting media was exchanged with fresh growth media and incubated for 48 h. Cells transfected with naked pDNA and FuGENE HD/pDNA complex were used as passive control and positive control, respectively. To score the transfection efficiency at the cellular level, the percentages of GFP positive cells were analyzed by FACS using a flowcytometer. The images of GFP positive cells were visualized at 20× magnification using a FV300 confocal laser scanning microscope.

Furthermore, the role of mannose receptor mediated uptake of polymer/pDNA polyplexes for enhanced gene transfection was confirmed by performing the transfection assay in the presence of externally added mannose. RAW 264.7 cells were pre-incubated for 20 min with 20

mM of D-mannose, and the transfection studies were carried out as described above. All transfections assays were conducted as a replicate of four.

5.2.12. Immunization of mice

Female Balb/c mice of 6 weeks old were used to evaluate immune responses and in vivo biocompatibility of the different DNA vaccine formulations. Mice were housed in a pathogen free temperature controlled facility (72 ± 2°F) with daily cycles of 12 h light and 12 h dark. The mice were allowed free access to certified standard pelleted rodent food and tap water. After a seven day acclimation period, mice were divided into seven groups with six mice in each group; the details about the grouping structure are depicted in Table 6. All animal studies were conducted as approved by the Institutional Animal Care and Use Committee (IACUC) at North Dakota State University (Protocol # A13035).

Table 6. The grouping structure for in vivo studies.

Group Number	Treatment
1	Phosphate buffered saline (Control)
2	Naked HBV DNA vaccine (Passive control)
3	FuGENE HD + HBV DNA vaccine
4	NAC-6 (15) + HBV DNA vaccine
5	NAC-6 (15)-Man + HBV DNA vaccine
6	AGC-F + HBV DNA vaccine
7	AGC-F-Man + HBV DNA vaccine

On the day before immunization, hair on the dorsal skin of the tail base of the mice was closely shaved using an electric clipper with great care to avoid any damage to the skin. An area

of the skin was swabbed with 70% v/v isopropyl alcohol before intradermal injection. Each mouse was injected with a single formulation containing 20 µg of HBV DNA (pHBsAg) vaccine (delivered by two injections each of ~ 50 µL) using a 31 G needle. After two weeks of primary immunization, mice were boosted with the same formulation at an equivalent dose. The control group was injected with 100 µL of phosphate buffer saline alone.

5.2.13. Detection of HBsAg-specific IgG antibody

Blood samples (~ 100 µL) were collected from submandibular facial vein of the mice into standard eppendorf tube and allowed to clot at room temperature for 30 min. The serum was harvested by centrifuging blood samples at 1500 × g for 10 min in a refrigerated centrifuge and stored in -80°C until further analysis. The level of anti-HBsAg IgG in serum samples were determined by enzyme linked immunosorbent assay (ELISA) using high-binding capacity 96-well Nunc-Immuno MaxiSorp microplates (Nalge Nunc Intl., Rochester, NY, USA). For ELISA, each well of the microplates was coated with 100 µL of 10 µg/mL of HBsAg (subtype: ayw) in coating buffer overnight at 4°C. The plates were washed five times with PBS containing 0.2% (v/v) Tween 20 (PBST). Each well of the microplates was then treated with 150 µL of 3% BSA in coating buffer at room temperature for 2 h to block the nonspecific binding and washed five times with PBST. After that, 100 µL of diluted serum samples (1:10000 dilution) was added to each well and incubated at room temperature for 2 h. Sera was removed by washing the microplates five times with PBST and each well was then incubated with 100 µL (1:5000 dilution) of horseradish peroxidase conjugated goat anti-mouse IgG polyclonal antibody (Gene Tex, Irvine, CA, USA). After 1 h incubation at room temperature, the plates were washed five times with PBST and 100 µL 3,3′,5,5′-tetramethylbenzidine-liquid-1-component (Amresco LLC, Solon, Ohio, USA) was added to each well and incubated for 30 min at room temperature. The

reaction was stopped by treatment with 2 M H_2SO_4 and the absorbance was measured at 450 nm. The amount of anti-HBsAg IgG in serum was converted to mIU with the help of a calibration curve generated by a serially diluted standard antibody (Gene Tex, Irvine, CA, USA).

5.2.14. Cellular immune responses

Cellular immune responses with HBV DNA vaccine were investigated by isolating splenocytes from each mouse 6 weeks after primary immunization. The spleens were mashed through 70 µm sterile nylon cell strainer using the plunger end of the 5 mL syringe. The splenocytes were collected, treated with lysis buffer (8.29 g NH_4Cl, 1 g $KHCO_3$, 37.2 mg Na_2-EDTA in 1 L deionized water, pH adjusted to 7.2) to eliminate erythrocytes, washed, and resuspended in RPMI 1640 medium containing 10% FBS (Dong et al., 2012). Cell viability of the splenocytes was determined by Trypan Blue exclusion method.

5.2.14.1. Lymphoproliferation assay

The isolated lymphocytes were plated in 96-well plates at a density of 1×10^5 cells/well in 150 µL RPMI 1640 medium supplemented with 10% FBS. The cells were stimulated in vitro with HBsAg (1 µg/well) immediately and cultured at 37°C in 5% CO_2 for 72 h. At the end of incubation, 20 µL of MTT solution (5 mg/mL) was added to each of the wells and incubated for another 3 h at 37°C. The cultured medium of each well was discarded and the formazan crystals produced by viable cells were dissolved in 150 µL of dimethyl sulfoxide. The absorbance was recorded at 570 nm and the proliferation responses for different immunization groups were calculated.

5.2.14.2. Cytokine measurements

To further characterize the cell-mediated immune responses with the different HBV DNA vaccine formulations, the production of interleukin-4 (IL-4) and interferon-γ (IFN-γ) were

monitored. The lymphocytes were treated in identical fashion as for lymphoproliferation assay and at the end of 72 h incubation, the supernatants culture medium was collected for cytokine measurement. The levels of IL-4 and IFN-γ were quantified using commercial ELISA kits (Enzo Life Sciences Int'l Inc., Plymouth Meeting, PA, USA) as per manufacturer's instructions. A range of serially diluted recombinant mouse IL-4 and IFN-γ served as the standard for IL-4 and IFN-γ, respectively.

5.2.15. In vivo toxicity

Mice were examined for daily food intake, weight loss, any distress, and mortality throughout the study period. At the end of the study period, the animals were sacrificed and histological examination of the highly perfused tissues such as liver, kidney, and heart was performed. The liver sections were observed for ballooning of hepatocytes, enlargement of nuclei or kupffer cells, and granulomas (Semete et al., 2010; Tseng et al., 2012). Heart was also examined for signs of necrosis or extravasation of red blood cells (Abdelhalim, 2011). Kidneys were observed for inflammation and necrosis (Barathmanikanth et al., 2010).

5.2.16. Statistical analysis

Data are expressed as mean ± SD. For in vitro cytotoxicity and transfection efficiency studies, four replicates were used to calculate mean and SD. Statistical analyses were performed using two tailed Student's t-test and ANOVA. A p value of less than 0.05 was considered to be significant.

5.3. Results and discussion

5.3.1. Synthesis and characterization of mannosylated polymers

The mannosylated chitosan derivatives were synthesized in a two-step reaction as illustrated in Figure 41. The grafting of hydrophobic moiety such as L-phenylalanine or hexanoic

acid onto chitosan backbone was carried out by EDC/NHS mediated coupling reaction. Subsequently, the hydrophobically modified chitosan was mannosylated by the thiourea reaction between primary amines of chitosan derivatives and the isothiocyanate group of α-D-mannopyranosylphenyl isothiocyanate. The chemical composition of the synthesized copolymers was analyzed by ^{1}H NMR spectroscopy (Figure 47). After mannosylation of hydrophobically modified chitosan, the proton peaks of phenylisothiocyanate of α-D-mannopyranosylphenyl isothiocyanate appeared at 7.2-7.4 ppm. The degree of substitution of mannose onto chitosan backbone was determined by elemental analysis and was found to be ~ 5%.

5.3.2. Size and zeta potential of polymer/pDNA polyplexes

Hydrodynamic size and surface charge of a polyplex are important physical factors governing its access and passage through the target site; hence these parameters have a significant impact on gene transfection (Anderson et al., 2005; Green et al., 2006; Thomas and Klibanov, 2003). Generally, particles within size ranges of 50 to several hundred nanometers are favorable for cellular uptake via endocytosis (Liu and Reineke, 2005). Similarly, the positive surface charge of polyplexes is essential for binding to the negatively charged cell membrane, which subsequently influences efficient intracellular trafficking (Pack et al., 2005). The polyplex formation occurs due to electrostatic interaction between the positively charged primary amino groups present on the glucosamine units of mannosylated chitosan and the negatively charged phosphate groups of pDNA. The average particle diameters of the polyplexes formed at different weight ratios were determined by DLS method. As depicted in Table 7, the stable and uniform polyplexes were formed at pH 6.5 and the size of the polyplexes tended to decrease with increasing polymer/pDNA weight ratio. At a particular weight ratio, the size of the NAC-6(15)-Man/pDNA polyplexes were significantly ($p < 0.05$) higher than AGC-F-

Man/pDNA polyplexes indicating formation of less compact polyplexes by NAC-6(15)-Man polymer.

At the weight ratio of 1, both of the polyplexes had nearly neutral surface charges. When the polymer/pDNA weight ratio increased to 5, the zeta potential of the polyplexes increased sharply. Zeta potential of the polyplexes further increased with the increased polymer/pDNA weight ratios. Thus, the results of DLS study confirmed the formation of nanosized polyplexes with net positive surface charge which is crucial for cell attachment and uptake process.

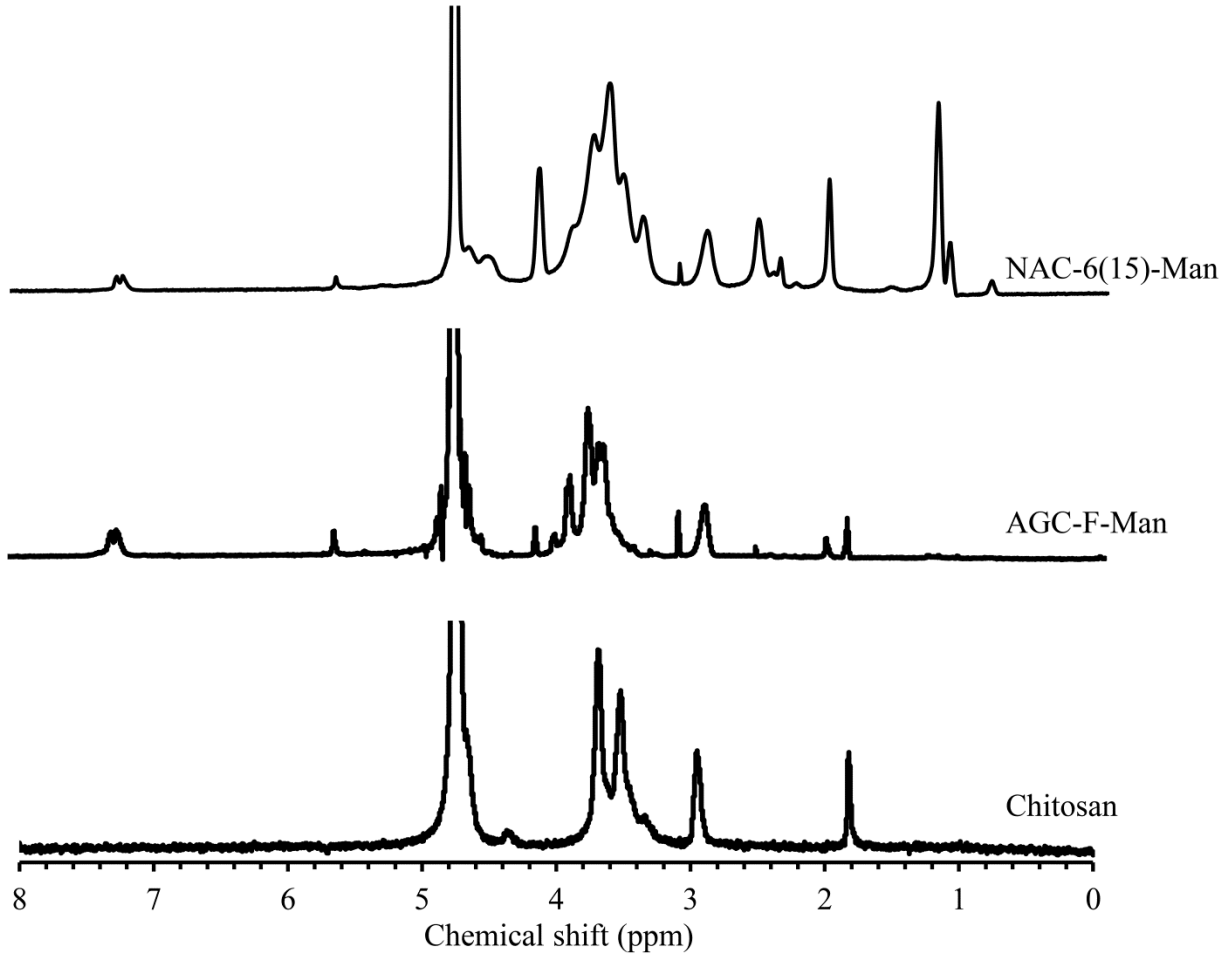

Figure 47. ^{1}H NMR spectra of chitosan, AGC-F-Man, and NAC-6(15)-Man in D_2O at 25°C.

Table 7. Particle sizes and zeta potentials of polyplexes in 20 mM sodium acetate buffer at pH 6.5. Data represents the mean ± SD (n = 6).

	Size (nm)		Zeta potential (mV)	
Polymer/pDNA weight ratio	AGC-F-Man	NAC-6-(15)-Man	AGC-F-Man	NAC-6-(15)-Man
1	268.7 ± 4.6	372.7 ± 8.9	3.7 ± 0.8	-3.5 ± 0.6
5	228.5 ± 4.4	320.4 ± 6.5	18.9 ± 0.9	13.2 ± 0.5
10	205.0 ± 4.5	279.1 ± 5.3	20.3 ± 0.7	16.2 ± 0.6
20	190.9 ± 4.3	258.5 ± 7.2	21.6 ± 0.8	19.7 ± 0.8
30	179.8 ± 3.8	247.3 ± 8.5	23.4 ± 0.8	20.2 ± 0.7
40	168.8 ± 4.6	242.5 ± 6.4	25.9 ± 0.9	20.7 ± 1.1
50	162.6 ± 3.0	236.7 ± 7.9	26.7 ± 0.8	21.2 ± 0.7

5.3.3. DNA binding study

For efficient DNA vaccine delivery, it is important that pDNA is condensed into stable polyplexes to protect the pDNA from extracellular enzymatic degradation and to allow for adequate cell uptake. The pDNA binding efficiency of mannosylated chitosan derivatives was monitored by agarose gel retardation assay using naked pDNA as a control. Polyplexes, formulated at different weight ratios from 0.2 to 50, were electrophoresed to determine the optimal weight ratio required for complete condensation of the pDNA. As shown in Figure 48A, the presence of a partly dissociated pDNA band in lane ‘b’ indicated the formation of physically unstable polyplexes at the weight ratio of 0.2. When the polymer/pDNA weight ratios increased

to ≥ 5, movement of pDNA was completely retarded, indicating formation of tight polyplexes between polymer and pDNA.

5.3.4. Protection of pDNA against nucleases

DNase I is a nonspecific endonuclease that catalyzes the hydrolytic cleavage of DNA to release di-, tri-, and oligonucleotides (Kunitz, 1950). Thus, the integrity of pDNA in the presence of DNase I is essential to ensure desired function of transferred pDNA in vitro or in vivo (Katayose and Kataoka, 1998). The protective effect of polyplexes against endonuclease degradation was authenticated using DNase I protection assay. As demonstrated in Figure 48B, the naked pDNA was completely digested by the DNase I as indicated by absence of band for pDNA. The pDNA exhibited no evidence of degradation when complexed with mannosylated polymers. The results of DNase I protection assay clearly demonstrate that, under physiological conditions where presence of different endonucleases significantly affect the integrity of pDNA, the mannosylated polymers provide efficient protection of condensed pDNA and are suitable for in vivo conditions.

5.3.5. In vitro release study

Once the polyplexes reach the cytoplasm, a very tight binding between pDNA and its vectors imposes difficulty in unpacking of the condensed pDNA, and thereby hinders gene transfection (Schaffer et al., 2000). Thus, the release profile of condensed pDNA plays a critical role to moderate the overall gene expression. Incorporation of hydrophobic segments to the polymeric backbone has emerged as an efficient strategy to reduce polymer/pDNA binding force (Pack et al., 2005). To simulate the existing pH environment of cytoplasm and nucleus, PBS at pH 7.4 was used as the release media. Figure 49 revealed the cumulative in vitro release profile of pDNA from the polyplexes after 48 h of incubation. The cumulative release of pDNA from

chitosan/pDNA polyplexes was less than 10%, while a relatively rapid release of pDNA was observed for polyplexes prepared with mannosylated polymers. Mannosylated polymers had a cumulative release of ~ 30%, but no significant differences ($p > 0.05$) existed between the two mannosylated polymers.

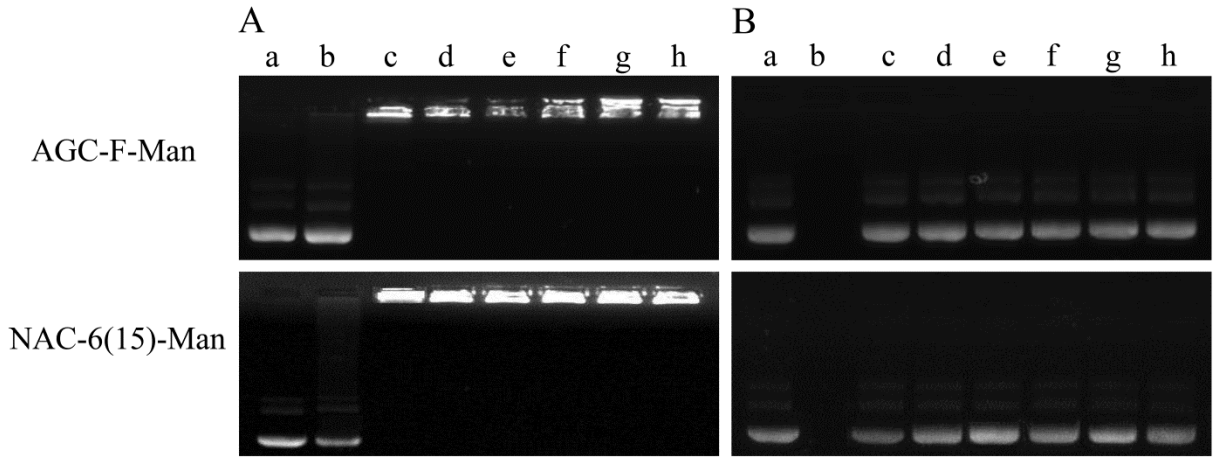

Figure 48. (A) Agarose gel retardation assay of AGC-F-Man/pDNA and NAC-6(15)-Man/pDNA polyplexes at different weight ratios. Lane a: naked DNA; Lanes b-h: polymer/pDNA polyplexes at the weight ratios of 0.2, 5, 10, 20, 30, 40, and 50, respectively. (B) DNase I protection assay of AGC-F-Man/pDNA and NAC-6(15)-Man/pDNA polyplexes prepared at different weight ratios. Lane a: naked DNA; Lane b: naked DNA + DNase I; Lanes c-h: polymer/pDNA polyplexes (at the weight ratios of 5, 10, 20, 30, 40, and 50, respectively) + DNase I.

Hydrophobic modification of chitosan facilitates the pDNA dissociation due to the hydrophobicity-induced weakening of the electrostatic interaction between the pDNA and polymer (Wang et al., 2011). Mannosylation of hydrophobically modified chitosan only slightly enhanced the pDNA release rate. Therefore, the enhanced pDNA release profiles along with the excellent pDNA protection ability of the mannosylated polymers render them suitable as an efficient carrier for pDNA delivery.

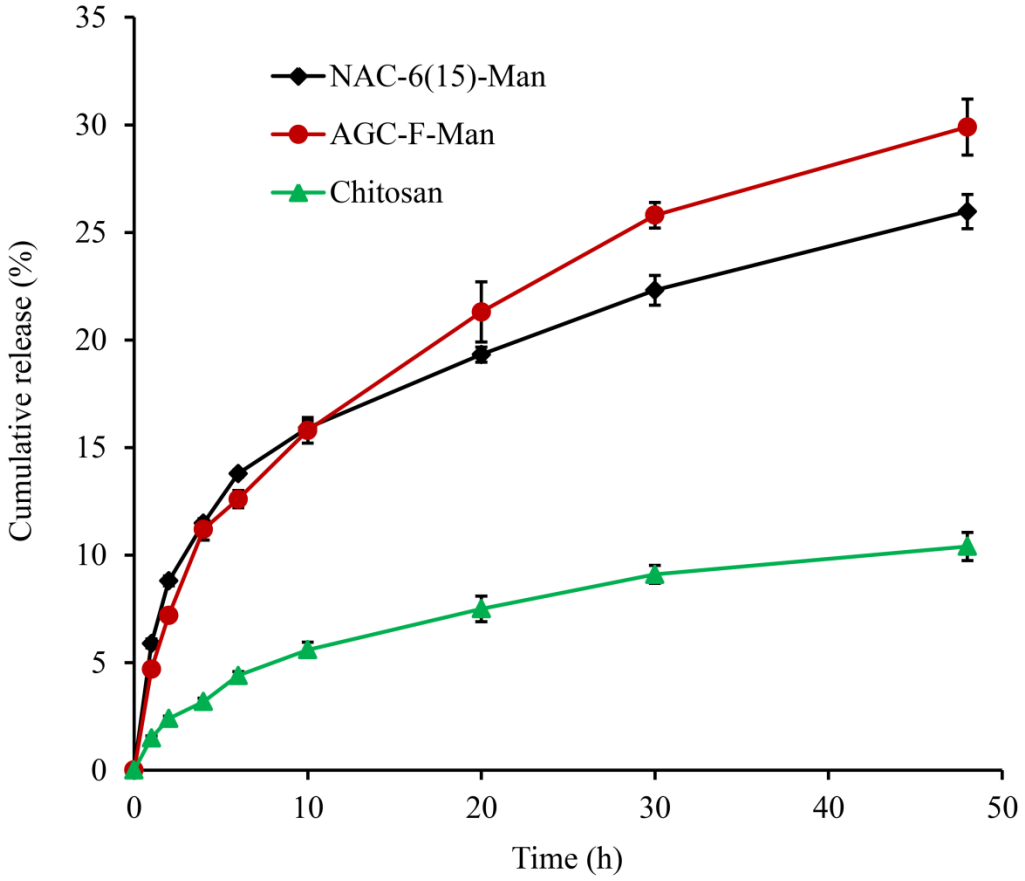

Figure 49. Cumulative pDNA release profiles of different polyplexes. Polyplexes were prepared at the weight ratio of 40 and were incubated in PBS (pH 7.4) at 37°C in a reciprocal shaking water bath at 100 rpm. Data represents the mean ± SD (n = 4).

5.3.6. In vitro cytotoxicity study

Cytotoxicity of cationic gene delivery systems is considered as one of the major limiting factors for their in vivo applications. Hence, in vitro cytotoxicity of mannosylated polymers was evaluated by MTT assay. As shown in Figure 50A, mannosylated polymers displayed no alteration in cell viability up to a concentration of 1 mg/mL, which was 20-fold higher than the maximum polymer concentration applied in gene transfection experiments. The cytotoxicity of the polymer/pDNA polyplexes at different weight ratios varied from 5-50 was further assessed in RAW 264.7 cells by MTT assay. As depicted in Figure 50B, polymer/pDNA polyplexes at different weight ratios did not change the cell viability compared to the control. The cell viability

results show great promise for the prospects of mannosylated chitosan derivatives for repeated administration of large quantities of genes of interest.

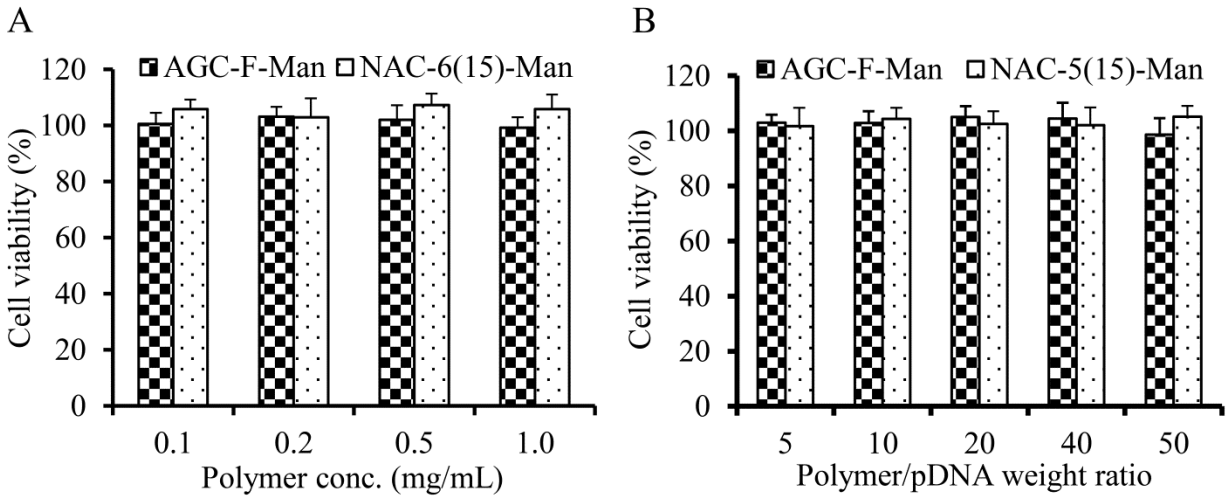

Figure 50. In vitro cytotoxicity of (A) mannosylated polymers and (B) polymer/pDNA polyplexes in RAW 264.7 cells. Data represents the mean ± SD (n = 4).

5.3.7. Cellular uptake study

The grafting of mannose as a ligand into the gene delivery vectors for specific recognition by antigen presenting cells may enhance the gene transfer across the cell membrane. Hence, the cellular uptake of polyplexes was also determined in RAW 264.7 cells (Díaz-Moscoso et al., 2011). Cells were incubated with FITC-labeled polymers/pDNA polyplexes at 37°C for 4 h and then visualized and photographed by confocal microscopy. As depicted in Figure 51, the chitosan/pDNA polyplexes exhibited the lowest number of FITC-positive cells while the mannosylated polymers/pDNA polyplexes showed maximum internalization followed by hydrophobically modified chitosan.

Since AGC-F and NAC-6(15) polymers are comprised of cationic amine groups and hydrophobic moieties in their structure, both electrostatic attraction and hydrophobic interactions facilitate the adsorption mediated endocytosis process (Piest and Engbersen, 2010). The

internalization of mannosylated polymer/pDNA polyplexes further improved due to the mannose receptor mediated uptake. The confocal images also signify that chitosan/pDNA polyplexes were mainly accumulated around the perinuclear section of the cytoplasm whereas a strong overlap of polyplexes and nuclei was evident in case of mannosylated polymer/pDNA. Nuclei of cells were stained with DAPI, showing blue fluorescence. There was no visual difference in uptake process of the two mannosylated polymers.

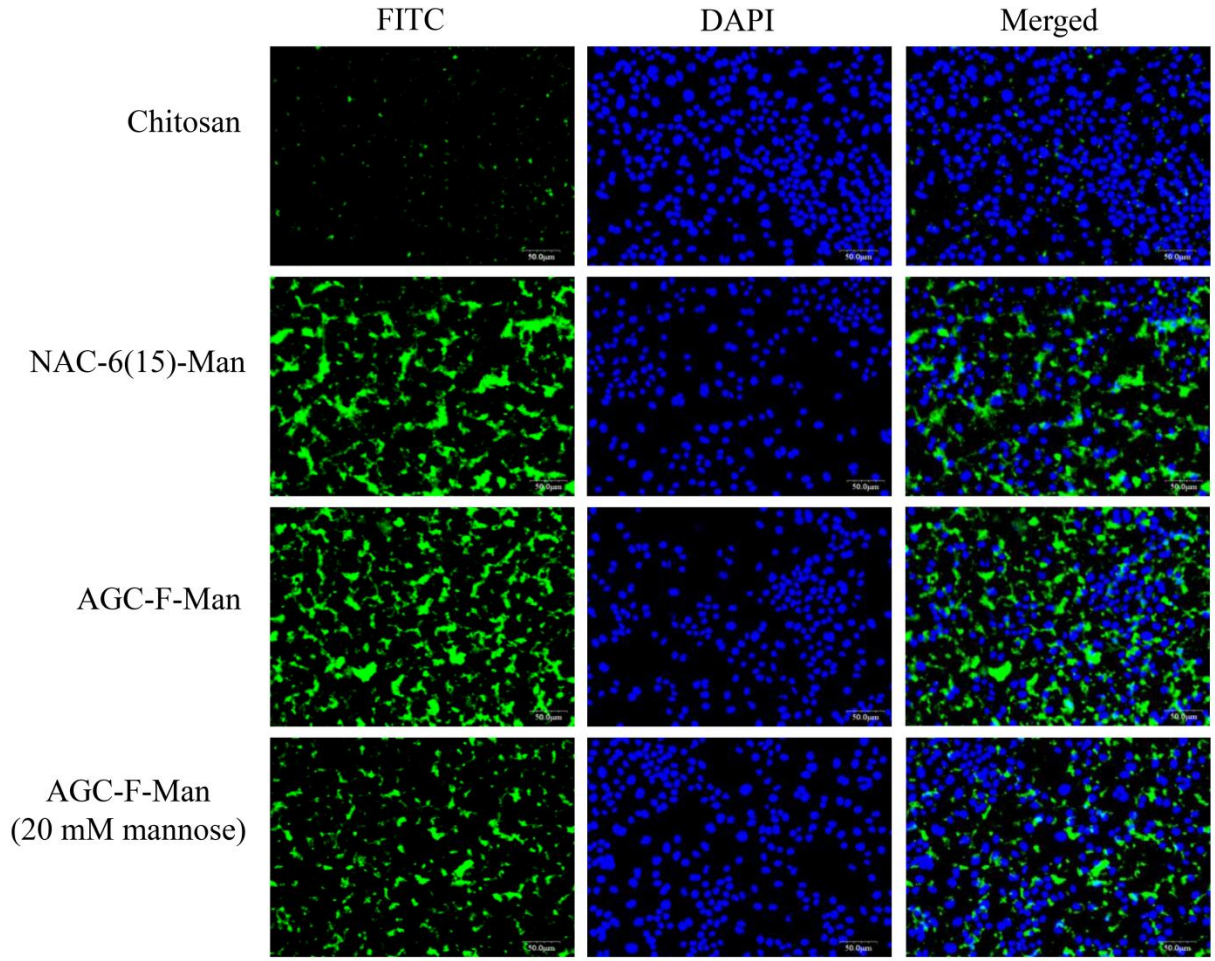

Figure 51. Cellular uptake of FITC-labeled mannosylated polyplexes in RAW 264.7 cells. Cells were incubated with different polyplexes at 37°C for 4 h. The nuclei of the cells were stained with DAPI. The image shows an overlap of the nuclei (blue) and polyplexes (green) after uptake of polyplexes by RAW 264.7 cells.

In order to further examine the mechanism of cellular uptake of mannosylated polyplexes, a competition experiment was performed with mannose. As is shown in Figure 51, the mean fluorescence intensity of RAW 264.7 cells pre-incubated with mannose was 3-4-fold lower than that of cells without mannose treatment. These results clearly suggest the involvement of mannose receptor in the uptake of the mannosylated polymer/pDNA.

5.3.8. In vitro gene transfection

A desirable level of gene expression is the central issue in the design of suitable gene delivery vector. To address whether monnosylation of hydrophobically modified chitosan could enhance its gene delivery efficacy, we compared the transfection efficiency of AGC-F-Man/pDNA and NAC-6(15)-Man/pDNA polyplexes with that of AGC-F/pDNA, NAC-6(15)/pDNA, and chitosan/pDNA polyplexes in RAW 264.7 mouse macrophage and DC 2.4 mouse dendritic cells, having abundant mannose receptors. In RAW 264.7 cells, the AGC-F-Man/pGFP polyplexes exhibited the optimum level of transfection with 42.3% of GFP positive cells, which was 20-fold higher than chitosan/pGFP polyplexes and 1.5-fold higher compared to AGC-F/pGFP polyplexes (Figure 52). Moreover, the gene transfection efficiency of AGC-F-Man/pGFP polyplexes was 1.6-fold higher than the commercially available nonviral gene delivery vector FuGENE HD. There was no significant difference ($p > 0.05$) in gene transfection efficiency of the two mannosylated polymers. The maximum transfection achieved with NAC-6(15)-Man/pDNA polyplexes was 40.5%, while NAC-6(15)/pDNA polyplexes resulted in 24.4% of GFP transfected cells. The trend of transfection efficacy of different polyplexes was further confirmed in DC 2.4 cells (Figure 53). However, the overall transfection efficiency was lower than that in RAW 264.7 cells. Results of quantitative analysis were in complete agreement with the confocal images of GFP transfected cells (Figure 54).

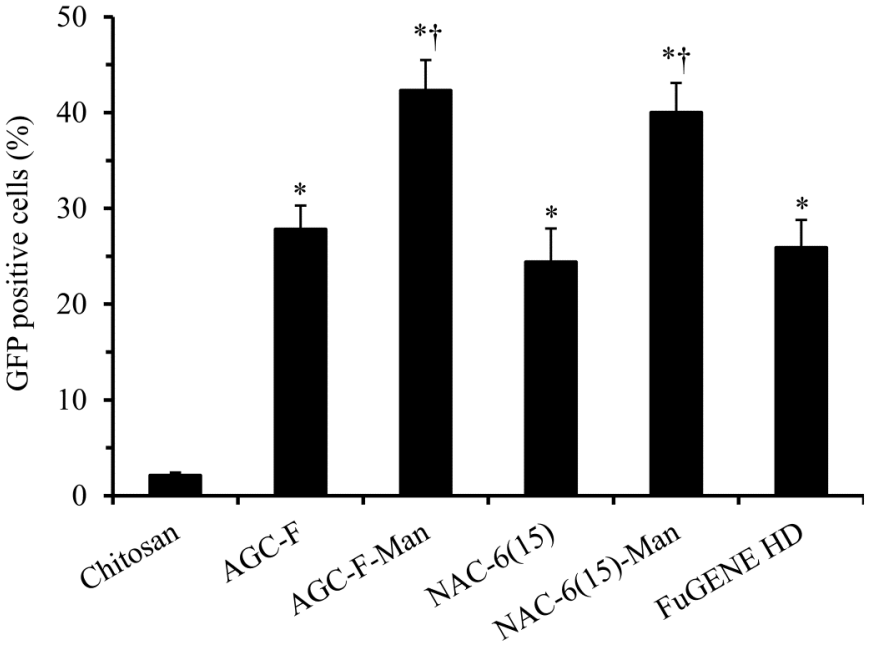

Figure 52. In vitro transfection efficiency of different formulations in RAW 264.7 cells. Data represents the mean ± SD (n = 4). ['*' significantly ($p < 0.05$) higher than chitosan; '†' significantly ($p < 0.05$) higher than FuGENE HD].

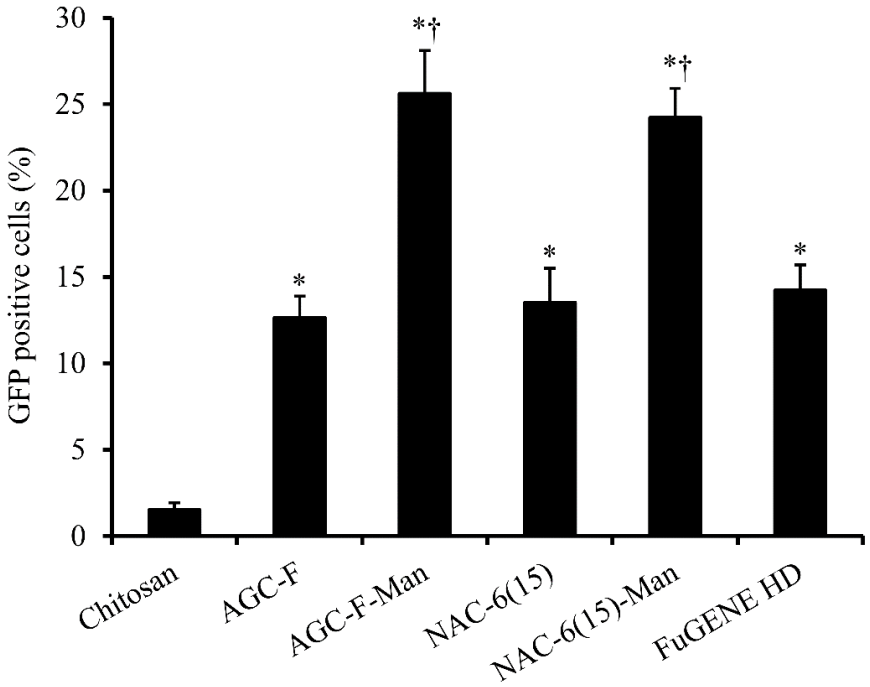

Figure 53. In vitro transfection efficiency of different formulations in DC 2.4 cells. Data represents the mean ± SD (n = 4). ['*' significantly ($p < 0.05$) higher than chitosan; '†' significantly ($p < 0.05$) higher than FuGENE HD].

To confirm the role of mannose receptor-mediated endocytosis of mannosylated polymer/pDNA polyplexes, the transfection efficacy of different polyplexes were investigated in the presence of 20 mM mannose as a competitor for mannosylated polymer/pDNA polyplexes (Park et al., 2008). The transfection efficiencies of AGC-F-Man/pDNA and NAC-6(15)-Man/pDNA polyplexes prepared at the weight ratio of 40 were significantly ($p < 0.05$) inhibited in the presence of externally added mannose, while the transfection efficiencies of chitosan/pDNA, AGC-F/pDNA, and NAC-6(15)/pDNA polyplexes were not changed (Figure 55). Hence the results of in vitro gene transfection experiments clearly demonstrate the importance of mannose grafting to improve the APCs transfecting capacity of chitosan as observed in AGC-F-Man and NAC-6(15)-Man.

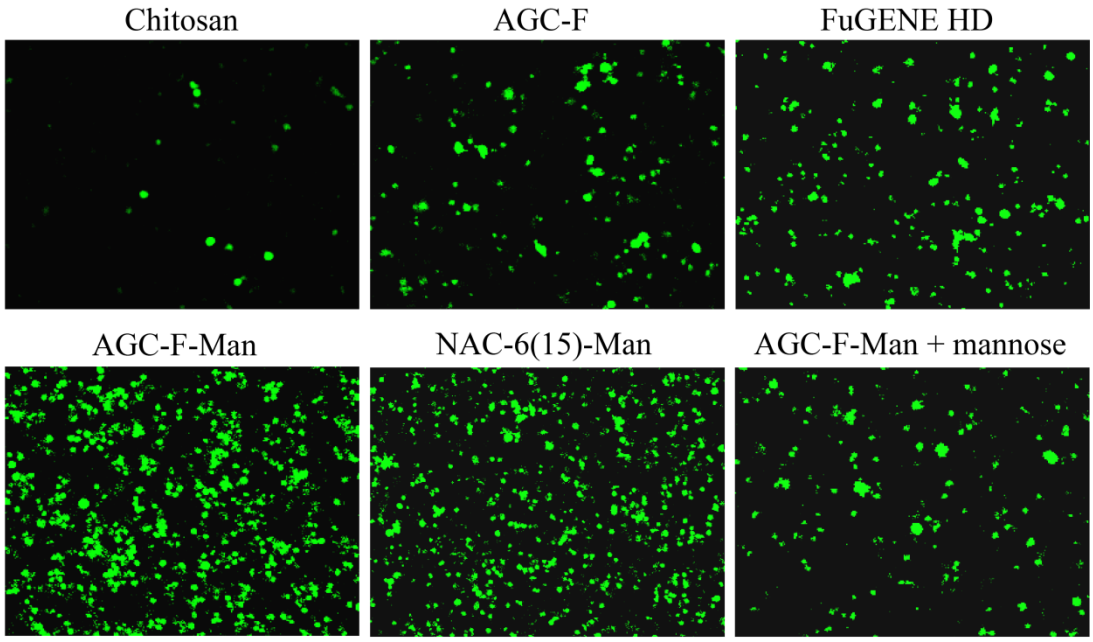

Figure 54. Confocal microscopic images of GFP positive RAW 264.7 cells after 48 h of transfection. Images were taken at 20× magnification.

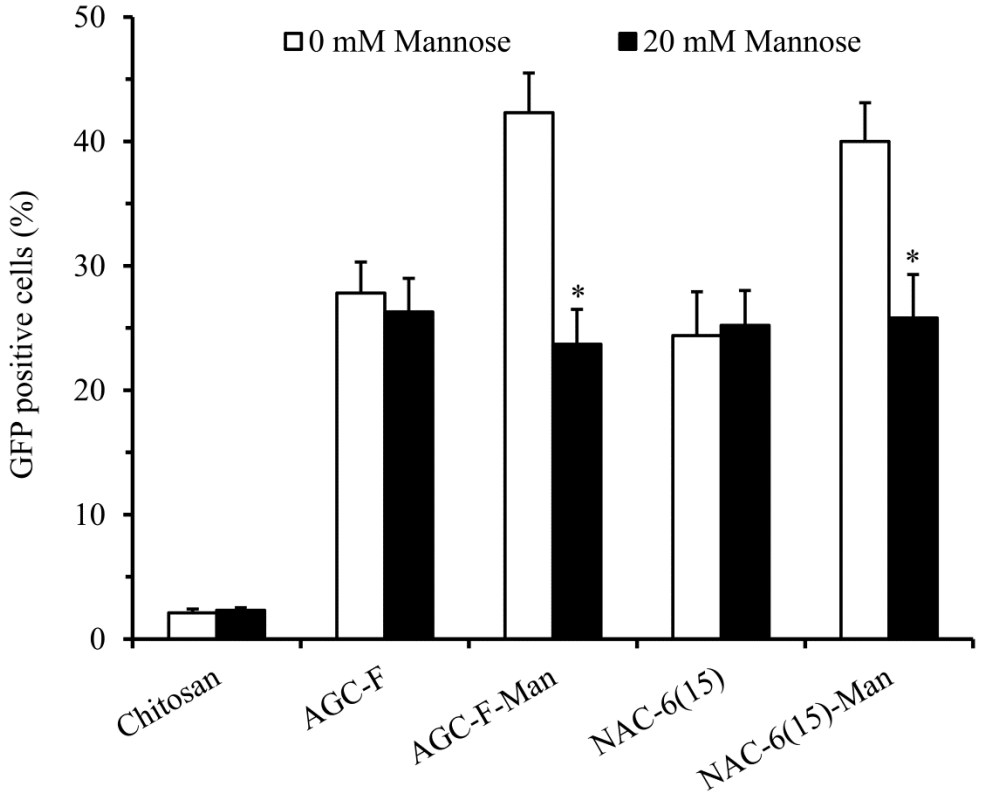

Figure 55. In vitro competition assay in Raw 264.7 cells. Data represents the mean ± SD (n = 4). [‘*’ significantly ($p < 0.05$) different from control].

5.3.9. Detection of HBsAg-specific IgG antibody

Hepatitis B virus infection is still one of the major global health problems and is the primary cause of chronic liver disease (Larkin et al., 1999). Although, HBV DNA vaccines offered an attractive approach against HBV infection, its immunogenicity still needs to be improved in order to use them routinely for human immunization. Lack of safe and efficient DNA delivery systems is the primary reason for the lower efficacy of DNA vaccine observed in higher animals and humans. Several immunological investigations have demonstrated that gene expression and subsequent activation of dendritic cells are the key events in the development of efficient immunity following DNA immunization (Akbari et al., 1999; You et al., 2001). Thus,

the APCs targeted mannosylated polymers could be used as a potential adjuvant to enhance the cellular and humoral immune responses induced by the DNA vaccine.

ELISA was used to quantify the level of anti-HBsAg antibody in mice serums. The levels of anti-HBsAg antibody induced by different vaccine formulations were expressed in terms of mIU/mL (Figure 56). Results showed that, at all time-points measured, mice immunized with mannosylated formulations induced significantly ($p < 0.05$) higher antibody titers compared with other groups. A clinically protective antibody level (> 10 mIU/mL) was observed in serums of mice immunized with intradermal injections of all other formulations including naked DNA vaccine (Mahor et al., 2007). However, the levels of HBsAg-specific antibody elicited by the mannosylated formulations were 1150-fold greater than the antibody induced by naked DNA injection after 6 weeks of primary immunization. Moreover, there were no significance differences in the antibody level when AGC-F-Man and NAC-6(15)-Man were used as adjuvant. These results clearly suggest that mannosylated chitosan derivatives can serve as potential carriers for HBV DNA vaccine to improve HBV-specific immune responses.

5.3.10. Lymphoproliferation assay

The ability of T cells to proliferate in response to their cognate antigen has traditionally been used as an indicator of the presence of antigen-specific CD4+ helper T cells (Clay et al., 2001). Lymphoproliferation assay was performed by isolating splenocytes from immunized mice after 6 weeks of primary immunization, re-stimulated in vitro with HBsAg antigen, and cultured at 37°C in 5% CO_2 environment. The HBV-specific T cells started to proliferate in response to antigen activation. After 72 h of incubation, the degree of lymphoproliferation was measured by MTT assay. As depicted in Figure 57, the results showed that AGC-F-Man/pHBsAg and NAC-6(15)-Man/pHBsAg polyplexes induced significantly ($p < 0.05$) higher degree of

lymphoproliferation than all other formulations. These results suggested that mice immunized with AGC-F-Man/pHBsAg and NAC-6(15)-Man/pHBsAg polyplexes induced efficient specific T cell response against HBV which is critical for long term immunity.

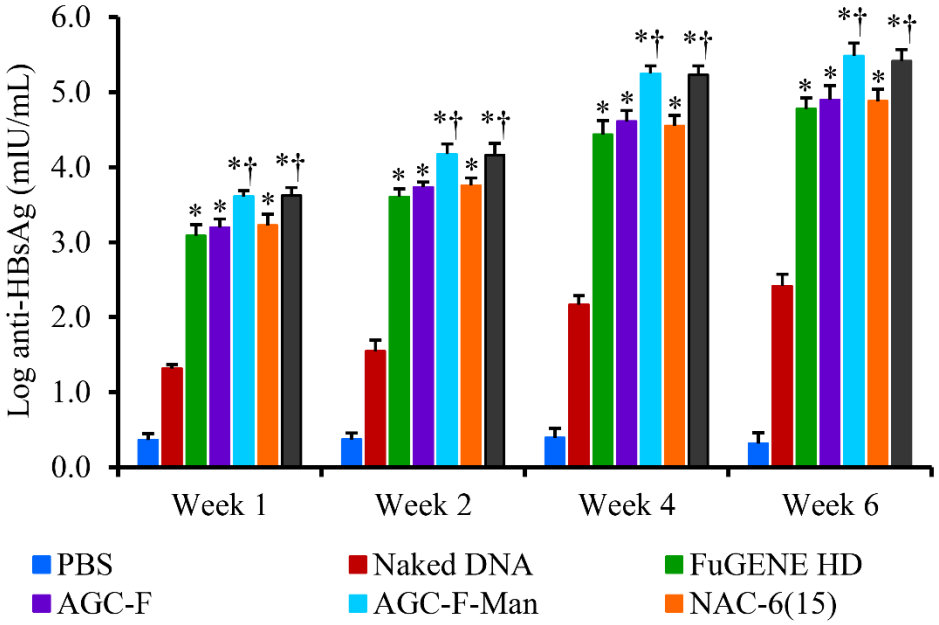

Figure 56. Levels of anti-HBsAg antibody in mice serum. Data represents the mean ± SD (n = 6). ['*' significantly ($p < 0.05$) higher than naked DNA; '†' significantly ($p < 0.05$) higher than FuGENE HD].

5.3.11. Cytokine measurements

Cytokines play an important role in the modulation of immune responses. The level of cytokines (IFN-γ and IL-4) released from re-stimulated splenocytes of immunized mice were measured in the supernatant of culture medium after 72 h of incubation. Cytokine profiling was performed to distinguish between Th1 (IFN-γ) and Th2 (IL-4) immune responses. As shown in Figure 58, AGC-F-Man/pHBsAg and NAC-6(15)-Man/pHBsAg polyplexes produced a stronger induction of IFN-γ than control and all other formulations. Several investigators have reported that splenic macrophages, Kupffer cells, and dendritic cells play a critical role in IFN-γ secretion

(Sakurai et al., 2002; Schattenberg et al., 2000). Thus, this finding confirms the ability of the mannosylated polymer/pHBsAg polyplexes to efficiently transfect APCs.

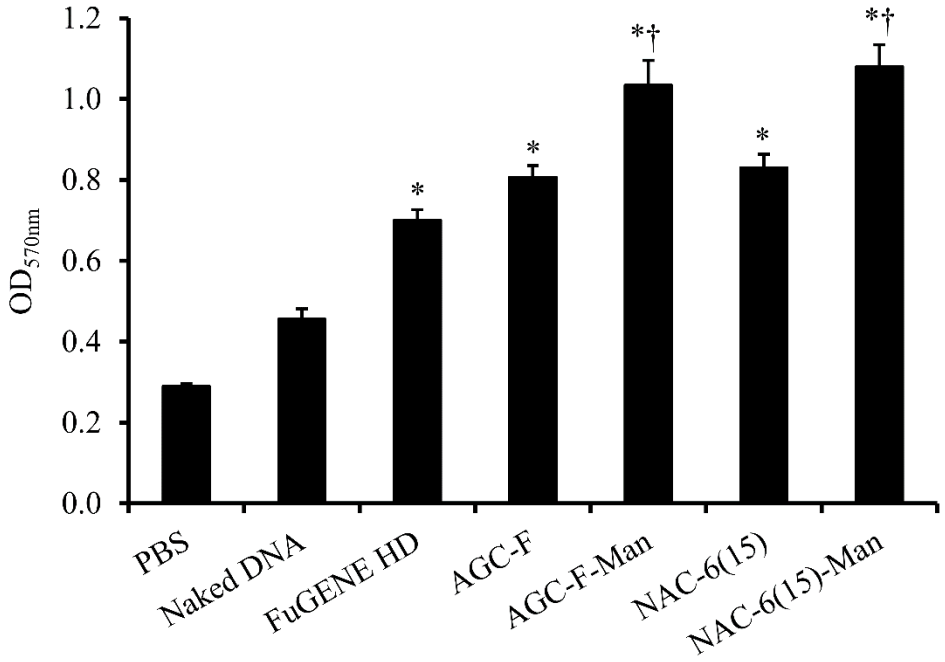

Figure 57. Lymphoproliferation assay. Data represents the mean ± SD (n = 6). ['*' significantly ($p < 0.05$) higher than naked DNA; '†' significantly ($p < 0.05$) higher than FuGENE HD].

However, there was no significant ($p > 0.05$) increase in IL-4 level after stimulation with HBsAg (Figure 59). These results suggested that the DNA vaccine efficacy was enhanced primarily by shifting helper T cells towards differentiation to Th1 cells when mannosylated polymers were used as DNA vaccine adjuvants. This enhanced level of IFN-γ is evidenced for the strong cellular immunity that is essential to eliminate virus infected cells (Constant and Bottomly, 1997).

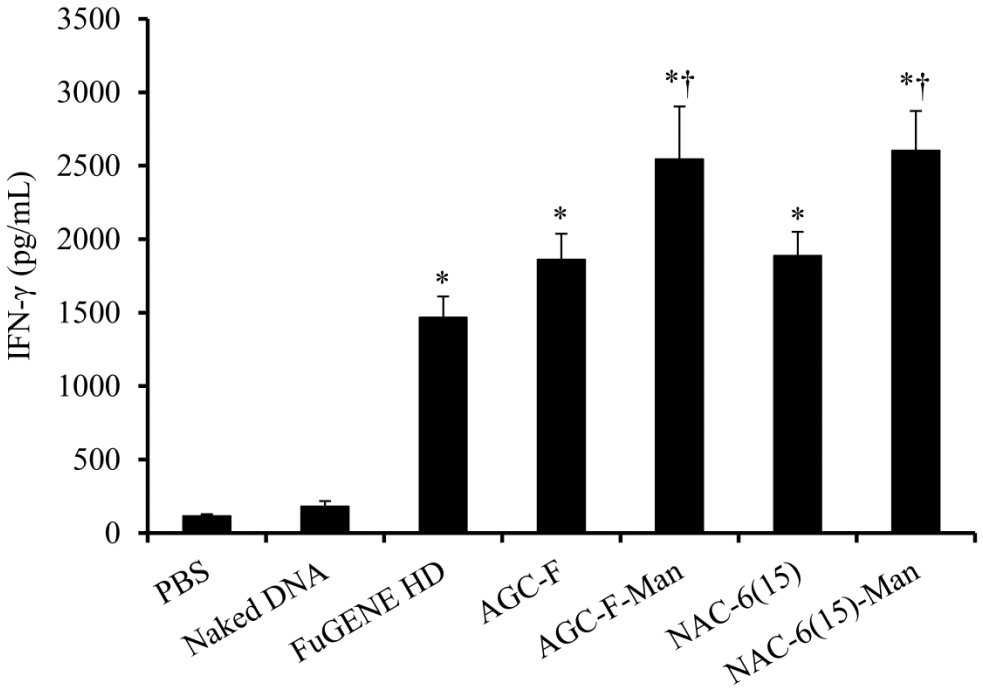

Figure 58. IFN-γ levels determined in cell culture supernatants of splenocytes. Data represents the mean ± SD (n = 6). ['*' significantly ($p < 0.05$) higher than naked DNA; '†' significantly ($p < 0.05$) higher than FuGENE HD].

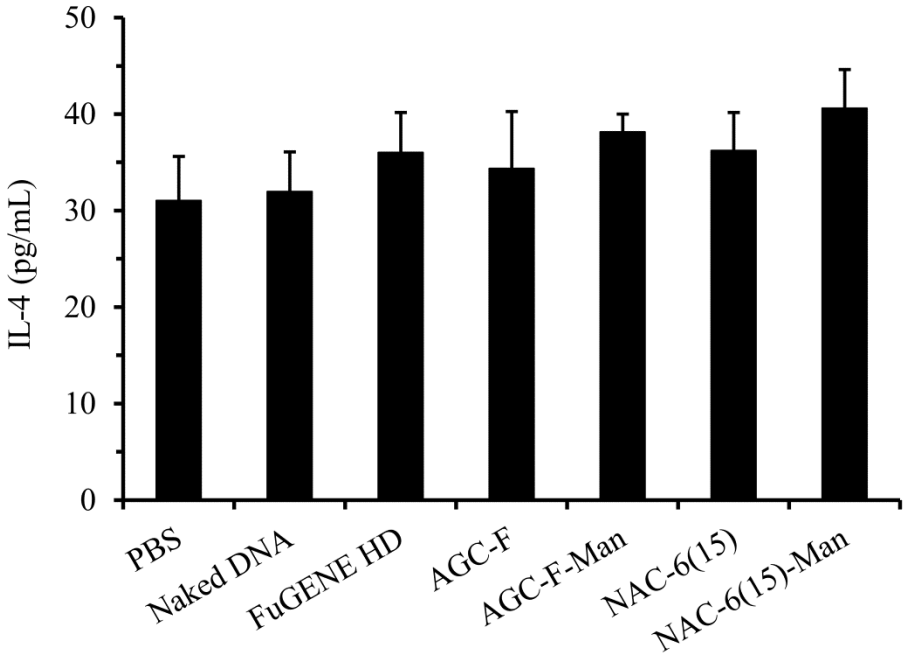

Figure 59. IL-4 levels determined in cell culture supernatants of splenocytes. Data represents the mean ± SD (n = 6).

5.3.12. In vivo toxicity

No signs of toxicity were observed when mice were administered with different HBV DNA vaccine formulations. The cationic polymers can induce inflammation and tissue necrosis (Jones et al., 2005). Thus, histological examination of the highly perfused tissues of the treated animals was also performed to evaluate in vivo biocompatibility of HBV DNA vaccine formulations. The tissue sections from the animals administered with PBS were used as control.

Hematoxylin-eosin staining of the treated tissue sections revealed no alterations in the morphological appearance of the tissues. Tissue sections collected from liver (Figure 60), heart (Figure 61), and kidney (Figure 62) of the treated animals did not show any necrosis, inflammation or enlargement of nuclei and were comparable to the tissue sections obtained from control animals.

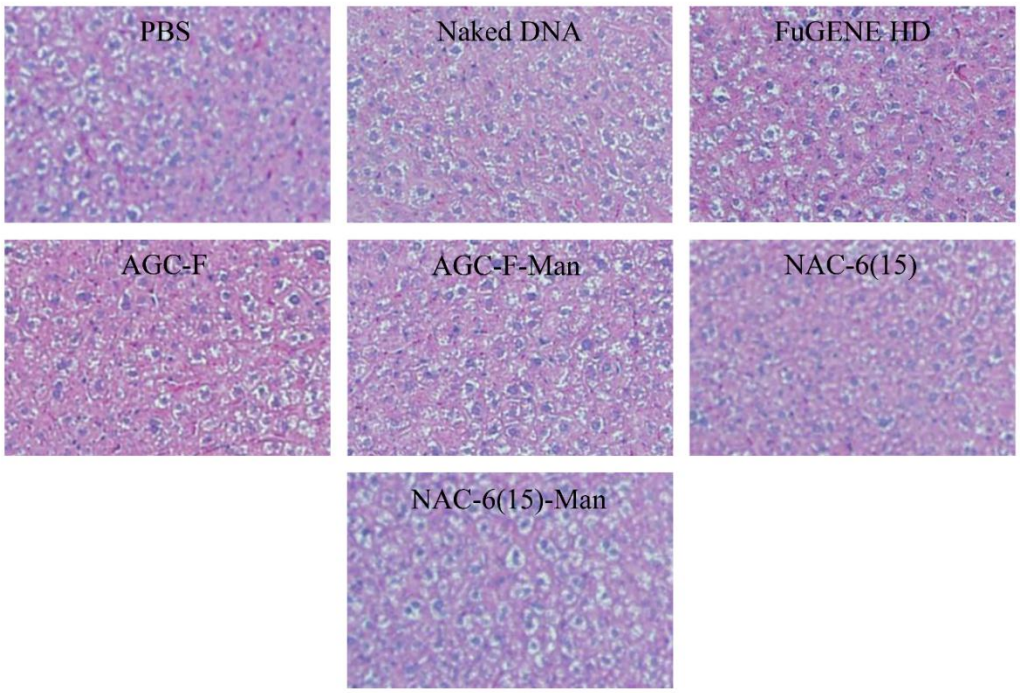

Figure 60. Histological examination of liver after immunization with different HBV DNA vaccine formulations. Organs were collected at the end of the study (6 weeks after primary immunization). The tissue section from mice administered with PBS was used as control.

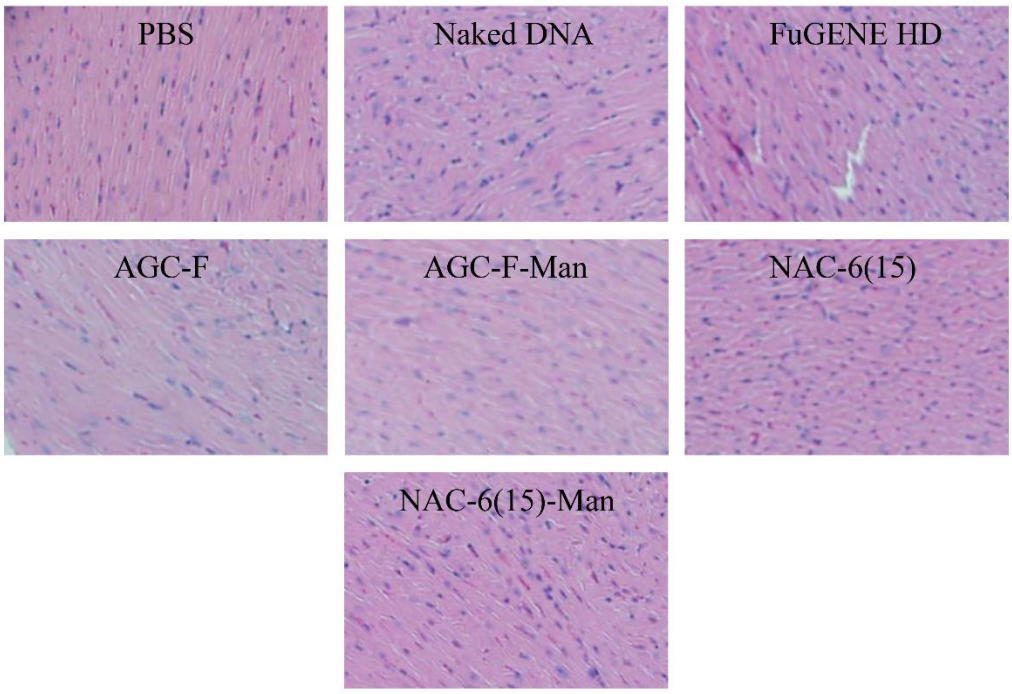

Figure 61. Histological examination of heart sections after immunization with different HBV DNA vaccine formulations.

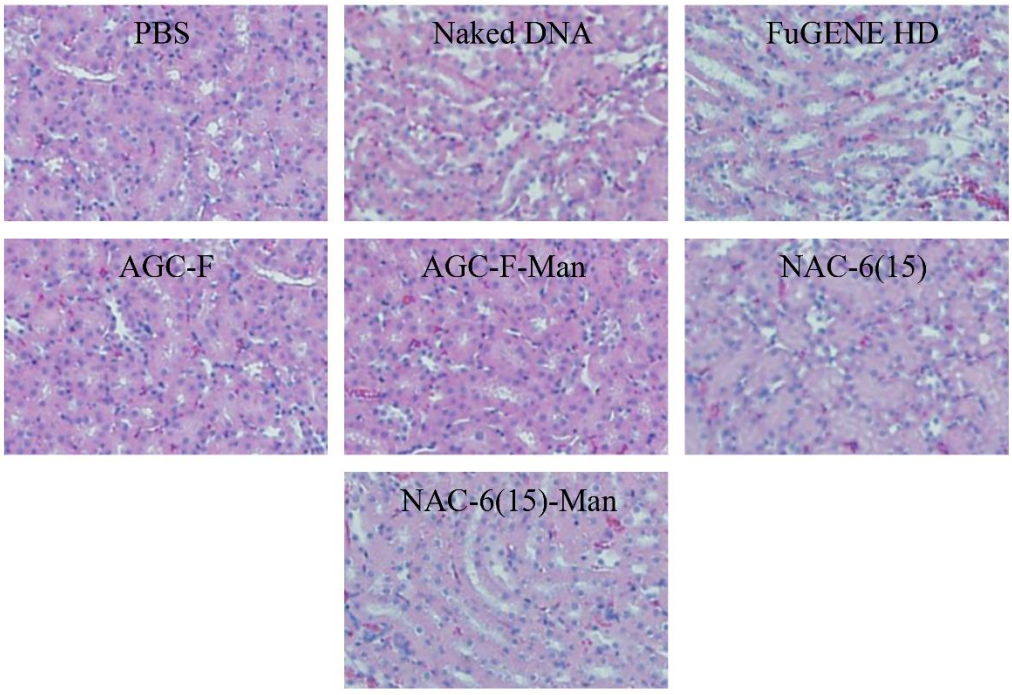

Figure 62. Histological examination of kidney sections after immunization with different HBV DNA vaccine formulations.

5.4. Conclusions

In this study, hydrophobically modified mannosylated chitosan derivatives were synthesized and evaluated as a gene or DNA vaccine carrier to specifically target antigen presenting cells. The mannosylated polymers demonstrated superior ability to form nanoscale polyplexes with pDNA and had suitable physicochemical properties for a DNA delivery system. This copolymer exhibited good in vitro and in vivo biocompatibility, and enhanced gene transfer efficiency and specificity when compared with FuGENE HD. The mannosylated polymers induced significantly higher immune responses in Balb/c mice using hepatitis B surface antigen encoding pDNA as a model DNA vaccine. These results illustrate that the mannosylated polymers can serve as a promising adjuvants for the targeted delivery of gene or DNA vaccine to APCs.

6. SUMMARY, CONCLUSIONS, AND FUTURE DIRECTIONS

6.1. Summary and conclusions

Gene therapy has emerged as a promising therapeutic strategy for the treatment of a wide range of inherited or acquired diseases. Genes are the blueprints for proteins, which act as building blocks for tissue, as well as critical regulators of biochemical reactions taking place inside all living cells. Errors in genes lead to disruptions in their expression and may result in disease. Conventional therapeutics can only mitigate symptoms of diseases and hence the results of treatments are often temporary. Gene therapy can eliminate the root causes of numerous diseases by replacing or repairing the patient's genetic code.

DNA vaccine is a relatively new branch in the field of gene therapy. It involves the direct administration of a pDNA code for an antigenic protein of a pathogen against which an immune response is sought. DNA vaccines have great potential in treatment and prevention of cancers and infectious diseases. Several advantages are associated with DNA immunization, e.g., relatively inexpensive to produce, heat stable, induce both cellular and humoral immune response, and no risk of reversion to pathogenicity. More importantly, DNA vaccines utilize host cells as bioreactors for in situ production of antigenic proteins. The endogenously produced antigens use both MHC I and MHC II pathways for antigen presentation and thereby induce strong cellular and humoral immune responses. Therefore, the DNA vaccines can be potentially useful for prophylactic as well as therapeutic purposes.

However, naked DNA is highly susceptible to nuclease degradation, shows poor cellular uptake, and low transfection efficiency. Therefore, the basic challenge for gene therapy is to design safe and effective carriers that assist efficient transfer of the therapeutic gene to targeted cells without degradation of the delivered gene. Recombinant viruses such as lentivirus,

retrovirus, adenovirus, and adeno-associated viruses have been widely studied for this purpose and epitomize the vast majority of clinical trials. As of June 2012, there has been over 1843 gene therapy clinical trials worldwide, ~ 68% of which have used various viral vectors. In spite of some limited success with recombinant viral vectors, there is still no FDA approved gene therapy products. Moreover, use of viral vectors in humans has been associated with inflammation, immunogenicity, cancers, and even death in a few cases. Therefore, viral-based delivery systems need to be reevaluated with respect to their safety issues for human gene therapy. Nonviral polymeric vectors have drawn increasing attention since their emergence, owing to their distinct advantages which include ease of synthesis, unrestricted gene loading capacity, low immunogenicity against the vector, and better safety profile.

The goal of this study was to design, synthesize, and evaluate polymer based nonviral vectors, which can effectively deliver loaded pDNA into the target cells without causing any harmful side effects. We have selected low molecular weight chitosan as a polymeric backbone because of its excellent biocompatibility, biodegradability, negligible cytotoxicity, low immunogenicity, and high cationic charge density. However, the clinical applications of unmodified chitosan have been limited by its low gene transfection efficiency. Studies have reported that the low transfection efficiency of chitosan is primarily attributed to the poor cellular uptake and inefficient release of pDNA from chitosan/pDNA polyplexes.

To overcome these challenges, a series of fatty acids with increasing chain length (N-hexanoic, N-octanoic, and N-decanoic acid) were utilized to synthesize N-acyl chitosan derivatives (NAC). The influence of fatty acid chain length was investigated by assessing the water solubility, particle size, zeta potential, pDNA binding affinity, pDNA release, cellular uptake, in vitro biocompatibility, and transfection efficiencies.

Hydrophobic modifications of chitosan enhanced its adsorption on cell surfaces and facilitated endocytosis of polymer/pDNA polyplexes. Furthermore, hydrophobic segments in chitosan assisted dissociation of polymer/pDNA polyplexes to promote intracellular release of pDNA which otherwise would be tightly bound through ionic interactions between phosphate groups of pDNA and amino groups of chitosan. Conjugation of hydrophobic segments to chitosan resulted in amphiphilic cationic polymers which could easily self-organize to form micelles in aqueous milieu. These polymeric micelles not only facilitate efficient pDNA condensation, but also improve the stability of pDNA polyplexes for in vitro and in vivo environments.

These NAC polymers effectively condensed pDNA resulting in the size range of 220-340 nm with net positive charge. NAC polymers also showed good pDNA binding capacity, high protection of pDNA from nuclease degradation and excellent biocompatibility. Transfection efficiency of chitosan, in HEK 293 cells, was enhanced 15-25-fold after coupling with fatty acid and increased with a decrease in fatty acyl chain length of NAC. Among different graft polymers N-acyl derivative of hexanoic acid (NAC-6) demonstrated significantly ($p < 0.05$) higher transfection efficiency in comparison to other NAC polymers as well as standard commercial nonviral transfecting agent FuGENE HD.

Our next aim was to gain insight about the optimum degree of N-acyl substitution of chitosan to control the degree of interaction between the NAC-6 polymer and its pDNA cargo. The NAC-6 with different substitution degrees (5%, 15%, and 25%) of hexanoic acid were synthesized and the influence of degree of substitution was examined in terms of pDNA binding strength, polyplex stability, in vitro pDNA release, cellular uptake, biocompatibility, and transfection efficiency in HEK 293 cells.

All of the NAC-6 polymers showed good pDNA condensing capacity and efficient protection of pDNA from DNase I. A positive correlation of higher degree of haxanoic acid substitution with increased pDNA release was evident, which suggested the reduction in pDNA binding strength of polymer at higher degree of hexanoic acid substitution. We demonstrated that the intermediate level of hydrophobic modification (i.e., 15% of hexanoic acid substitution) of chitosan with NAC-6(15) was favorable for pDNA delivery as suggested by 7-fold improvement in cellular internalization and 31-fold enhancement in transgene expression compared to unmodified chitosan. Moreover, NAC-6(15) polymer exhibited 1.33-fold higher gene expression in comparison to the marketed nonviral vector FuGENE HD. The degree of hexanoic acid substitution did not affect the in vitro biocompatibility of the polymers or polymer/pDNA polyplexes. These finding suggests that the promising future NAC-6(15) graft polymer as a nonviral gene delivery vector due to its superior transfection efficiency and biocompatibility.

Peptide conjugated chitosan polymers have recently received increasing attention in drug and gene delivery applications due to their distinct benefits of enhanced cell adsorption as well as excellent safety profile. However, the transfection potential of hydrophobic amino acid grafted chitosan has yet to be explored. In order to explore the gene transfer capacity of amino acid grafted chitosan (AGC) derivatives, chitosan was conjugated with a series of hydrophobic amino acids with increasing relative hydrophobicity indices ranging from 41 to 100. The graft polymers were characterized with respect to their pDNA binding efficiency, in vitro pDNA release profile, cellular uptake, in vitro transfection efficiency, cytotoxicity, and blood compatibility.

AGC polymers effectively bound and condensed pDNA to form cationic polyplexes in the size range of 155-263 nm, demonstrated excellent blood compatibility, and cell viability. Hydrophobic amino acid substitution contributed to enhance pDNA release at cytosolic pH. The

resultant polyplex showed 3.4-5.4-fold greater cellular uptake and 13-30-fold higher transfection efficiency in HEK 293 cells as compared to unmodified chitosan. Moreover, both cellular uptake and transfection efficiency improved with the increasing amino acid hydrophobicity. The AGC polymer with L-phenylalanine substitution (AGC-F) showed higher gene transfection efficiency with ~ 83% of GFP positive HEK 293 cells in comparison to other AGC polymers and FuGENE HD (~ 69% of GFP positive cells). These data demonstrate AGC-F polymer as a promising novel nonviral gene delivery vector.

A major shortcoming of chitosan-based gene delivery vectors is its poor cell specificity. The efficient delivery of antigen-encoded DNA into specific cells is of paramount importance to successful DNA vaccine development. Professional APCs such as dendritic cells and macrophages play a central role in the induction of immune responses to foreign antigens. It has also been reported that professional APCs overexpress mannose receptor on their cell surface. Hence, we have taken a novel approach to improve the cell specificity of the polymeric DNA vectors by conjugating mannose ligand to AGC-F and NAC-6(15) polymers. The mannosylated polymers were characterized with respect to their pDNA binding efficiency, in vitro and in vivo biocompatibility, APC targeting ability, cellular uptake, and in vitro gene transfection efficiency in RAW 264.7 and DC 2.4 cells. The DNA vaccine delivery potency of the polymers was evaluated by comparing the cellular and humoral immune responses induced by the different formulations in Balb/c mice.

The mannosylation of polymers did not alter the pDNA binding and protective capacity and biocompatibility of the polymers. We demonstrated that the APC targeting ability and cellular uptake of the polyplexes were significantly improved upon mannosylation. Mannosylated polymers such as AGC-F-Man and NAC-6(15)-Man significantly ($p < 0.05$)

increased the gene transfection efficiency of the polyplexes in RAW 264.7 and DC 2.4 cells. We demonstrated that mannosylated polymers induced more than 1150-fold greater antibody level and significantly ($p < 0.05$) stronger cellular immune responses compared with naked HBV DNA vaccine. The serums of mice immunized with mannosylated polymer/pHBsAg polyplexes demonstrated 2.6-fold higher anti-HBsAg antiboby titers than the mice immunized with FuGENE HD/pHBsAg complexes. However, there were no significant differences in the immune responses when AGC-F-Man and NAC-6(15)-Man were used as adjuvant. Thus, our results suggest a promising future for mannosylated chitosan derivative as an adjuvant for DNA vaccine delivery.

In conclusion, a series of hydrophobically modified chitosan derivatives was synthesized in order to find the optimum chain length, degree of substitution, and hydrophobicity which were then evaluated for gene delivery application. The two promising polymers were selected and mannosylated to examine their potency as in vivo DNA vaccine adjuvant. Moreover, the administration of hepatitis B DNA vaccine using these mannosylated polymers exhibited efficient cellular and immune responses in Balb/c mice model, indicating their promising future as adjuvant for HBV and other DNA vaccine deliver.

6.2. Future directions

The observations of this dissertation can direct several future researches in the field. We have used 91% deacetylated low molecular chitosan (Mw ~ 50 kDa) to synthesize hydrophobically modified chitosan derivatives. The availability of chitosan with a variety of molecular weights and degree of deacetylation as well as the availability of large number of hydrophobic moieties with diverse chemical structures could lead to some interesting

combinations. The attachment of cell penetrating peptide in combination with targeting ligand mannose can further enhance the gene transfer capacity of these polymers to APCs.

Our results demonstrated that these mannosylated polymers effectively target the RAW 264.7 macrophage cells; hence these delivery systems could be used for the targeted delivery of drugs or genes for the treatment of rheumatoid arthritis, acquired immune deficiency syndrome, leishmaniasis, tuberculosis, and many other diseases. In addition, a potential future approach could be the combination of these mannosylated polymers with other physical techniques of gene transfer. For example, the use of microneedle could be an interesting approach to improve the overall immune responses elicited by these DNA vaccine formulations.

7. LITERATURE CITED

Abbas, A.K., Lichtman, A.H., Pober, J.S., 1994. Antigen processing and presentation to T lymphocytes, in: Abbas, A.K., Lichtman, A.H., Pober, J.S. (Eds.), Cellular and molecular immunology. WB Saunders, Philadelphia, PA, pp. 115–135.

Abdelhalim, M.A., 2011. Exposure to gold nanoparticles produces cardiac tissue damage that depends on the size and duration of exposure. Lipids Health Dis. 10, 205.

Aderem, A., Underhill, D.M., 1999. Mechanisms of phagocytosis in macrophages. Annu. Rev. Immunol. 17, 593–623.

Akbari, O., Panjwani, N., Garcia, S., Tascon, R., Lowrie, D., Stockinger, B., 1999. DNA vaccination: transfection and activation of dendritic cells as key events for immunity. J. Exp. Med. 189, 169–178.

Akinc, A., Langer, R., 2002. Measuring the pH environment of DNA delivered using nonviral vectors: implications for lysosomal trafficking. Biotechnol. Bioeng. 78, 503–508.

Al-Dosari, M.S., Gao, X., 2009. Nonviral gene delivery: principle, limitations, and recent progress. AAPS J. 11, 671–681.

Al-Dosari, M.S., Knapp, J.E., Liu, D., 2006. Activation of human CYP2C9 promoter and regulation by CAR and PXR in mouse liver. Mol. Pharm. 3, 322–328.

Anderson, D.G., Akinc, A., Hossain, N., Langer, R., 2005. Structure/property studies of polymeric gene delivery using a library of poly(beta-amino esters). Mol. Ther. 11, 426–434.

Andre, F., Mir, L.M., 2004. DNA electrotransfer: its principles and an updated review of its therapeutic applications. Gene Ther. 11, S33–42.

Bailey, C.J., Crystal, R.G., Leopold, P.L., 2003. Association of adenovirus with the microtubule organizing center. J. Virol. 77, 13275–13287.

Banatvala, J.E., Van Damme, P., 2003. Hepatitis B vaccine – do we need boosters? J. Viral Hepat. 10, 1–6.

Barathmanikanth, S., Kalishwaralal, K., Sriram, M., Pandian, S.R., Youn, H.S., Eom, S., Gurunathan, S., 2010. Anti-oxidant effect of gold nanoparticles restrains hyperglycemic conditions in diabetic mice. J. Nanobiotechnol. 8, 16.

Behr, J.P., 1997. The proton sponge: a trick to enter cells the viruses did not exploit. Chimia 51, 34–36.

Benns, J.M., Mahato, R.I., Kim, S.W., 2002. Optimization of factors influencing the transfection efficiency of folate-PEG-folate-graft-polyethylenimine. J. Control. Release 79, 255–269.

Boussif, O., Lezoualc'h, F., Zanta, M.A., Mergny, M.D., Scherman, D., Demeneix, B., Behr, J.P., 1995. A versatile vector for gene and oligonucleotide transfer into cells in culture and in vivo: polyethyleneimine. Proc. Natl. Acad. Sci. USA 92, 7297–7301.

Burton, E.A., Glorioso, J.C., 2000. Herpes simplex virus vector-based gene therapy for malignant glioma. Gene Ther. Mol. Biol. 5, 131–145.

Carrillo-Carrasco, N., Chandler, R.J., Chandrasekaran, S., Venditti, C.P., 2010. Liver-directed recombinant adeno-associated viral gene delivery rescues a lethal mouse model of methylmalonic acidemia and provides long-term phenotypic correction. Hum. Gene Ther. 21, 1147–1154.

Casettari, L., Vllasaliu, D., Lam, J.K., Soliman, M., Illum, L., 2012. Biomedical applications of amino acid-modified chitosans: a review. Biomaterials 33, 7565–7583.

Cattoglio, C., Facchini, G., Sartori, D., Antonelli, A., Miccio, A., Cassani, B., Schmidt, M., von Kalle, C., Howe, S., Thrasher, A.J., Aiuti, A., Ferrari, G., Recchia, A., Mavilio, F., 2007. Hot spots of retroviral integration in human CD34+ hematopoietic cells. Blood 110, 1770–1778.

Chae, S.Y., Son, S., Lee, M., Jang, M.K., Nah, J.W., 2005. Deoxycholic acid-conjugated chitosan oligosaccharide nanoparticles for efficient gene carrier. J. Control. Release 109, 330–344.

Chailertvanitkul, V.A., Pouton, C.W., 2010. Adenovirus: a blueprint for non-viral gene delivery. Curr. Opin. Biotechnol. 21, 627–632.

Chan, C.L., Majzoub, R.N., Shirazi, R.S., Ewert, K.K., Chen, Y.J., Liang, K.S., Safinya, C.R., 2012. Endosomal escape and transfection efficiency of PEGylated cationic liposome–DNA complexes prepared with an acid-labile PEG-lipid. Biomaterials 33, 4928–4935.

Chang, K.L., Higuchi, Y., Kawakami, S., Yamashita, F., Hashida, M., 2010. Efficient gene transfection by histidine-modified chitosan through enhancement of endosomal escape. Bioconjugate Chem. 21, 1087–1095.

Check, E., 2005. Gene therapy put on hold as third child develops cancer. Nature 433, 561.

Chen, X., Ding, S., Qu, G., Zhang, C., 2008a. Synthesis of novel chitosan derivatives for micellar solubilization of cyclosporine A. J. Bioact. Compat. Polym. 23, 563–578.

Chen, S., Cheng, S.X., Zhuo, R.X., 2011. Self-assembly strategy for the preparation of polymer-based nanoparticles for drug and gene delivery. Macromol. Biosci. 11, 576–589.

Chen, H.H., Ho, Y.P., Jiang, X., Mao, H.Q., Wang, T.H., Leong, K.W., 2008b. Quantitative comparison of intracellular unpacking kinetics of polyplexes by a model constructed from quantum Dot-FRET. Mol. Ther. 16, 324–332.

Choate, K.A., Khavari, P.A., 1997. Direct cutaneous gene delivery in a human genetic skin disease. Hum. Gene Ther. 8, 1659–1665.

Choksakulnimitr, S., Masuda, S., Tokuda, H., Takakura, Y., Hashida, M., 1995. In vitro cytotoxicity of macromolecules in different cell culture systems. J. Control. Release 34, 233–241.

Choosakoonkriang, S., Lobo, B.A., Koe, G.S., Koe, J.G., Middaugh, C.R., 2003. Biophysical characterization of PEI/DNA complexes. J. Pharm. Sci. 92, 1710–1722.

Clay, T.M., Hobeika, A.C., Mosca, P.J., Lyerly, H.K., Morse, M.A., 2001. Assays for monitoring cellular immune responses to active immunotherapy of cancer. Clin. Cancer Res. 7, 1127–1135.

Conner, S.D., Schmid, S.L., 2003. Regulated portals of entry into the cell. Nature 422, 37–44.

Constant, S.L., Bottomly, K., 1997. Induction of Th1 and Th2 CD4+ T cell responses: the alternative approaches. Annu. Rev. Immunol. 15, 297–322.

Curiel, D.T., Agarwal, S., Wagner, E., Cotton, M., 1991. Adenovirus enhancement of transferrin-polylysine-mediated gene delivery. Proc. Natl. Acad. Sci. USA 88, 8850–8854.

Deng, C.X., Sieling, F., Pan, H., Cui, J., 2004. Ultrasound induced cell membrane porosity. Ultrasound Med. Biol. 30, 519–526.

Díaz-Moscoso, A., Guilloteau, N., Bienvenu, C., Méndez-Ardoy, A., Blanco, J.L., Benito, J.M., Le Gourriérec, L., Di Giorgio, C., Vierling, P., Defaye, J., Mellet, C.O., Fernández, J.M., 2011. Mannosyl-coated nanocomplexes from amphiphilic cyclodextrins and pDNA for site-specific gene delivery. Biomaterials 32, 7263–7273.

Dodane, V., Vilivalam, V.D., 1998. Pharmaceutical applications of chitosan. Pharm. Sci. Technol. Today 1, 246–253.

Domard, A., 1987. pH and c.d. measurements on a fully deacetylated chitosan: application to CuII–polymer interactions. Int. J. Biol. Macromol. 9, 98–104.

Dong, G.H., Wang, J., Zhang, Y.H., Liu, M.M., Wang, D., Zheng, L., Jin, Y.H., 2012. Induction of p53-mediated apoptosis in splenocytes and thymocytes of C57BL/6 mice exposed to perfluorooctane sulfonate (PFOS). Toxicol. Appl. Pharmacol. 264, 292–299.

Donnelly, J.J., Ulmer, J.B., Shiver, J.W., Liu, M.A., 1997. DNA vaccines. Annu. Rev. Immunol. 15, 617–648.

Du, Z., Chen, M., He, Q., Zhou, Y., Jin, T., 2012. Polymerized spermine as a novel polycationic nucleic acid carrier system. Int. J. Pharm. 434, 437–443.

Du, Y.Z., Lu, P., Zhou, J.P., Yuan, H., Hu, F.Q., 2010. Stearic acid grafted chitosan oligosaccharide micelle as a promising vector for gene delivery system: factors affecting the complexation. Int. J. Pharm. 391, 260–266.

Duceppe, N., Tabrizian, M., 2010. Advances in using chitosan-based nanoparticles for in vitro and in vivo drug and gene delivery. Expert Opin. Drug Deliv. 7, 1191–1207.

During, M.J., 1997. Adeno-associated virus as a gene delivery system. Adv. Drug Deliv. Rev. 27, 83–94.

Elouahabi, A., Ruysschaert, J.M., 2005. Formation and intracellular trafficking of lipoplexes and polyplexes. Mol. Ther. 11, 336–347.

Encke, J., zu Putlitz, J., Wands, J.R., 1999. DNA vaccines. Intervirology 42, 117–124.

Fabre, J.W., Grehan, A., Whitehorne, M., Sawyer, G.J., Dong, X., Salehi, S., Eckley, L., Zhang, X., Seddon, M., Shah, A.M., Davenport, M., Rela, M., 2008. Hydrodynamic gene delivery to the pig liver via an isolated segment of the inferior vena cava. Gene Ther. 15, 452–462.

Felgner, P.L., Gadek, T.R., Holm, M., Roman, R., Chan, H.W., Wenz, M., Northrop, J.P., Ringold, G.M., Danielsen, M., 1987. Lipofection: a highly efficient, lipid-mediated DNA-transfection procedure. Proc. Natl. Acad. Sci. USA 84, 7413–7417.

Ferrara, K.W., 2010. Driving delivery vehicles with ultrasound. Adv. Drug Deliv. Rev. 60, 1097–1102.

Ferrari, C., Penna, A., Bertoletti, A., Valli, A., Antoni, A.D., Giuberti, T., Cavalli, A., Petit, M.A., Fiaccadori, F., 1990. Cellular immune response to hepatitis B virus-encoded antigens in acute and chronic hepatitis B virus infection. J. Immunol. 145, 3442–3449.

Filion, D., Lavertu, M., Buschmann, M.D., 2007. Ionization and solubility of chitosan solutions related to thermosensitive chitosan/glycerol-phosphate systems. Biomacromolecules 8, 3224–3234.

Fischer, D., Li, Y.X., Ahlemeyer, B., Krieglstein, J., Kissel T., 2003. In vitro cytotoxicity testing of polycations: influence of polymer structure on cell viability and hemolysis. Biomaterials 24, 1121–1131.

Friend, D.S., Papahadjopoulos, D., Debs, R.J., 1996. Endocytosis and intracellular processing accompanying transfection mediated by cationic liposomes. Biochim. Biophys. Acta 1278, 41–50.

Gabrielson, N.P., Pack, D.W., 2006. Acetylation of polyethylenimine enhances gene delivery via weakened polymer/DNA interactions. Biomacromolecules 7, 2427–2435.

Gabrielson, N.P., Pack, D.W., 2009. Efficient polyethylenimine-mediated gene delivery proceeds via a caveolar pathway in HeLa cells. J. Control. Release 136, 54–61.

Gao, S., Chen, J., Dong, L., Ding, Z., Yang, Y.H., Zhang, J., 2005. Targeting delivery of oligonucleotide and plasmid DNA to hepatocyte via galactosylated chitosan vector. Eur. J. Pharm. Biopharm. 60, 327–334.

Gao, X., Kim, K.S., Liu, D., 2007. Nonviral gene delivery: what we know and what is next. AAPS J. 9, 92–104.

Gao, Y., Zhang, Z., Chen, L., Gu, W., Li, Y., 2009. Synthesis of 6-N,N,N-trimethyltriazole chitosan via "click chemistry" and evaluation for gene delivery. Biomacromolecules 10, 2175–2182.

Ge, Y., Zhang, Y., He, S., Nie, F., Teng, G., Gu, N., 2009. Fluorescence modified chitosan-coated magnetic nanoparticles for high-efficient cellular imaging. Nanoscale Res. Lett. 4, 287–295.

Gehl, J., 2003. Electroporation: theory and methods, perspectives for drug delivery, gene therapy and research. Acta Physiol. Scand. 177, 437–447.

Genta, I., Perugini, P., Pavanetto, F., 1998. Different molecular weight chitosan microspheres: influence on drug loading and drug release. Drug Dev. Ind. Pharm. 24, 779–784.

Germershaus, O., Mao, S.R., Sitterberg, J., Bakowsky, U., Kissel, T., 2008. Gene delivery using chitosan, trimethyl chitosan or polyethylenglycol-graft-trimethyl chitosan block copolymers: establishment of structure-activity relationships in vitro. J. Control. Release 125, 145–154.

Gershon, H., Ghirlando, R., Guttman, S.B., Minsky, A., 1993. Mode of formation and structural features of DNA-cationic liposome complexes used for transfection. Biochemistry 32, 7143–7151.

Ginn, S.L., Alexander, I.E., Edelstein, M.L., Abedi, M.R., Wixon, J., 2013. Gene therapy clinical trials worldwide to 2012 – an update. J. Gene Med. 15, 65–77.

Glover, D.J., Lipps, H.J., Jans, D.A., 2005. Non-viral approaches towards safe, stable therapeutic gene expression in humans. Nat. Rev. Genet. 6, 299–310.

Godbey, W.T., Wu, K.K., Mikos, A.G., 1999. Poly(ethylenimine) and its role in gene delivery. J. Control. Release 60, 149–160.

Gopal, V., Xavier, J., Dar, G.H., Jafurulla, M., Chattopadhyay, A., Rao, N.M., 2011. Targeted liposomes to deliver DNA to cells expressing 5-HT receptors. Int. J. Pharm. 419, 347–354.

Gosselin, M.A., Guo, W., Lee, R.J., 2001. Efficient gene transfer using reversibly cross-linked low molecular weight polyethylenimine. Bioconjugate Chem. 12, 989–994.

Goswami, S., Mukherjee, R., Mukherjee, R., Jana, S., Maity, A.C., Adak, A.K., 2005. Simple and efficient synthesis of 2,7-difunctionalized-1,8-naphthyridines. Molecules 10, 929–936.

Greber, U.F., Way, M., 2006. A superhighway to virus infection. Cell 124, 741–754.

Green, J.J., Shi, J., Chiu, E., Leshchiner, E.S., Langer, R., Anderson, D.G., 2006. Biodegradable polymeric vectors for gene delivery to human endothelial cells. Bioconjugate Chem. 17, 1162–1169.

Guliyeva, U., Oner, F., Ozsoy, S., Haziroğlu, R., 2006. Chitosan microparticles containing plasmid DNA as potential oral gene delivery system. Eur. J. Pharm. Biopharm. 62, 17–25.

Guo, X., Huang, L., 2012. Recent advances in nonviral vectors for gene delivery. Acc. Chem. Res. 45, 971–979.

Hacein-Bey-Abina, S., von Kalle, C., Schmidt, M., Le Deist, F., Wulffraat, N., McIntyre, E., Radford, I., Villeval, J.L., Fraser, C.C., Cavazzana-Calvo, M., Fischer A., 2003. A serious adverse event after successful gene therapy for X-linked severe combined immunodeficiency. New Engl. J. Med. 348, 255–256.

He, C.H., Tabata, Y., Gao, J.Q., 2010. Non-viral gene delivery carrier and its three-dimensional transfection system. Int. J. Pharm. 386, 232–242.

Heller, R., Jaroszeski, M., Atkin, A., Moradpour, D., Gilbert, R., Wands, J., Nicolau, C., 1996. In vivo gene electroinjection and expression in rat liver. FEBS Lett. 389, 225–228.

Hillaireau, H., Couvreur, P., 2009. Nanocarriers' entry into the cell: relevance to drug delivery. Cell. Mol. Life Sci. 66, 2873–2896.

Hirano, S., Kaneko, H., Kitagawa, M., 1991. N-lower-fatty-acyl derivatives of chitosan as adsorbents for lysozyme and chitinase. Agric. Biol. Chem. 55, 1683–1684.

Hoekstra, D., Rejman, J., Wasungu, L., Shi, F., Zuhorn, I., 2007. Gene delivery by cationic lipids: in and out of an endosome. Biochem. Soc. Trans. 35, 68–71.

Hoggard, M.K., Varum, K.M., Issa, M., Danielsen, S., Christensen, B.E., Stokke, B.T., Artursson, P., 2004. Improved chitosan mediated gene delivery based on easily dissociated chitosan polyplexes of highly defined chitosan oligomers. Gene Ther. 11, 1441–1452.

Huang, M., Fong, C.W., Khorc, E., Lim, L.Y., 2005. Transfection efficiency of chitosan vectors: effect of polymer molecular weight and degree of deacetylation. J. Control. Release 106, 391–406.

Hu, F.Q., Zhao, M.D., Yuan, H., You, J., Du, Y.Z., Zeng, S., 2006. A novel chitosan oligosaccharide-stearic acid micelles for gene delivery: properties and in vitro transfection studies. Int. J. Pharm. 315, 158–166.

Huebener, N., Fest, S., Strandsby, A., Michalsky, E., Preissner, R., Zeng, Y., Gaedicke, G., Lode, H.N., 2008. A rationally designed tyrosine hydroxylase DNA vaccine induces specific antineuroblastoma immunity. Mol. Cancer Ther. 7, 2241–2251.

Ishii, T., Okahata, Y., Sato, T., 2001. Mechanism of cell transfection with plasmid/chitosan complexes. Biochim. Biophys. Acta 1514, 51–64.

Jayakumar, R., Chennazhi, K.P., Muzzarelli R.A.A., Tamura, H., Nair, S.V., Selvamurugan, N., 2010. Chitosan conjugated DNA nanoparticles in gene therapy. Carbohydr. Polym. 79, 1–8.

Jazi, M.H., Dabaghian, M., Tebianian, M., Gharagozlou, M.J., Ebrahimi, S.M., 2012. In vivo electroporation enhances immunogenicity and protection against influenza A virus challenge of an M2e-HSP70c DNA vaccine. Virus Res. 167, 219–225.

Jones, S.W., Christison, R., Bundell, K., Voyce, C.J., Brockbank, S.M., Newham, P., Lindsay, M.A., 2005. Characterisation of cell-penetrating peptide-mediated peptide delivery. Br. J. Pharmacol. 145, 1093–1102.

Jones, D.S., Mawhinney, H.J., 2005. Chitosan, in: Rowe, R.C, Sheskey, P.J, Owen, S.C (Eds.), Handbook of pharmaceutical excipients, 5th edn. Pharmaceutical Press and American Pharmacists Association, Washington DC, pp. 159–162.

Kainthan, R.K., Gnanamani, M., Ganguli, M., Ghosh, T., Brooks, D.E., Maiti, S., Kizhakkedathu, J.N., 2006. Blood compatibility of water soluble hyperbranched

polyglycerol-based multivalent cationic polymers and their interaction with DNA. Biomaterials 27, 5377–5390.

Kang, M.L., Cho, C.S., Yoo, H.S., 2009. Application of chitosan microspheres for nasal delivery of vaccines. Biotechnol. Adv. 27, 857–865.

Kay, M.A., Glorioso, J.C., Naldini, L., 2001. Viral vectors for gene therapy: the art of turning infectious agents into vehicles of therapeutics. Nat. Med. 7, 33–40.

Katayose, S., Kataoka, K., 1998. Remarkable increase in nuclease resistance of plasmid DNA through supramolecular assembly with poly(ethylene glycol)-poly(L-lysine) block copolymer. J. Pharm. Sci. 87, 160–163.

Kawabata, K., Takakura, Y., Hashida, M., 1995. The fate of plasmid DNA after intravenous injection in mice: involvement of scavenger receptors in its hepatic uptake. Pharm. Res. 12, 825–830.

Kiang, T., Wen, J., Lim, H.W., Leong, K.W., 2004. The effect of the degree of chitosan deacetylation on the efficiency of gene transfection. Biomaterials 25, 5293–5301.

Kim, J.W., Gulley, J.L., 2012. Poxviral vectors for cancer immunotherapy. Expert Opin. Biol. Ther. 12, 463–478.

Kim, T.H., Ihm, J.E., Choi, Y.J., Nah, J.W., Cho, C.S., 2003. Efficient gene delivery by urocanic acid-modified chitosan. J. Control. Release 93, 389–402.

Kim, T.H., Jiang, H.L., Jere, D., Park, I.K., Cho, M.H., Nah, J.W., Choi, Y.J., Akaike, T., Cho, C.S., 2007. Chemical modification of chitosan as a gene carrier in vitro and in vivo. Prog. Polym. Sci. 32, 726–753.

Kim, T.H., Nah, J.W., Cho, M.H., Park, T.G., Cho, C.S., 2006. Receptor-mediated gene delivery into antigen presenting cells using mannosylated chitosan/DNA nanoparticles. J. Nanosci. Nanotechnol. 6, 2796–2803

Klein, R.M., Wolf, E.D., Wu, R., Sanford, J.C., 1992. High-velocity microprojectiles for delivering nucleic acids into living cells. Biotechnology 24, 384–386.

Kong, F., Zhou, F., Ge, L., Liu, X., Wang, Y., 2012. Mannosylated liposomes for targeted gene delivery. Int. J. Nanomedicine 7, 1079–1089.

Koping-Hoggard, M., Tubulekas, I., Guan, H., Edwards, K., Nilsson, M., Varum, K.M., Artursson, P., 2001. Chitosan as a nonviral gene delivery system. Structure-property relationships and characteristics compared with polyethylenimine in vitro and after lung administration in vivo. Gene Ther. 8, 1108–1121.

Koping-Hoggard, M., Varum, K.M., Issa M., Danielsen, S., Christensen, B.E., Stokke, B.T., Artursson, P., 2004. Improved chitosan-mediated gene delivery based on easily dissociated chitosan polyplexes of highly defined chitosan oligomers. Gene Ther. 11, 1441–1452.

Kunitz, M., 1950. Crystalline desoxyribonuclease; digestion of thymus nucleic acid; the kinetics of the reaction. J. Gen. Physiol. 33, 363–377.

Kursa, M., Walker, G.F., Roessler, V., Ogris, M., Roedl, W., Kircheis, R., Wagner, E., 2003. Novel shielded transferrin-polyethylene glycol-polyethylenimine/DNA complexes for systemic tumor-targeted gene transfer. Bioconjugate Chem. 14, 222–231.

Lavanchy, D., 2004. Hepatitis B virus epidemiology, disease burden, treatment, and current and emerging prevention and control measures. J. Viral Hepat.11, 97–107.

Larkin, J., Clayton, M., Sun, B., Perchonock, C.E., Morgan, J.L., Siracusa, L.D., Michaels, F.H., Feitelson, M.A., 1999. Hepatits B virus transgenic mouse model of chronic liver disease. Nat. Med. 5, 907–912.

Layek, B., Singh, J., 2012. N-hexanoyl N-octanoyl and N-decanoyl chitosans: binding affinity, cell uptake, and transfection. Carbohydr. Polym. 89, 403–410.

Layek, B., Singh, J., 2013a. Amino acid grafted chitosan for high performance gene delivery: comparison of amino acid hydrophobicity on vector and polyplex characteristics. Biomacromolecules 14, 485−494.

Layek, B., Singh, J., 2013b. Caproic acid grafted chitosan cationic nanocomplexes for enhanced gene delivery: effect of degree of substitution. Int. J. Pharm. 447, 182−191.

Lee, M.K., Chun, S.K., Choi, W.J., Kim, J.K., Choi, S.H., Kim, A., Oungbho, K., Park, J.S., Ahn, W.S., Kim, C.K., 2005. The use of chitosan as a condensing agent to enhance emulsion-mediated gene transfer. Biomaterials 26, 2147–2156.

Lee, K.Y., Kwon, I.C., Jo, W.H., Jeong, S.Y., 2005. Complex formation between plasmid DNA and self-aggregates of deoxycholic acid-modified chitosan. Polymer 46, 8107–8112.

Lee, K.Y., Kwon, I.C., Kim, Y.H.; Jo, W.H., Jeong, S.Y., 1998. Preparation of chitosan self-aggregates as a gene delivery system. J. Control. Release 51, 213−220.

Lee, D., Zhang, W., Shirley, S.A., Kong, X., Hellermann, G.R., Lockey, R.F., Mohapatra, S.S., 2007. Thiolated chitosan/DNA nanocomplexes exhibit enhanced and sustained gene delivery. Pharm. Res. 24, 157–167.

Leitner, W.W., Ying, H., Restifo, N.P., 2000. DNA and RNA-based vaccines: principles, progress and prospects. Vaccine 18, 765–777.

Levy, M.Y., Barron, L.G., Meyer, K.B., Szoka, F.C., Jr., 1996. Characterization of plasmid DNA transfer into mouse skeletal muscle: evaluation of uptake mechanism, expression and secretion of gene products into blood. Gene Ther. 3, 201–211.

Li, C., Bowles, D.E., van Dyke, T., Samulski, R.J., 2005. Adeno-associated virus vectors: potential applications for cancer gene therapy. Cancer Gene Ther. 12, 913–925.

Li, Z.T., Guo, J., Zhang, J.S., Zhao, Y.P., Lv, L., Ding, C., Zhang, X.Z., 2010. Chitosan-graft-polyethylenimine with improved properties as a potential gene vector. Carbohydr. Polym. 80, 254–259.

Lin, M.T.S., Pulkininen, L., Uitto, J., Yoon, K., 2000. The gene gun: current applications in cutaneous gene therapy. Int. J. Dermatol. 39, 161–170.

Liu, Y.M., Reineke, T.M., 2005. Hydroxyl stereochemistry and amine number within poly(glycoamidoamine)s affect intracellular DNA delivery. J. Am. Chem. Soc. 127, 3004–3015.

Liu, W.G., Yao, K.D., 2002. Chitosan and its derivatives–a promising nonviral vector for gene transfection. J. Control. Release 83, 1–11.

Liu, W.G., Zhang, X., Sun, S.J., Sun, G.J., Yao, K.D., Liang, D.C., Guo, G., Zhang, J.Y., 2003. N-alkylated chitosan as a potential nonviral vector for gene transfection. Bioconjugate Chem. 14, 782–789.

Liu, Z., Zhang, Z., Zhou, C., Jiao, Y., 2010. Hydrophobic modifications of cationic polymers for gene delivery. Prog. Poly. Sci. 35, 1144–1162.

Lu, S., Wang, S., Grimes-Serrano, J.M., 2008. Current progress of DNA vaccine studies in humans. Expert Rev. Vaccines 7, 175–191.

Lu, B., Wang, C.F., Wu, D.Q., Li, C., Zhang, X.Z., Zhuo, R.X., 2009. Chitosan based oligoamine polymers: synthesis, characterization, and gene delivery. J. Control. Release 137, 54–62.

Ma, P.L., Lavertu, M., Winnik, F.M., Buschmann, M.D., 2009. New insights into chitosan–DNA interactions using isothermal titration microcalorimetry. Biomacromolecules 10, 1490–1499.

Mahor, S., Rawat, A., Dubey, P.K., Gupta, P.N., Khatri, K., Goyal, A.K., Vyas, S.P., 2007. Cationic transfersomes based topical genetic vaccine against hepatitis B. Int. J. Pharm. 340, 13–19.

Malmo, J., Vårum, K.M., Strand, S.P., 2011. Effect of chitosan chain architecture on gene delivery: comparison of self-branched and linear chitosans. Biomacromolecules 12, 721–729.

Mansouri, S., Lavigne, P., Corsi, K., Benderdour, M., Beaumont, E., Fernandes, J.C., 2004. Chitosan-DNA nanoparticles as non-viral vectors in gene therapy: strategies to improve transfection efficacy. Eur. J. Pharm. Biopharm. 57, 1–8.

Mao, H.Q., Roy, K., Troung-Le, V.L., Janes, K.A., Lin, K.Y., Wang, Y., August, J.T., Leong, K.W., 2001. Chitosan–DNA nanoparticles as gene carriers: synthesis, characterization and transfection efficiency. J. Control. Release 70, 399–421.

Mao, S., Shuai, X., Unger, F., Simon, M., Bi, D., Kissel, T., 2004. The depolymerization of chitosan: effects on physicochemical and biological properties. Int. J. Pharm. 281, 45–54.

Mao, S., Sun, W., Kissel, T., 2010. Chitosan-based formulations for delivery of DNA and siRNA. Adv. Drug Deliv. Rev. 62, 12–27.

Medi, B.M., Hoselton, S., Marepalli, R.B., Singh, J., 2005. Skin targeted DNA vaccine delivery using electroporation in rabbits. I: efficacy. Int. J. Pharm. 294, 53–63.

Medina-Kauwe, L.K., Xie, J., Hamm-Alvarez, S., 2005. Intracellular trafficking of nonviral vectors. Gene Ther. 12, 1734–1751.

Mellman, I., Steinman, R.M., 2001. Dendritic cells: specialized and regulated antigen processing machines. Cell 106, 255–258.

Mhashilkar, A., Chada, S., Roth, J.A., Ramesh, R., 2001. Gene therapy. Therapeutic approaches and implications. Biotechnol. Adv. 19, 279–297.

Michel, M.L., Loirat, D., 2001. DNA vaccines for prophylactic or therapeutic immunization against hepatitis B. Intervirology 44, 78–87.

Miller, D. L., Pislaru, S.V., Greenleaf, J.E., 2002. Sonoporation: mechanical DNA delivery by ultrasonic cavitation. Somat. Cell Mol. Genet. 27, 115–134.

Mintzer, M.A., Simanek, E.E., 2009. Nonviral vectors for gene delivery. Chem. Rev. 109, 259–302.

Mir, L.M., Bureau, M.F., Gehl, J., Rangara, R., Rouy, D., Caillaud, J.M., Delaere, P., Branellec, D., Schwartz, B., Scherman, D., 1999. High efficiency gene transfer into skeletal muscle mediated by electric pulses. Proc. Natl. Acad. Sci. USA 96, 4262–4267.

Mislick, K.A., Baldeschwieler, J.D., Kayyem, J.F., Meade, T.J, 1995. Transfection of folate-polylysine DNA complexes: evidence for lysosomal delivery. Bioconjugate Chem. 6, 512–515.

Miyazaki, M., Obata, Y., Abe, K., Furusu, A., Koji, T., Tabata, Y., Kohno, S., 2006. Gene transfer using nonviral delivery systems. Perit. Dial. Int. 26, 633–640.

Miyazawa, N., Leopold, P.L., Hackett, N.R., Ferris, B., Worgall, S., Falck-Pedersen, E., Crystal, R.G., 1999. Fiber swap between adenovirus subgroups B and C alters intracellular trafficking of adenovirus gene transfer vectors. J. Virol. 73, 6056–6065.

Monera, O.D., Sereda, T.J., Zhou, N.E., Kay, C.M., Hodges, R.S., 1995. Relationship of side chain hydrophobicity and alpha-helical propensity on the stability of the single-stranded amphipathic alpha-helix. J. Pept. Sci. 1, 319–329.

Montini, E., Cesana, D., Schmidt, M., Sanvito, F., Ponzoni, M., Bartholomae, C., Sergi Sergi, L.S., Benedicenti, F., Ambrosi, A., Di Serio, C., Doglioni, C., von Kalle, C., Naldini, L., 2006. Hematopoietic stem cell gene transfer in a tumor-prone mouse model uncovers low genotoxicity of lentiviral vector integration. Nat. Biotechnol. 24, 687–696.

Muzzarelli, R.A.A., Frega, N., Miliani, M., Muzzarelli, C., Cartolari, M., 2000. Interactions of chitin, chitosan, N-lauryl chitosan and N-dimethylaminopropyl chitosan with olive oil. Carbohydr. Polym. 43, 263–268.

Nam, H.Y., Kwon, S.M., Chung, H., Lee, S.Y., Kwon, S.H., Jeon, H., Kim, Y., Park, J.H., Kim, J., Her, S., Oh, Y.K., Kwon, I.C., Kim, K., Jeong, S.Y., 2009. Cellular uptake mechanism and intracellular fate of hydrophobically modified glycol chitosan nanoparticles. J. Control. Release 135, 259–267.

Needham, C.J., Williams, A.K., Chew, S.A., Kasper, F.K., Mikos, A.G., 2012. Engineering a polymeric gene delivery vector based on poly(ethylenimine) and hyaluronic acid. Biomacromolecules 13, 1429–1437.

Nemerow, G.R., Stewart, P.L., 1999. Role of αv integrins in adenovirus cell entry and gene delivery. Microbiol. Mol. Biol. Rev. 63, 725–734.

Neumann, E., Schaefer-Ridder, M., Wang, Y., Hofschneider, P.H., 1982. Gene transfer into mouse lyoma cells by electroporation in high electric fields. Embo. J. 1, 841–845.

Newman, C.M., Bettinger, T., 2007. Gene therapy progress and prospects: ultrasound for gene transfer. Gene Ther. 14, 465–475

Niidome, T., Huang, L., 2002. Gene therapy progress and prospects: nonviral vectors. Gene Ther. 9, 1647–1652.

Pack, D.W., Hoffman, A.S., Pun, S., Stayton, P.S., 2005. Design and development of polymers for gene delivery. Nat. Rev. Drug Discov. 4, 581–593.

Park, I.Y., Kim, I.Y., Yoo, M.K., Choi, Y.J., Cho, M.H., Cho, C.S., 2008. Mannosylated polyethylenimine coupled mesoporous silica nanoparticles for receptor-mediated gene delivery. Int. J. Pharm. 359, 280–287.

Park, I.K., Park, Y.H., Shin, B.A., Choi, E.S., Kim, Y.R., Akaike, T., Cho, C.S., 2000. Galactosylated chitosan-graft-dextran as hepatocyte-targeting DNA carrier. J. Control. Release 69, 97–108.

Pichon, C., Goncalves, C., Midoux, P., 2001. Histidine-rich peptides and polymers for nucleic acids delivery. Adv. Drug Deliv. Rev. 53, 75–94.

Piest, M., Engbersen, J.F.J., 2010. Effects of charge density and hydrophobicity of poly(amido amine)s for non-viral gene delivery. J. Control. Release 148, 83–90.

Pillai, C.K.S., Paul, W., Sharma, C.P., 2009. Chitin and chitosan polymers: chemistry, solubility and fiber formation. Prog. Polym. Sci. 34, 641–678.

Pitt, W.G., Husseini, G.A., Staples, B.J., 2004. Ultrasonic drug delivery–a general review. Expert Opin. Drug Deliv. 1, 37–56.

Poeschla, E.M., Wong-Staal, F., Looney, D.J., 1998. Efficient transduction of nondividing human cells by feline immunodeficiency virus lentiviral vectors. Nature Med. 4, 354–357.

Prabaharan, M., 2008. Review paper: chitosan derivatives as promising materials for controlled drug delivery. J. Biomater. Appl. 23, 5–36.

Prata, C.A.H., Zhang, X.X., Luo, D., McIntosh, T.J., Barthelemy P., Grinstaff M.W., 2008. Lipophilic peptides for gene delivery. Bioconjugate Chem. 19, 418–420.

Rane, K.D., Hoover, D.G., 1999. Production of chitosan by fungi. Food Biotechnol. 7, 11–33.

Rao, N.M., Gopal, V., 2006. Cell biological and biophysical aspects of lipid-mediated gene delivery. Biosci. Rep. 26, 301–324.

Raper, S.E., Chirmule, N., Lee, F.S., Wivel, N.A., Bagg, A., Gao, G.P., Wilson, J.M., Batshaw, M.L., 2003. Fatal systemic inflammatory response syndrome in a ornithine transcarbamylase deficient patient following adenoviral gene transfer. Mol. Genet. Metab. 80, 148–158.

Ravi Kumar, M.N., Sameti, M., Mohapatra, S.S., Kong, X., Lockey, R.F., Bakowsky, U., Lindenblatt, G., Schmidt, H., Lehr, C.M., 2004. Cationic silica nanoparticles as gene carriers: synthesis, characterization and transfection efficiency in vitro and in vivo. J. Nanosci. Nanotechnol. 4, 876–881.

Rendi-Wagner, P., Wiedermann, G., Stemberger, H., Kollaritsch, H., 2002. New vaccination strategies for low- and non-responders to hepatitis B vaccine. Wien. Klin. Wochenschr. 114, 175–180.

Rinaudo, M., 2006. Chitin and chitosan: properties and applications. Prog. Polym. Sci. 31, 603–632.

Riva, R., Ragelle, H., des Rieux, A., Duhem, N., Jerome, C., Preat, V., 2011. Chitosan and chitosan derivatives in drug delivery and tissue engineering. Adv. Polym. Sci. 244, 19–44.

Robbins, P.D., Ghivizzani, S.C., 1998. Viral vectors for gene therapy. Pharmacol. Ther. 80, 35–47.

Romøren, K., Pedersen, S., Smistad, G., Evensen, Ø., Thu, B.J., 2003. The influence of formulation variables on in vitro transfection efficiency and physicochemical properties of chitosan-based polyplexes. Int. J. Pharm. 261, 115–127.

Rottinghaus, S.T., Poland, G.A., Jacobson, R.M., Barr, L.J., Roy, M.J., 2003. Hepatitis B DNA vaccine induces protective antibody responses in human non-responders to conventional vaccination. Vaccine 21, 4604–4608.

Rudzinski, W.E., Aminabhavi, T.M., 2010. Chitosan as a carrier for targeted delivery of small interfering RNA. Int. J. Pharm. 399, 1–11.

Ruponen, M., Yla-Herttuala, S., Urtti, A., 1999. Interactions of polymeric and liposomal gene delivery systems with extracellular glycosaminoglycans: physicochemical and transfection studies. Biochim. Biophys. Acta 1415, 331–341.

Sajomsang, W., Ruktanonchai, U., Gonil, P., Mayen, V., Opanasopit, P., 2009. Methylated N-aryl chitosan derivative/DNA complex nanoparticles for gene delivery: synthesis and structure–activity relationships. Carbohydr. Polym. 78, 743–752.

Sakurai, F., Terada, T., Yasuda, K., Yamashita, F., Takakura, Y., Hashida, M., 2002. The role of tissue macrophages in the induction of proinflammatory cytokine production following intravenous injection of lipoplexes. Gene Ther. 9, 1120–1126.

Sato, T., Ishii, T., Okahata, Y., 2001. In vitro gene delivery mediated by chitosan. Effect of pH, serum, and molecular mass of chitosan on the transfection efficiency. Biomaterials 22, 2075–2080.

Schaffer, D.V., Fidelman, N.A., Dan, N., Lauffenburger, D.A., 2000. Vector unpacking as a potential barrier for receptor-mediated polyplex gene delivery. Biotechnol. Bioeng. 67, 598–606.

Schattenberg, D., Schott, M., Reindl, G., Krueger, T., Tschoepe, D., Feldkamp, J., Scherbaum, W.A., Seissler, J., 2000. Response of human monocyte-derived dendritic cells to immunostimulatory DNA. Eur. J. Immunol. 30, 2824–2831.

Semete, B., Booysen, L., Lemmer, Y., Kalombo, L., Katata, L., Verschoor, J., Swai, H.S., 2010. In vivo evaluation of the biodistribution and safety of PLGA nanoparticles as drug delivery systems. Nanomedicine 6, 662–671.

Sharma, G., Modgil, A., Layek, B., Arora, K., Sun, C., Law, B., Singh, J., 2013. Cell penetrating peptide tethered bi-ligand liposomes for delivery to brain in vivo: biodistribution and transfection. J. Control. Release. 167, 1–10.

Sharma, S., Mukkur, T.K.S., Benson, H.A.E., Chen, Y., 2012. Enhanced immune response against pertussis toxoid by IgA-loaded chitosan–dextran sulfate nanoparticles. J. Pharm. Sci. 101, 233–244.

Shea, L.D., Segura, T., 2001. Materials for non-viral gene delivery. Annu. Rev. Mater. Res. 31, 25–46.

Shu, X.Z., Zhu, K.J., 2002. The influence of multivalent phosphate structure on the properties of ionically cross-linked chitosan films for controlled drug release. Eur. J. Pharm. Biopharm. 54, 235–243.

Smith-Arica, J.R., Bartlett, J.S., 2001. Gene therapy: recombinant adeno-associated virus vectors. Curr. Cardiol. Rep. 3, 43–49.

Smith, A.E., 1995. Viral vectors in gene therapy. Annu. Rev. Microbiol. 49, 807–838.

Son, S.H., Chae, S.Y., Choi, C.Y., Kim, M.Y., Ngugen, V.G., Jang, M.K., Nah, J.W., Kweon, J.K., 2004. Preparation of a hydrophobized chitosan oligosaccharide for application as an efficient gene carrier. Macromol. Res. 12, 573–580.

Srivastava, I.K., Margaret, A.L., 2003. Gene vaccines. Ann. Inter. Med. 138, 550–559.

Strand, S.P., Lelu, S., Reitan, N.K., de Lange Davies C., Artursson, P., Vårum, K.M., 2010. Molecular design of chitosan gene delivery systems with an optimized balance between polyplex stability and polyplex unpacking. Biomaterials 31, 975–987.

Suda, T., Liu, D., 2007. Hydrodynamic gene delivery: its principles and applications. Mol. Ther. 15, 2063–2069.

Suda, T., Suda, K., Liu, D., 2008. Computer-assisted hydrodynamic gene delivery. Mol. Ther. 16, 1098–1104.

Sun, X., Chen, S., Han, J., Zhang, Z., 2012. Mannosylated biodegradable polyethyleneimine for targeted DNA delivery to dendritic cells. Int. J. Nanomedicine 7, 2929–2942.

Tang, D.C., DeVit, M., Johnston, S.A., 1992. Genetic immunization is a simple method for eliciting an immune response. Nature 356, 152–154.

Tang, M.X., Szoka, F.C., 1997. The influence of polymer structure on the interactions of cationic polymers with DNA and morphology of the resulting complexes. Gene Ther. 4, 823–832.

Taylor, M.E., Conary, J.T., Lennartz, M.R., Stahl, P.D., Drickamer, K., 1990. Primary structure of the mannose receptor contains multiple motifs resembling carbohydrate-recognition domains. J. Biol. Chem. 265, 12156–12162.

Thanou, M., Florea, B.I., Geldof, M., Junginger, H.E., Borchard, G., 2002. Quaternized chitosan oligomers as novel gene delivery vectors in epithelial cell lines. Biomaterials 23, 153–159.

Thibault, M., Astolfi, M., Tran-Khanh, N., Lavertu, M., Darras, V., Merzouki, A., Buschmann, M.D., 2011. Excess polycation mediates efficient chitosan-based gene transfer by promoting lysosomal release of the polyplexes. Biomaterials 32, 4639–4646.

Thiersch, M., Rimann, M., Panagiotopoulou, V., Öztürk, E., Biedermann, T., Textor, M., Lühmann, T.C., Hall, H., 2013. The angiogenic response to PLL-g-PEG-mediated HIF-1α plasmid DNA delivery in healthy and diabetic rats. Biomaterials 34, 4173–4182.

Thomas, C.E., Ehrhardt, A., Kay, M.A., 2003. Progress and problems with the use of viral vectors for gene therapy. Nat. Rev. Genet. 4, 346–358.

Thomas, M., Ge, Q., Lu, J.J., Chen, J., Klibanov, A., 2005. Cross-linked small polyethylenimines: while still nontoxic, deliver DNA efficiently to mammalian cells in vitro and in vivo. Pharm. Res. 22, 373–380.

Thomas, M., Klibanov, A.M., 2003. Non-viral gene therapy: polycation-mediated DNA delivery. Appl. Microbiol. Biotechnol. 62, 27–34.

Tian, H., Lin, L., Chen, J., Chen, X., Park, T.G., Maruyama, A., 2011. RGD targeting hyaluronic acid coating system for PEI-PBLG polycation gene carriers. J. Control. Release 155, 47–53.

Tien, C.L., Lacroix, M., Szabo, P.I., Mateescu, M.A., 2003. N-acylated chitosan: hydrophobic matrices for controlled drug release. J. Control. Release 93, 1–13.

Toh, E.K.W., Chen, H.Y., Lo, Y.L., Huang, S.J., Wang, L.F., 2011. Succinated chitosan as a gene carrier for improved chitosan solubility and gene transfection. Nanomed. Nanotechnol. Biol. Med. 7, 174–183.

Tseng, M.T., Lu, X., Duan, X., Hardas, S.S., Sultana, R., Wu, P., Unrine, J.M., Graham, U., Butterfield, D.A., Grulke, E.A., Yokel, R.A., 2012. Alteration of hepatic structure and oxidative stress induced by intravenous nanoceria. Toxicol. Appl. Pharmacol. 260, 173–182.

Uchida, M., Natsume, H., Kobayashi, D., Sugibayashi, K., Morimoto, Y., 2002. Effects of particle size, helium gas pressure and microparticle dose on the plasma concentration of indomethacin after bombardment of indomethacin-loaded poly-L-lactic acid microspheres using a Helios gun system. Biol. Pharm. Bull. 25, 690–693.

Ulmer, J.B., Deck, R.R., Dewitt, C.M., Donnhly, J.I., Liu, M.A., 1996. Generation of MHC class I-restricted cytotoxic T lymphocytes by expression of a viral protein in muscle cells: antigen presentation by non-muscle cells. Immunology 89, 59–67.

Varkouhi, A.K., Scholte, M., Storm, G., Haisma, H.J., 2011. Endosomal escape pathways for delivery of biologicals. J. Control. Release 151, 220–228.

Verma, I.M., Somia, N., 1997. Gene therapy–promises, problems and prospects. Nature 389, 239–242.

Vigna, E., Naldini, L., 2000. Lentiviral vectors: excellent tools for experimental gene transfer and promising candidates for gene therapy. J. Gene Med. 2, 308–316.

Villemejane, J., Mir, L.M., 2009. Physical methods of nucleic acid transfer: general concepts and applications. Br. J. Pharmacol. 157, 207–219.

WHO, 2009. Weekly epidemiological record. 84, 405–420.

Walther, W., Stein, U., 2000. Viral vectors for gene transfer: a review of their use in the treatment of human diseases. Drugs 60, 249–271.

Wang, Q.Z., Chen, X.G., Liu, N., Wang, S.X., Liu, C.S., Meng, X.H., Liu, C.G., 2006. Protonation constants of chitosan with different molecular weight and degree of deacetylation. Carbohydr. Polym. 65, 194–201.

Wang, B., He, C., Tang, C., Yin, C., 2011. Effects of hydrophobic and hydrophilic modifications on gene delivery of amphiphilic chitosan based nanocarriers. Biomaterials 32, 4630–4638.

Wang, D.S., Panje, C., Pysz, M.A., Paulmurugan, R., Rosenberg, J., Gambhir, S.S., Schneider, M., Willmann, J.K., 2012. Cationic versus neutral microbubbles for ultrasound-mediated gene delivery in cancer. Radiology 264, 721–732.

Wang, J., Zhu, R., Gao, B., Wu, B., Li, K., Sun, X., Liu, H., Wang, S., 2014. The enhanced immune response of hepatitis B virus DNA vaccine using SiO_2@LDH nanoparticles as an adjuvant. Biomaterials 35, 466–478.

Wasungu, L., Hoekstra, D., 2006. Cationic lipids, lipoplexes and intracellular delivery of genes. J. Control. Release 116, 255–264.

Wieland, S., Chisari, F., 2005. Stealth and cunning: hepatitis B and hepatitis C viruses. J. Virol. 79, 9369–9380.

Wiethoff, C.M., Middaugh, C.R., 2003. Barriers to nonviral gene delivery. J. Pharm. Sci. 92, 203–217.

Wong, S.Y., Pelet, J.M., Putnam, D., 2007. Polymer systems for gene delivery–past, present, and future. Prog. Polym. Sci. 32, 799–837.

Wright, J.F., Qu, G., Tang, C., Sommer, J.M., 2003. Recombinant adeno-associated virus: formulation challenges and strategies for a gene therapy vector. Curr. Opin. Drug Discov. Devel. 6, 174–178.

Wu, G.Y., Wu, C.H., 1987. Receptor-mediated in vitro gene transformation by a soluble DNA carrier system. J. Biol. Chem. 262, 4429–4432.

Yamada, T., Iwasaki, Y., Tada, H., Iwabuki, H., Chuah, M.K., VandenDriessche, T., Fukuda, H., Kondo, A., Ueda, M., Seno, M., Tanizawa, K., Kuroda, S., 2003. Nanoparticles for the delivery of genes and drugs to human hepatocytes. Nat. Biotechnol. 21, 885–890.

Yang, J., Liu, Y., Wang, H., Liu, L., Wang, W., Wang, C., Wang, Q., Liu, W., 2012. The biocompatibility of fatty acid modified dextran-agmatine bioconjugate gene delivery vector. Biomaterials 33, 604–613.

Yang, X., Yuan, X., Cai, D., Wang, S., Zong, L., 2009. Low molecular weight chitosan in DNA vaccine delivery via mucosa. Int. J. Pharm. 375, 123–132.

Ye, Y.Q., Yang, F.L., Hu, F.Q., Du, Y.Z., Yuan, H., Yu, H.Y., 2008. Core-modified chitosan-based polymeric micelles for controlled release of doxorubicin. Int. J. Pharm. 352, 294–301.

Yoksan, R., Akashi, M., 2009. Low molecular weight chitosan-g-L-phenylalanine: preparation, characterization, and complex formation with DNA. Carbohydr. Polym. 75, 95–103.

Yoo, H.S., Lee, J.E., Chung, H., Kwon, I.C., Jeong, S.Y., 2005. Self-assembled nanoparticles containing hydrophobically modified glycol chitosan for gene delivery. J. Control. Release 103, 235–243.

You, Z., Huang, X., Hester, J., Toh, H.C., Chen, S.Y., 2001. Targeting dendritic cells to enhance DNA vaccine potency. Cancer Res. 61, 3704–3711.

Yuan, H., Lu, L.J., Du, Y.Z., Hu, F.Q., 2011. Stearic acid-g-chitosan polymeric micelle for oral drug delivery: in vitro transport and in vivo absorption. Mol. Pharm. 8, 225–238.

Zelikin, A.N., Putnam, D., Shastri, P., Langer, R., Izumrudov, V.A., 2002. Aliphatic ionenes as gene delivery agents: elucidation of structure-function relationship through modification of charge density and polymer length. Bioconjugate Chem. 13, 548–553.

Zhang, G., Gao, X., Song, Y.K., Vollmer, R., Stolz, D.B., Gasiorowski, J.Z., Dean, D.A., Liu, D., 2004. Hydroporation as the mechanism of hydrodynamic delivery. Gene Ther. 11, 675–682.

Zhang, X., Godbey, W.T., 2006. Viral vectors for gene delivery in tissue engineering. Adv. Drug Deliv. Rev. 58, 515–534.

Zhang, S., Xu, Y., Wang, B., Qiao, W., Liu, D., Li, Z., 2004. Cationic compounds used in lipoplexes and polyplexes for gene delivery. J. Control. Release 100, 165–180.

Zhou, Y., Yang, B., Ren, X., Liu, Z., Deng, Z., Chen, L., Deng, Y., Zhang, L.M., Yang, L., 2012. Hyperbranched cationic amylopectin derivatives for gene delivery. Biomaterials 33, 4731–4740.

Zhu, A.P., Pan, Y.N., Liao, T.Q., Zhao, F., Chen, T., 2008. The synthesis and characterization of polymerizable and biocompatible N-maleic acyl-chitosan. J. Biomed. Mater. Res. B Appl. Biomater. 85, 489–495.

Ziady, A.G., Gedeon, C.R., Miller, T., Quan, W., Payne, J.M., Hyatt, S.L., Fink, T.L., Muhammad, O., Oette, S., Kowalczyk, T., Pasumarthy, M.K., Moen, R.C., Cooper, M.J., Davis, P.B., 2003. Transfection of airway epithelium by stable PEGylated poly-L-lysine DNA nanoparticles in vivo. Mol. Ther. 8, 936–947.

Zou, Q., Zhong, Y., Su, H., Kang, Y., Jin, J., Liu, Q., Geng, S., Zhao, G., Wang, B., 2010. Enhancement of humoral and cellular responses to HBsAg DNA vaccination by immunization with praziquantel through inhibition TGF-β/Smad2,3 signaling. Vaccine 28, 2032–2038.

Zuhorn, I.S., Kalicharan, R., Hoekstra, D., 2002. Lipoplex-mediated transfection of mammalian cells occurs through the cholesterol-dependent clathrin-mediated pathway of endocytosis. J. Biol. Chem. 277, 18021–18028.